ASSESSING THE EVOLUTION OF DISSOLVED INORGANIC CARBON AND STABLE CARBON ISOTOPES IN SURFACE WATERS

By

PRIDE T. ABONGWA
Master of Science in Hydrology and Water Resources
UNESCO-IHE Institute of Water Education
Delft, The Netherlands
2004

Bachelor of Science in Geology
University of Buea
Buea, Cameroon
1999

Submitted to the Faculty of the
Graduate College of the
Oklahoma State University
in partial fulfillment of
the requirements for
the Degree of
DOCTOR OF PHILOSOPHY
July, 2014

ASSESSING THE EVOLUTION OF DISSOLVED INORGANIC CARBON AND STABLE CARBON ISOTOPES IN SURFACE WATERS

Dissertation Approved

Dr. Eliot Atekwana

Dissertation Adviser

Dr. Tracy Quan

Dr. James Puckette

Dr. Todd Halihan

Dr. Gail Wilson

ACKNOWLEDGEMENTS

I thank everyone who has assisted and supported me throughout my educational career. I heartily thank my Ph.D. adviser, Dr. Eliot Atekwana. His guidance, continual mentorship, and involvement in every step in the way right down to the last detail brought this work to fruition. The numerous late nights he kept discussing and advising on the direction of the work and as well as the prompt nature in which he reviewed my manuscripts and return written material speaks of his immense dedication, interest and commitment to my work. I thank my committee members Dr. Tracy Quan, Dr. Todd Halihan, Dr. James Puckette and Dr. Gail Wilson, for their critique, input, help and guidance to make my work a realization. I especially thank Dr. Todd Halihan and Dr. James Puckette for their field assistance and logistic support in the 'carbonate springs' project.

I thank the various head of the Boone Pickens School of Geology during my stay: Dr. Jay Gregg, Dr. Eliot Atekwana and Dr. Estella Atekwana for their vision, advice, support, mentorship and encouragement.

I acknowledge all faculty and staff members whom I interacted with and was fortunate to benefit from their generosity, guidance and advice on related and other non-related dissertation issues. I specifically thank Dr. Joseph Donoghue and Dr. Tracy Quan for permitting me to use their laboratory space for my experiments.

I thank the Alumni of the Boone Pickens School of Geology for providing the funds that were awarded to me via the graduate alumni fellowship throughout my Ph.D. study. I thank the

Boone Pickens School of Geology for providing funds through the ‘student enrichment fund’ which I used for travel to present my work at international conferences. I am particularly grateful for the friends that I made throughout my stay here at Oklahoma State University. I thank the executive and scholarship committee of the National Association of Black Geoscientist (NABG) for their financial support towards the completion of my Ph.D. degree.

I am indebted to my colleagues: Eric Akoko, Keller Flinton, Christopher Geyer, Emily Guderian, Cass Luckette, Nicole Paizis and Rawlings Akondi for their field and laboratory assistance.I thank my family for their complete support both financially and morally throughout all these years of studies. To my siblings Florence, Victor, Bernadette and Derick for their constant calls, emails and messages of encouragement and to that, I say a big thank you. I am where I am today because of my parents, my dad, Joseph Abongwa (of blessed memory) and my mum, Alice Abongwa for nursing me and laying the right foundation at the early stages of my life. I specifically would thank my mum for her prayers, extreme protection, love, vision, and care up to this present moment and for this, mummy; I will always remain indebted to you. My special thanks also go to my uncle, John Abongwa for his assistance, guidance and support throughout these years.

Finally, I heartily thank my sweetheart, my wife and the love of my life, Mollie for her dedication, love, prayers, perseverance, support and her ability to endure throughout all these years of my Ph.D. studies. My children Pearl and Joseph kept the fire burning in me.

Name: PRIDE TAMASANG BONGWA

Date of Degree: JULY, 2014

Title of Study: ASSESSING THE EVOLUTION OF DISSOLVED INORGANIC CARBON AND STABLE CARBON ISOTOPES IN SURFACE WATERS

Major Field: GEOLOGY

Abstract: Documenting the transformation of dissolved inorganic carbon (DIC) during the interaction of surface waters with atmospheric $CO_{2(g)}$ is vital for understanding carbon cycling. We conducted field and laboratory experiments that mimic the continuum of changes in DIC concentrations and stable carbon isotope ratio of DIC ($\delta^{13}C_{DIC}$) over space and time. At partial pressures of CO_2 (pCO_2) greater than atmospheric, the DIC concentrations decreased due to CO_2 outgassing accompanied by continued enrichment in $\delta^{13}C_{DIC}$. Over time and space, as the pCO_2 approaches equilibrium with atmospheric CO_2, the DIC concentration increases by evaporation. The outgassing of CO_2 and the continuous exchange of carbon with atmospheric CO_2 would drive the surface water to equilibrium conditions through kinetic and equilibrium isotopic fractionation. In surface water systems such as carbonate springs that evolve to calcite saturation, significant $\delta^{13}C_{DIC}$ enrichment that occurs after calcite supersaturation is dominated by equilibrium isotopic effect, despite conditions conducive for calcite precipitation. We hypothesize that the chemical and isotopic behavior observed for the field and laboratory experiments may characterize other carbonate-rich waters (streams and lakes) evolving in contact with the atmosphere. Addition of precipitation to surface water dilutes solutes and DIC according to the dilution proportion causing differential evolution of the $\delta^{13}C_{DIC}$. Continuous invasion of $CO_{2(g)}$ into surface water forms carbonic acid and causes the preferential incorporation of the heavier $^{13}CO_2$ into the liquid phase causing the surface water to be enriched in $\delta^{13}C_{DIC}$. The effect of precipitation on surface water is important from the initial stages of dilution to the equivalence of about 10 hour of reaction time based on the results of this experiment. We suggest that experimentation designed to study carbon evolution in surface waters while minimizing carbon evolution based on the effect of dilution should wait for at least 10 hours after a precipitation event before sampling.

TABLE OF CONTENTS

TABLE OF FIGURES

I. ASSESSING THE TEMPORAL EVOLUTION OF DISSOLVED INORGANIC CARBON IN WATERS EXPOSED TO ATMOPSHERIC $CO_{2(g)}$: A LABORATORY APPROACH

II. CONTROLS ON THE CHEMICAL AND ISOTOPIC COMPOSITION OF CARBONATE SPRINGS DURING EVOLUTION TO SATURATION WITH RESPECT TO CALCITE

LIST OF TABLES

I. ASSESSING THE TEMPORAL EVOLUTION OF DISSOLVED INORGANIC CARBON IN WATERS EXPOSED TO ATMOPSHERIC $CO_{2(g)}$: A LABORATORY APPROACH

II. CONTROLS ON THE CHEMICAL AND ISOTOPIC COMPOSITION OF CARBONATE SPRINGS DURING EVOLUTION TO SATURATION WITH RESPECT TO CALCITE

GENERAL INTRODUCTION

1. Motivation

The earth's climate is greatly impacted by the carbon cycle, which is regulated by the level of $CO_{2(g)}$ in the atmosphere (e.g., Houghton et al., 1998; Ikeda and Tajika, 2002). Current estimates suggest that inland surface water releases ~1.2 Pg C $year^{-1}$ to the atmosphere, making inland surface waters a vital component of the global carbon cycle (Tranvik et al., 2009). Also, the oceanic carbon reservoir is partly derived from contributions of carbon from continents via rivers, as well as from ocean productivity (Hein and Sand–Jensen, 1997). Since the ocean partly receives its carbon from inland water systems, knowledge of the processes that impact carbon dynamics in inland surface waters becomes an important consideration in understanding global carbon cycling.

Surface water receives influx of dissolved inorganic (DIC) and water from groundwater and precipitation which occurs at different magnitude and temporal and spatial scales. In surface water, competing processes that produce $CO_{2(g)}$ (e.g., aquatic respiration, photo-oxidation) or remove $CO_{2(g)}$ will affect the DIC pool and the $\delta^{13}C_{DIC}$ (e.g., Atekwana and Krishnamurthy, 1998; Telmer and Veizer, 1999; Cartwright, 2010; Zeng and Masiello, 2011; Shin et al., 2011). In addition to the processes (photosynthesis, respiration and water-rock interactions) that add or remove carbon from surface water DIC pool, there is also carbon isotopic exchange that occurs during DIC-atmospheric $CO_{2(g)}$ interaction. The loss, gain or exchange of carbon between

surface water DIC and atmospheric $CO_{2(g)}$ causes changes in the $\delta^{13}C_{DIC}$ because these processes are isotopically fractionating (Clark and Fritz, 1997). The partial pressure of $CO_{2(g)}$ (pCO_2) is a determining factor of how DIC in a solution that interacts with atmospheric $CO_{2(g)}$ behaves chemically (e.g., Pawellek and Veizer, 1994; Richey et al., 2002; Mayorga et al., 2005; Wachniew, 2006; Doctor et al., 2008). Therefore the carbon lost or gained or exchanged from the solution will depend on the chemical transformation between DIC and $CO_{2(g)}$ ($CO_3^{2-} \leftrightarrow HCO_3^- \leftrightarrow CO_{2(aq)} \leftrightarrow CO_{2(g)}$) (e.g., Telmer and Veizer, 1999; Cartwright, 2010, Shin et al., 2011; Abongwa and Atekwana, 2013) Thus, the DIC concentrations in conjunction with the $\delta^{13}C_{DIC}$ can be used in understanding aspects of carbon interaction between surface water DIC and atmospheric $CO_{2(g)}$. Surface water systems with relatively low Ca^{2+} concentrations will not evolve to calcite supersaturation and this is expected to affect the overall behavior of DIC in such surface waters. Therefore, studies of the behavior of DIC in surface waters that do not evolve to calcite saturation is an important consideration in the understanding of the processes and mechanisms that affect DIC evolution in surface water systems.

During surface water-atmospheric $CO_{2(g)}$ interaction, evolution of the water to calcite supersaturation could cause calcite precipitation, hence removing carbon from the DIC pool (e.g., Atekwana and Krishnamurthy, 1998; Cartwright, 2010, Zeng and Masiello, 2011). Although the removal of carbon from surface water is possible during carbonate precipitation, it is not clear how this will affect the overall evolution of DIC in surface waters that interact with atmospheric $CO_{2(g)}$. Hence, studying surface waters which evolved to calcite supersaturation may provide information that characterize carbonate-rich waters and also determine how fast it could take for such carbonate-rich waters to precipitate carbonates. Precipitation adds water into surface water systems causing solute and DIC dilution which affects the chemical and isotopic

behavior of DIC. Yet, the effects of dilution on carbon evolution in surface waters that interacts with atmospheric $CO_{2(g)}$ is not known. Investigating the evolution of DIC in surface water perturbed by rainfall is an important geochemical consideration in the understanding of carbon behavior during surface water DIC-atmospheric $CO_{2(g)}$ interactions. Dilution would change the $\delta^{13}C_{DIC}$ signature of surface and sequential monitoring of the $\delta^{13}C_{DIC}$ composition over time and/or space could be used to evaluate the effect of dilution on carbon evolution in surface waters. The residence time of water in rivers vary between 3 to 19 days (Basu and Pick, 1996) and knowing how long the effect of dilution would last in surface water could be important in determining when to commence hydrogeochemical studies that minimize surface water dilution effect.

2. Problems, hypothesis and objectives

The questions addressed in this research are as follows:

(1) How does DIC evolve in surface water undersaturated with respect to calcite?

(2) How does DIC behave in surface water that evolves to calcite supersaturation?

(3) During surface water DIC-atmospheric $CO_{2(g)}$ interactions, does perturbation by rainfall affects the DIC evolution?

The goal of this research was to investigate the processes and mechanisms that affect DIC evolution and $\delta^{13}C_{DIC}$ composition during surface water DIC-atmospheric $CO_{2(g)}$ interaction.

The hypotheses tested were:

(1) *During short to long term surface water DIC-atmospheric $CO_{2(g)}$ interaction, variable changes in the DIC concentrations will be accompanied by continuous enrichment in $\delta^{13}C_{DIC}$ until chemical and isotopic equilibrium is achieved.*

(2) *The chemical and isotopic behavior that characterizes carbonate-rich determines when such systems start precipitating calcite.*

(3) *Precipitation by rain or snow-melt which dilute surface water DIC concentrations will only change the initial chemical and isotopic composition and not influence the evolution that occurs during the interaction of surface water and atmospheric $CO_{2(g)}$.*

The objectives of this study were:

Hypothesis 1: *to develop models that characterize the evolutionary pathways of DIC in surface water exposed to atmospheric $CO_{2(g)}$ over time,*

Hypothesis 2: *to generate information on DIC-$\delta^{13}C_{DIC}$ models from field and laboratory data that characterize water evolution through calcite saturation and,*

Hypothesis 3: *to conduct a comparative assessment of the effect of DIC dilution by precipitation on DIC chemical and isotopic evolution.*

The hypotheses were tested and the project objectives met by using natural and artificial solutions and conducting field and laboratory experiments that trace and model carbon interactions of surface water DIC and atmospheric $CO_{2(g)}$. Measurements of DIC, Ca^{2+} and Mg^{2+} concentrations, $\delta^{13}C_{DIC}$, temperature and pH and calculations of the $pCO_{2(g)}$ and saturation indices of calcite (SIc) were used as inputs to develop models for carbon dynamics in surface waters.

3. Significance of study

We developed models based on DIC-$\delta^{13}C_{DIC}$ behavior in surface waters that would be used to guide interpretation of the processes and mechanisms associated with surface water DIC-atmospheric $CO_{2(g)}$ interaction. Documenting the transformation of DIC and $\delta^{13}C_{DIC}$ composition during the interaction of surface waters (e.g., rivers, lakes) with atmospheric $CO_{2(g)}$ is vital for understanding carbon cycling on a local, regional and global scale.

The results of this study could also be applied to surface waters that evolved to calcite supersaturation such that the $\delta^{13}C_{DIC}$ will be used to track isotopic fractionation accompanying carbon loss to the atmosphere, to precipitation of calcite or from carbon exchange with atmospheric $CO_{2(g)}$. The chemical and isotopic behavior observed from this study could be used to characterize carbonate-rich waters evolving in contact with the atmosphere.

Precipitation (rain or melted snow) dilutes surface water but its effect on the evolution of DIC and $\delta^{13}C_{DIC}$ in surface waters are not known. This study determines if such dilution will cause surface water to lose CO_2 through degassing, gain CO_2 through invasion or drive the system towards equilibration by carbon exchange with atmospheric $CO_{2(g)}$. Also, the result of this study will provide estimate based on a time frame as to when the effect of dilution becomes non-significant.

CHAPTER I

ASSESSING THE TEMPORAL EVOLUTION OF DISSOLVED INORGANIC CARBON IN WATERS EXPOSED TO ATMOPSHERIC $CO_{2(g)}$: A LABORATORY APPROACH

Pride T. Abongwa and Eliot A. Atekwana
Journal of Hydrology 505 (2013), 250-265
Boone Pickens School of Geology, 105 Noble Research Center, Oklahoma State University, Stillwater OK, 74078, USA.

Abstract

Documenting the transformation of dissolved inorganic carbon (DIC) during the interaction of surface waters (e.g., rivers, lakes) with atmospheric $CO_{2(g)}$ is vital for understanding carbon cycling. Investigations that mimic the continuum of changes in DIC concentrations and stable carbon isotope ratio of DIC ($\delta^{13}C_{DIC}$) to equilibrium with atmospheric $CO_{2(g)}$ are difficult to conduct in natural settings because of multiple processes that occur in the water column, the interaction between water and sediments or rocks in stream channels and lake beds, as well as the variability in water residence times. Thus, laboratory simulations of the spectrum of DIC

transformation provide insights which reduce the ambiguity in describing the mechanisms that control the behavior of DIC during surface water-atmospheric $CO_{2(g)}$ interaction. To test how surface water-atmospheric $CO_{2(g)}$ interaction affects DIC concentrations and $\delta^{13}C_{DIC}$, we used three types of samples: (1) we prepared an artificial solution using $NaHCO_3$ where the DIC concentration is near chemical equilibrium and the $\delta^{13}C_{DIC}$ is far from isotopic equilibrium with atmospheric $CO_{2(g)}$, (2) natural groundwater where the DIC concentration and the $\delta^{13}C_{DIC}$ are both sufficiently far from chemical and isotopic equilibrium with atmospheric $CO_{2(g)}$ and (3) lake water where the DIC concentration and the $\delta^{13}C_{DIC}$ are near chemical and isotopic equilibrium with atmospheric $CO_{2(g)}$. These samples allowed us to ascertain when only chemical or isotopic changes are occurring, or when both chemical and isotopic changes are occurring. The $NaHCO_3$ solution was prepared by dissolving ~6 g of laboratory grade $NaHCO_3$ salt in 20 L of deionized water. Groundwater was collected from Stillwater, Oklahoma (36° 08′ 22.20″ N, 97° 03′ 22.66″ W) and lake water was collected from Lake McMurtry, Stillwater, Oklahoma (36° 10′ 49.37″ N, 97° 10′ 52.9″ W). The solution of $NaHCO_3$, and groundwater (potential source of surface water) and lake water samples were exposed to the atmosphere in a laboratory setting for 850 to 1000 hours until their DIC attained chemical and isotopic equilibrium with atmospheric $CO_{2(g)}$. All samples were prepared in duplicate and one set was agitated to simulate mixing in surface waters. The DIC concentrations of the $NaHCO_3$ samples increased without C loss and the $\delta^{13}C_{DIC}$ was enriched to a steady state for the mixed sample. The increase in the DIC concentrations was modeled as evaporation and not as $CO_{2(g)}$ invasion since the pCO_2 was higher than atmospheric throughout the experiment. The enrichment in the $\delta^{13}C_{DIC}$ was modeled as equilibrium carbon isotopic exchange with atmospheric $CO_{2(g)}$. The DIC concentrations in the mixed groundwater sample initially decreased due to $CO_{2(g)}$ outgassing and the accompanying

enrichment in $\delta^{13}C_{DIC}$ was modeled as kinetic isotopic fractionation. After the initial decrease, the DIC concentrations increased continuously while the $\delta^{13}C_{DIC}$ was enriched to a steady state. Overall, the unmixed groundwater sample showed similar temporal $\delta^{13}C_{DIC}$ trends to the mixed groundwater sample, even though the unmixed sample did not achieve isotopic equilibrium with atmospheric $CO_{2(g)}$. Both the mixed and unmixed lake samples showed only small increases in temporal DIC concentrations and a slight initial decrease, followed by a small enrichment in the $\delta^{13}C_{DIC}$ during the experiment. The minor changes suggest that the lake samples were closer to chemical and carbon isotopic equilibrium with atmospheric $CO_{2(g)}$. The results of this study would apply in settings where the predominant process controlling carbon cycling is the interaction between the surface water DIC and atmospheric $CO_{2(g)}$.

Keywords: Dissolved inorganic carbon; Evaporation; Isotopic fractionation; Stable carbon isotopes; Surface water-atmosphere interaction

1. Introduction

Inland surface waters serve as conduits for carbon transfer from the terrestrial to the atmospheric reservoir (Cole et al., 2007). Current estimates suggest that inland surface water releases ~1.2 Pg C $year^{-1}$ to the atmosphere, making inland surface waters a vital component of the global carbon cycle (Tranvik et al., 2009). The transfer of carbon to the atmosphere occurs in the form of $CO_{2(g)}$ primarily from rivers and lakes. The loss of $CO_{2(g)}$ to the atmosphere, influx of $CO_{2(g)}$ from the atmosphere or equilibrium exchange of carbon between dissolved inorganic carbon (DIC) and atmospheric $CO_{2(g)}$ will change the chemical and isotopic composition of DIC

in rivers (e.g., Pawellek and Veizer, 1994; Atekwana and Krishnamurthy, 1998; Telmer and Veizer, 1999; Richey et al., 2002; Mayorga et al., 2005; Wachniew, 2006; Doctor et al., 2008) and lakes (e.g., Emerson, 1975; Anderson et al., 1999; Jonsson et al., 2003). Theoretically, the loss or gain of carbon and exchange of carbon between surface water DIC and atmospheric $CO_{2(g)}$ should change the isotopic composition of DIC ($\delta^{13}C_{DIC}$) because these processes result in isotopic fractionation (Clark and Fritz, 1997). During the transfer of $CO_{2(g)}$ across the gas-liquid interface, the isotopic fractionation is controlled by the relative diffusivities of ^{12}C vs. ^{13}C and has been described by kinetic isotopic fractionation (e.g., Usdowski and Hoefs, 1990; Zhang et al., 1995). The $\delta^{13}C_{DIC}$ of surface waters that lose or gain $CO_{2(g)}$ during the interaction with atmospheric $CO_{2(g)}$ can also be described by equilibrium isotopic fractionation (e.g., Zhang et al., 1995; Halas et al., 1997). In instances where the DIC in a solution is in chemical but not isotopic equilibrium with atmospheric $CO_{2(g)}$, carbon exchange will occur until isotopic equilibrium is achieved (Leśniak and Zawidzki, 2006).

The partial pressure of $CO_{2(g)}$ (pCO_2) is the determining factor of how DIC in a solution that interacts with the atmospheric $CO_{2(g)}$ behaves chemically. Therefore the net amount of carbon lost, gained or exchanged from the solution will depend on the chemical transformation between DIC and $CO_{2(g)}$ ($CO_3^{2-} \leftrightarrow HCO_3^- \leftrightarrow CO_{2(aq)} \leftrightarrow CO_{2(g)}$). Thus, DIC concentration in conjunction with the $\delta^{13}C_{DIC}$ measurements can be used in understanding aspects of carbon interaction between surface water DIC and atmospheric $CO_{2(g)}$. The systematics of DIC evolution in surface water is complicated by water column processes that affect carbon such as respiration which supplies carbon to the DIC pool along with photosynthesis and carbonate precipitation that remove carbon from the DIC pool (e.g., Atekwana and Krishnamurthy, 1998; Telmer and Veizer, 1999; Cartwright, 2010, Zeng and Masiello, 2011; Shin et al., 2011). Where the material lining

river channels or sediments lining lake beds are carbonates, weathering of the carbonates may affect the water column DIC pool (Doctor et al., 2008). Finally, the hydrologic status of the surface water is also important for understanding the evolution of DIC. In humid climates, groundwater is an important source of discharge to surface water which affects the DIC concentration and $\delta^{13}C_{DIC}$ concentrations of surface water. On the other hand, in arid environments, groundwater discharge to surface water may not occur and is not important in the evolution of DIC in streams. Surface water in arid climates may even undergo evaporation which will increase DIC concentrations (e.g., Akoko et al., 2012).

The different processes that affect the DIC pool in surface waters occur with variable intensity over different temporal and spatial scales. Thus, the residence time of water becomes an overall integrating factor for the different processes in surface water reservoirs. For example, in rivers, the evolution of DIC to chemical and isotopic equilibrium with atmospheric $CO_{2(g)}$ can be traced throughout the length of the river; here the length scale is translated to a time scale, ignoring all of the other complicating processes such as respiration, photosynthesis and water-rock interactions. The residence time of water in rivers vary between 3 to 19 days for temperate rivers (Basu and Pick, 1996). For all rivers on the continents, the average water residence time increases to 26 days, with an average of 60 days for the 50 largest rivers (Vörösmarty et al., 2000). In contrast, the spatial scale may not be important in lakes, therefore, DIC evolution to equilibrium with atmospheric $CO_{2(g)}$ could be related to time. Lakes have residence times that vary from 2 to 10^2 years (e.g., Quinn, 1992; Ambrosetti et al., 2003). The effect of long water residence time on $\delta^{13}C_{DIC}$ will depend on competing processes that produce $CO_{2(g)}$ (e.g., aquatic respiration, photo-oxidation) or remove $CO_{2(g)}$ (e.g., aquatic photosynthesis) in addition to carbon isotopic exchange.

The processes that control $CO_{2(g)}$ loss, $CO_{2(g)}$ gain and carbon exchange between DIC in surface waters and atmospheric $CO_{2(g)}$ can be elucidated by assessing the DIC concentrations and $\delta^{13}C_{DIC}$ over space and/or time until the system attains chemical and isotopic equilibrium. Because of the multiple processes and variable residence time, the continuum in the temporal behavior of DIC and $\delta^{13}C_{DIC}$ is difficult to capture in natural experiments. In practice, a long-term study of a range of surface waters that capture the continuum in the behavior of DIC and $\delta^{13}C_{DIC}$ is costly, time consuming and difficult to conduct. Laboratory simulations of the interaction of surface waters with atmospheric $CO_{2(g)}$ that achieve chemical and isotopic equilibrium can provide insights on surface water DIC-atmospheric $CO_{2(g)}$ interaction. Although laboratory simulations do not capture the nuances of the natural environment, they provide near ideal cases for the processes studied, and thus can guide interpretation of such processes when they dominate over others in the natural environment.

In this study, we investigated carbon cycling in surface waters where the predominant process controlling the carbon cycling is atmospheric $CO_{2(g)}$-surface water DIC interaction. We investigated the temporal chemical and $\delta^{13}C$ behavior of DIC in an artificial solution of $NaHCO_3$, natural groundwater and lake water exposed to atmospheric $CO_{2(g)}$ in a laboratory setting by making chemical and isotopic measurements for up to 850 to 1000 hours. We aimed to determine how the different processes such as $CO_{2(g)}$ loss, $CO_{2(g)}$ gain or carbon exchange can be elucidated from DIC concentrations and $\delta^{13}C_{DIC}$. We develop conceptual models that are applied to our results to characterize the chemical processes and isotopic fractionation from changes in the DIC concentrations and $\delta^{13}C_{DIC}$ and then fit these models to data from select surface waters to validate our results. Our models can adequately characterize surface waters in which DIC-atmospheric $CO_{2(g)}$ interaction dominates the cycling of carbon.

2. Methods

2.1 Theoretical considerations in experimental design

Two aspects that must be considered in order to assess $CO_{2(g)}$ behavior during the interaction between surface water and the atmosphere are: (1) the physical process involving the outgassing of $CO_{2(g)}$ from solutions to the atmosphere, influx of $CO_{2(g)}$ into solutions from the atmosphere or exchange of carbon between DIC and atmospheric $CO_{2(g)}$ and (2) the chemical process of the formation of $CO_{2(g)}$ from DIC or the transformation of $CO_{2(g)}$ to DIC ($CO_{2(g)} \leftrightarrow CO_{2(aq)} \leftrightarrow H_2CO_3 \leftrightarrow HCO_3^- \leftrightarrow CO_3^{2-}$) in the aqueous phase. The transfer of $CO_{2(g)}$ or carbon between solutions and atmospheric $CO_{2(g)}$ is diffusion controlled (Fig. 1). Air injection and supersaturation is common in turbulent streams and choppy lakes and would enhance $CO_{2(g)}$ diffusion across the air-water interface. The rate of $CO_{2(g)}$ transfer across the air-water interface is described by Fick's first law and modeled using a two-film diffusion model (Lewis and Whitman, 1924):

$$F = \left(\frac{1}{A}\right)\frac{dn}{dt} = D\frac{\Delta C}{z} = K_g\,(C_g - C_{sg}) = K_l\,(C_{sl} - C_l) \qquad (1)$$

where F is the flux in mols (n) per unit time (sec) per unit area A (cm^3), D is the diffusion coefficient (cm^3/sec) from a surface area of thickness z (cm), ΔC is the concentration difference (mol/cm^3) across the air-water interface, K_g and K_l are the exchange constants or transfer coefficients (cm/sec) of the $CO_{2(g)}$ molecules across the gas and liquid films, respectively, C_g and C_l are the $CO_{2(g)}$ concentrations (mol/cm^3) in the bulk gas and liquid and C_{sg} and C_{sl} are the $CO_{2(g)}$ concentrations (mol/cm^3) in the gas and liquid films.

For a solution with a pCO_2 that is different from atmospheric, the thickness of gas and liquid film layers is a limiting factor in the transfer of $CO_{2(g)}$ between the solution and the atmosphere.

The gas and liquid films represented by the surface layer thickness (z) vary inversely with the degree of turbulence (e.g., wind speed). Thus, a higher value of K_1 can be achieved by greater turbulence and conversely, with no turbulence, the value of K_1 will be small. In laboratory $CO_{2(g)}$ interaction experiments, K_1 can be maximized by agitating the solution and minimized by no agitation (Fig. I-1).

The concentration of DIC and the distribution of DIC species in natural waters exposed to a $CO_{2(g)}$ containing gas phase is controlled by carbonate equilibrium (Stumm and Morgan, 1981):

$$CO_{2(g)} + H_2O \leftrightarrow CO_{2(aq)} + H_2O \quad (2)$$

$$CO_{2(aq)} + H_2O \leftrightarrow H_2CO_3 \quad (3)$$

$$H_2CO_3 \leftrightarrow HCO_3^- + H^+ \quad (4)$$

$$HCO_3^- \leftrightarrow CO_3^{2-} + H^+ \quad (5)$$

The equilibrium concentration of $CO_{2(aq)}$ in the solution is determined by the temperature dependent Henry's Law constant (K_h) and the pCO_2 in the gas phase:

$$K_h = \frac{aH_2CO_3}{pCO_2} \quad (6)$$

where a is the activity.

Similarly, at equilibrium, the speciation between H_2CO_3 and HCO_3^- and between HCO_3^- and CO_3^{2-} is given by the first (K_1) and second (K_2) dissociation constants, respectively, such that:

$$K_1 = \frac{aH^+ * aHCO_3^-}{aH_2CO_3} \text{ and,} \quad (7)$$

$$K_2 = \frac{aH^+ * aCO_3^{2-}}{aHCO_3^-} \quad (8)$$

Therefore, the behavior of DIC in solution will depend on both the pCO_2 in the gas phase, the pCO_2 of the solution and the pH.

2.2 Sample selection

A way to test how surface water-atmospheric $CO_{2(g)}$ interaction affects DIC concentrations and $\delta^{13}C_{DIC}$ is to select solutions in which (1) the DIC concentration is near chemical equilibrium and the $\delta^{13}C_{DIC}$ is far from isotopic equilibrium with atmospheric $CO_{2(g)}$, (2) the DIC concentrations and the $\delta^{13}C_{DIC}$ are both sufficiently far from chemical and isotopic equilibrium with atmospheric $CO_{2(g)}$ and (3) the DIC concentrations and the $\delta^{13}C_{DIC}$ are near chemical and isotopic equilibrium with atmospheric $CO_{2(g)}$. These solutions will allow us to ascertain when only chemical or isotopic changes are occurring, or when both chemical and isotopic changes are occurring. For a solution in which the DIC concentration is near chemical equilibrium and the $\delta^{13}C_{DIC}$ is far from isotopic equilibrium with atmospheric $CO_{2(g)}$, we prepared an artificial solution using $NaHCO_3$. For a solution in which the DIC concentration and $\delta^{13}C_{DIC}$ are both far from chemical and isotopic equilibrium with atmospheric $CO_{2(g)}$, we used natural groundwater. For a solution with DIC concentration near chemical and isotopic equilibrium with atmospheric CO_2, we used lake water (see Table I-1 for the initial values of pCO_2 and $\delta^{13}C_{DIC}$).

2.3 Sample collection and experimental set-up

Acid pre-washed 25 L plastic buckets served as reactors for the experiments. The mixed and unmixed $NaHCO_3$ solutions were prepared by dissolving 5.5 g and 5.8 g of 99% laboratory grade $NaHCO_3$ salt (LCSX-0320-1, EMD Chemicals, Inc.), respectively in 20 L of deionized water. Groundwater was collected from Stillwater, Oklahoma (36° 08′ 22.20″ N, 97° 03′ 22.66″ W) by pumping into two acid pre-washed 25 L plastic containers with a submersible pump. Lake water was pumped into two acid pre-washed 25 L plastic containers with a submersible pump from

Lake McMurtry, Stillwater, Oklahoma (36° 10′ 49.37″ N, 97° 10′ 52.9″ W). Samples of both the groundwater and lake water were filtered through inline 0.45 μm Gelman filters (Pall Corporation) during collection and were immediately capped and transported to the laboratory. The lake water and groundwater samples collected in the 25 L reactors were collected with no headspace, thereby eliminating exchange of carbon between DIC and trapped atmospheric $CO_{2(g)}$ in the headspace during transportation and storage. Twenty liters of $NaHCO_3$ solutions were prepared in 25 L reactors in duplicate and the experiments were started immediately after sample preparation. Twenty liters of the groundwater and lake samples were dispensed into the 25 L reactors in duplicates. One set of the reactors containing the $NaHCO_3$, groundwater and lake water were agitated by circulating the water at a rate of ~10 L/min using a submersible pump (ViaAqua Powerhead, VA 360-906060; Foster and Smith Aquatics). All reactors were left opened and in contact with the laboratory atmosphere for the duration of the experiment which ranged from 850 to 1000 hours depending on the time it took for the mixed solutions to reach chemical and isotopic equilibrium.

2.4 Sampling and analysis

Measurements and sampling for determining the physical and chemical parameters and the $\delta^{13}C_{DIC}$ were conducted at 0, 0.5, 1, 2, 3, 4, 8 and 24 hours, followed by every 24 hours for 2 weeks and weekly after that. Temperature, pH and total dissolved solids (TDS) were measured using a Yellow Springs Instrument (YSI) multi-parameter probe calibrated to manufacturer's specifications. Water samples collected from each reactor were filtered through 0.45 μm nylon filters and the alkalinity was measured immediately after sampling by acid titration (Hach Company, 1992). Samples for anions and cations were collected in high density polyethylene

(HDP) bottles and the cation samples were acidified to a pH <2.0 using high purity HNO_3. The anions and cations were measured by ion chromatography (Dionex ICS 3000). Samples for DIC analysis were collected in pre-acidified (1 mL of 85% H_3PO_4) vaccutainer tubes and $CO_{2(g)}$ was extracted as described by Atekwana and Krishnamurthy (1998). The DIC concentrations were calculated from extracted $CO_{2(g)}$, then the $CO_{2(g)}$ was sealed in Pyrex tubes and analyzed for $\delta^{13}C_{DIC}$ using a Finnigan Delta Plus XL isotope ratio mass spectrometer. Laboratory air was collected periodically in pre-evacuated 1.5 L glass ampoules with the use of a vacuum line to purify the $CO_{2(g)}$. The purified $CO_{2(g)}$ was also sealed in Pyrex tubes and later analyzed for $\delta^{13}C$. Stable isotopes ratios of hydrogen (δD) and oxygen ($\delta^{18}O$) in select water samples were measured by a high temperature conversion elemental analyzer (Gehre et al., 2004) coupled to a Finnigan Delta Plus XL isotope ratio mass spectrometer. The stable isotope ratios are reported in the standard delta (δ) notation in per mil (‰):

$$\delta(‰) = \left(\left(R_{sample}/R_{standard}\right) - 1\right)$$

Where R is $^{13}C/^{12}C$, D/H, or $^{18}O/^{16}O$. The δ values are reported relative to the standards VPDB for C isotopes and VSMOW for H and O isotopes. Routine isotopic measurements of in-house standards and samples have an overall precision (1-sigma standard deviation) of better than 0.1‰ for $\delta^{13}C$, 0.2 for $\delta^{18}O$ and 2.0‰ for δD.

2.5 Geochemical Modeling

The computer program PHREEQC Version 2.8 (Parkhurst and Appelo, 1999) was used to calculate the pCO_2 of the samples using the DIC concentrations and the corresponding pH and temperature.

3. Results

3.1 pH, alkalinity, DIC, $\delta^{13}C_{DIC}$ and TDS

The pH, alkalinity concentrations, DIC concentrations, $\delta^{13}C_{DIC}$ and the TDS concentrations are presented in Table 1. After 300 hours, the pH of the mixed $NaHCO_3$ sample increased by less than 0.5 units, while the pH of the unmixed $NaHCO_3$ remained nearly constant during the experiment (Fig. I-2a). The pH of the mixed and unmixed groundwater samples increased markedly by 1.5 to 2.0 units, respectively for the first 200 hours, followed by a slower rise of less than 0.5 units (Fig. I-2b). The pH of the mixed and unmixed lake samples increased steadily by 0.48 units after 150 hours (Fig. I-2c).

The alkalinity concentrations for the mixed $NaHCO_3$ stayed at ~1.55 mM/L for the first 124 hours followed by a steady increase to 4.23 mM/L (171%). The alkalinity concentrations for the unmixed $NaHCO_3$ also stayed at ~1.55 mM/L for first 144 hours before increasing steadily to 1.96 mM/L (18%) (Fig. I-2d). In contrast, the alkalinity concentrations of the mixed groundwater sample decreased markedly from 2.94 to 2.30 mM/L (22%) for the first 200 hours, after which, the alkalinity concentrations increased to 2.49 mM/L (336 hours) and remained nearly constant (Fig. I-2e). The alkalinity concentrations of the unmixed groundwater sample varied from 3.13 to 3.24 mM/L (within 4%) for the first 124 hours and then decreased continuously from 3.24 to 2.85 mM/L (12%) from 124 hours to the end of the experiment. The alkalinity concentrations of the mixed lake sample increased from 1.38 to 1.90 mM/L (38%) and that of the unmixed lake sample increased by 20% from 1.38 to 1.65 mM/L (Fig. I-2f).

The DIC concentrations for the mixed $NaHCO_3$ sample increased from 4.20 to 5.35 mM C/L for the first 484 hours before increasing steeply (147%) to 10.36 mM C/L (Fig. I-3a). Overall,

the DIC concentrations for the unmixed $NaHCO_3$ sample increased steadily by 25% from 4.13 to 5.15 mM C/L (25%). The DIC concentrations for the mixed groundwater sample decreased from 8.51 to 5.78 mM C/L (32%) for the first 96 hours, after which, the DIC concentrations increased slowly from 5.78 to 7.48 mM C/L (29%) between 96 and 624 hours (Fig. I-3b). There was a very rapid increase in the DIC concentration of the mixed groundwater sample after 624 hours, reaching 11.85 mM C/L, which is a 39% increase from the initial concentration and a 105% increase from the lowest concentration (5.78 mM C/L). The DIC concentrations of the unmixed groundwater sample decreased continuously throughout the experiment from 8.26 to 6.90 mM C/L, which is a decrease of 16% (Fig. I-3b). The DIC concentrations of the mixed lake samples increased from 3.78 to 5.14 mM C/L (36%) by 524 hours before decreasing slightly to 4.61 mM C/L (Fig. I-3c). The DIC concentrations of the unmixed lake sample increased steadily from 3.53 to 5.13 (45%) for the duration of the experiment (Fig. I-3c).

The $\delta^{13}C_{DIC}$ of the mixed $NaHCO_3$ samples were enriched rapidly from -19.1 to -9.4‰ (9.7‰) for the first 200 hours followed by a slower enrichment from -9.4‰ to -4.2‰ (5.3‰) from 200 to 500 hours, and leveled-off at ~-4‰ (Fig. I-3d). The unmixed $NaHCO_3$ sample showed a steady enrichment with a 6.7‰ shift in $\delta^{13}C_{DIC}$ from -19.7 to -13.0‰ (Fig. I-3d). The $\delta^{13}C_{DIC}$ of the mixed groundwater sample were enriched rapidly from -12.1 to -6.1‰ (6‰) for the first 250 hours followed by a slower enrichment from -6.2 to -3.4‰ (3‰) from ~250 to 624 hours and reached steady state at ~-3‰ (Fig. I-3e). The $\delta^{13}C_{DIC}$ of the unmixed groundwater sample were enriched from -11.1 to -4.1‰ (7‰) from start to end of the experiment (Fig. I-3e). The $\delta^{13}C_{DIC}$ of the mixed lake water samples were depleted from -4.0 to -5.3‰ (1.3‰) from the start to 237 hours and then enriched from -5.3 to -4.3‰ (1.0%) from 237 hours (Fig. I-3f). The

$\delta^{13}C_{DIC}$ of the unmixed lake samples were depleted from -4.1 to -4.6‰ (0.5‰) for the first 284 hours and then enriched from -4.6 to -3.2‰ (1.4‰) from 284 hours (Fig. I-3f).

The TDS increased steadily by 31% from 213 to 280 mg/L in the first 388 hours for the mixed $NaHCO_3$ sample (Fig. I-4a). After 388 hours, the TDS increased sharply, reaching 520 mg/L (144%). The TDS of the unmixed $NaHCO_3$ increased steadily by 26% from 216 to 271 mg/L (Fig. I-4a). The TDS of the mixed groundwater sample decreased by 14% from 511 mg/L to 441 mg/L for the first 121 hours, and then increased continuously to 801 mg/L (95%) from 121 hours (Fig. I-4b). The unmixed groundwater sample showed only a slight increase in the TDS from 506 to 520 mg/L (3%) from the start to the end of experiment (Fig. I-4b). The lake samples showed a slow but steady increase in TDS throughout, increasing from 242 to 388 mg/L (60%) for the mixed lake sample and from 241 to 303 mg/L (20%) for the unmixed lake sample (Fig. I-4c).

4. Discussion

4.1 Chemical and isotopic behavior of DIC in solutions exposed to the atmosphere

The concentrations of DIC in the mixed and unmixed $NaHCO_3$ and groundwater samples exposed to the atmosphere exhibit different temporal chemical behaviors (Figs. I-3a and b). Between 0 to ~300 hours, the DIC concentrations for the mixed $NaHCO_3$ only marginally increased while that of the mixed groundwater decreased. After 300 hours, the DIC concentrations of both the $NaHCO_3$ and groundwater samples increased continuously to the end of the experiment. Despite the initial differences in the behavior of the DIC, the $\delta^{13}C_{DIC}$ for the

mixed $NaHCO_3$ (Fig. I-3d) and mixed groundwater (Fig. I-3e) samples exhibit similar behaviors, where the $\delta^{13}C_{DIC}$ were enriched and reached steady state by the end of the experiment. In contrast, the DIC concentrations of the unmixed $NaHCO_3$ increased continuously (Fig. I-3a) while that of the unmixed groundwater continuously decreased throughout the experiment (Fig. I-3b). Although the DIC concentrations of the unmixed $NaHCO_3$ and groundwater samples show different behaviors, their $\delta^{13}C_{DIC}$ were enriched continuously throughout the experiment without reaching steady state. The temporal behavior of the DIC and $\delta^{13}C_{DIC}$ of the lake samples are significantly different from the $NaHCO_3$ and groundwater samples. The DIC concentrations of the lake samples showed a slight continuous increase (Fig. I-3c), while the $\delta^{13}C_{DIC}$ exhibits a slight decrease early in the experiment (Fig. I-3f). Unlike the marked differences exhibited in the DIC and $\delta^{13}C_{DIC}$ behavior between the mixed and unmixed $NaHCO_3$ and groundwater samples, mixing does not appear to be relevant in the lake samples, as the behavior of DIC and the $\delta^{13}C_{DIC}$ are similar. Since the $NaHCO_3$, groundwater and lake samples were all exposed to the laboratory atmosphere, we attribute their different chemical and isotopic behavior to differences in their initial carbonate and isotopic equilibrium states. We argue that by evaluating the behavior of DIC relative to the $\delta^{13}C_{DIC}$, we can gain greater insights into how and why the different samples exhibit different chemical and isotopic behavior.

4.2 Conceptual models of the chemical and isotopic behavior of DIC in solutions interacting with atmospheric $CO_{2(g)}$

We describe conceptual models that explain the behavior of DIC and $\delta^{13}C_{DIC}$ in solutions that undergo chemical and isotopic alteration during the interaction with atmospheric $CO_{2(g)}$ (Fig. I-5). In the panels of Figure I-5, the initial DIC concentration and $\delta^{13}C_{DIC}$ is represented by the

filled squares. The temporal direction of evolution of the samples DIC is shown by small solid arrows while the temporal direction of the evolution of the $\delta^{13}C_{DIC}$ is shown by small dashed arrows. The overall evolution of the samples from both the DIC and $\delta^{13}C_{DIC}$ changes is shown by solid dots and the direction of evolution by the large solid arrows. A solution exposed to atmospheric $CO_{2(g)}$ can either lose $CO_{2(g)}$ to the atmosphere or gain $CO_{2(g)}$ from the atmosphere depending on the pCO_2 in the solution relative to that of the atmosphere (Stumm and Morgan, 1981). If the solution loses $CO_{2(g)}$, then the ratio of the DIC concentration at any time to that at the start (C_t/C_0) will move to the left on the DIC axis or to the right on the DIC axis if the solution gains DIC. If the DIC transformation results in carbon isotopic enrichment or depletion, the isotopic composition will move up or down on the $\delta^{13}C_{DIC}$ axis, respectively.

4.2.1 Model 1

This model represents a solution that loses $CO_{2(g)}$ to the atmosphere (Fig. I-5a) and it is likely to occur only in the early-time of the experiments. The $^{12}CO_{2(g)}$ is preferentially lost, leaving the residual DIC in solution enriched in the heavy $^{13}CO_{2(g)}$ (Mook et al., 1974; Szaran, 1998; Zhang et al., 1995). The loss of $CO_{2(g)}$ will shift the DIC concentration to the left on the DIC axis and enrichment during $CO_{2(g)}$ loss will shift up on the $\delta^{13}C_{DIC}$ axis. The overall evolution shows a negative slope in the DIC- $\delta^{13}C_{DIC}$ space.

4.2.2 Model 2

This model depicts a scenario where the DIC is in isotopic disequilibrium with atmospheric $CO_{2(g)}$. The DIC increases by evaporation and the $\delta^{13}C_{DIC}$ increases by carbon equilibration

during carbon exchange between DIC and atmospheric $CO_{2(g)}$. The increasing DIC concentration and the enrichment in $\delta^{13}C_{DIC}$ show an overall evolution with a positive slope in the DIC-$\delta^{13}C_{DIC}$ space (Fig. I-5b).

4.2.3 Model 3

If the pCO_2 of the solution is in equilibrium with atmospheric $CO_{2(g)}$, then the DIC concentration in solution will remain constant if the systems is not dominated by processes that concentrate carbon such as evaporation and the C_t/C_0 does not change (Fig. I-5c). If the $\delta^{13}C_{DIC}$ is lower than the isotopic value for a solution that is in isotopic equilibrium with atmospheric $CO_{2(g)}$, then isotopic exchange of carbon between DIC and the $CO_{2(g)}$ will result in enrichment of the $\delta^{13}C_{DIC}$. The evolution displays a vertical trend in the DIC-$\delta^{13}C_{DIC}$ space.

4.2.4 Model 4

In a situation in which the DIC concentrations increase from $CO_{2(g)}$ addition and the $\delta^{13}C$ of the residual DIC in solution does not change (Figure I-5d), the isotopic composition of the $CO_{2(g)}$ is such that isotopic fractionation of the carbon during $CO_{2(g)}$ dissolution and formation of DIC is similar to the $\delta^{13}C$ of the initial DIC in solution. Alternatively, a solution that has attained carbon isotopic equilibrium with atmospheric $CO_{2(g)}$ probably after long time period of exposure to atmospheric $CO_{2(g)}$ and has its DIC concentration continuously increased, say by evaporation, will exhibit a behavior shown by model 4 (Fig. I-5d). The evolution displays a horizontal trend in the DIC-$\delta^{13}C_{DIC}$ space.

4.2.5 Model 5

In natural waters interaction with $CO_{2(g)}$, an increase in DIC can result in a depletion in the $\delta^{13}C$ as seen in Figure I-5e. For this to happen, the pCO_2 of the atmosphere has to be higher than that of the solution. During the dissolution of $CO_{2(g)}$ the $^{12}CO_{2(g)}$ is preferentially incorporated in the liquid phase (e.g., Clark and Fritz, 1977). Similarly for solutions with high pH, $CO_{2(g)}$ invasion into the solution is such that ^{12}C is preferentially incorporated in solution (Usdowski and Hoefs, 1990) which will increase the DIC concentration and deplete $\delta^{13}C_{DIC}$ (Fig. I-5e). In both instances, the $\delta^{13}C_{DIC}$ becomes progressively negative with $CO_{2(g)}$ invasion and dissolution, and the evolution displays a negative slope in the DIC-$\delta^{13}C_{DIC}$ space.

4.2.6 Combination of different evolutionary pathways for DIC-$\delta^{13}C_{DIC}$ evolution

The conceptual DIC-$\delta^{13}C_{DIC}$ models presented in Figure I-5 describe the DIC-$\delta^{13}C_{DIC}$ evolution controlled by a single process that controls the DIC concentrations and the $\delta^{13}C_{DIC}$. If a solution evolves sequentially by different processes that follow different DIC-$\delta^{13}C_{DIC}$ pathways (e.g., $CO_{2(g)}$ loss followed by $CO_{2(g)}$ gain), then it is possible to track multiple evolutionary pathways by combining the different conceptual models as appropriate.

4.3 Chemical and isotopic behavior of DIC in the $NaHCO_3$, groundwater and lake water samples exposed to the atmosphere

To assess the DIC and $\delta^{13}C_{DIC}$ evolution of the $NaHCO_3$, groundwater and lake samples in this study, we use a combination of the conceptual DIC-$\delta^{13}C_{DIC}$ models presented in Figure I-5.

The relationships between C_t/C_0 vs. $\delta^{13}C_{DIC}$ for $NaHCO_3$, groundwater and lake samples are shown in Figure I-6. We have drawn polygons to enclose and label the different data groups on each of the panels which undergo DIC-$\delta^{13}C_{DIC}$ evolution that can be described by one or more of the five models presented. The large solid arrows point to the direction of the temporal evolution. We also present the least squares regression equation of C_t/C_0 vs. $\delta^{13}C_{DIC}$ and their r^2 values for the DIC-$\delta^{13}C_{DIC}$ evolution.

4.3.1 $NaHCO_3$ samples

The mixed $NaHCO_3$ sample is described initially by model 3 (open diamonds; Fig. I-6a) which has no slope because of nearly constant DIC during the enrichment of $\delta^{13}C_{DIC}$. The enrichment of $\delta^{13}C_{DIC}$ results from isotopic exchange of carbon with atmospheric $CO_{2(g)}$. This evolution represents a solution with a DIC concentration that is near chemical equilibrium with atmospheric $CO_{2(g)}$ and a $\delta^{13}C_{DIC}$ that is far from isotopic equilibrium with atmospheric $CO_{2(g)}$. The initial evolution is followed by a different evolutionary pathway shown by the segment of data that is depicted by model 2 (filled squares; Fig. I-6a) and best described by a positive increase in the DIC concentrations accompanied by an increase in $\delta^{13}C_{DIC}$. In the mixed $NaHCO_3$ sample, the estimated log pCO_2 using PHREEQC modeling code ranged from $10^{-3.1}$ to $10^{-3.2}$ atm. for the duration of the experiment. This range in pCO_2 values are higher than atmospheric (log pCO_2 of $10^{-3.5}$ atm.; Fig. I-7a), thereby, eliminating atmospheric $CO_{2(g)}$ as the source of the added DIC. The log pCO_2 ($10^{-3.4}$ atm.) of the laboratory air was slightly higher than expected outdoors ($10^{-3.5}$ atm.). We also expected the pCO_2 of the laboratory air to change because of air handling in a nearly closed loop and variable building occupancy by people. Because the samples were exposed to the atmosphere at room temperature, we attribute the increase in the DIC

concentrations to evaporation. The effect of evaporation will decrease the amount of water in the sample which will cause an apparent increase in solute concentrations (e.g., Stiller et al., 1985; Akoko et al., 2013). Evaporation over time will cause enrichment in the heavier hydrogen (δD) and oxygen isotope ($\delta^{18}O$) of the water (e.g., Clark and Fritz, 1997). The temporal stage where $\delta^{13}C_{DIC}$ in the $NaHCO_3$ has reached steady state, but the DIC concentration continuously increases can be interpreted as a state in which the carbon in DIC is in isotopic equilibrium with carbon of the atmospheric $CO_{2(g)}$ as depicted by model 4 (open squares; Fig. I-6a). The continuous increase in solute concentration is observed in the DIC (Fig. I-3a) and TDS (Fig. I-4a) concentrations and the effect of evaporation is clearly demonstrated in a plot of TDS vs. δD which shows a log-normal relationship ($r^2 = 0.981$; Fig. I-8).

The unmixed $NaHCO_3$ samples initially show clustering of data between $\delta^{13}C_{DIC}$ values of -19.7‰ and -17.3‰ (open diamonds; Fig. I-6b) corresponding to the first 300 hours, which is followed by a behavior characterized by model 2 (filled squares; Fig. I-6b). Thus, the unmixed $NaHCO_3$ samples evolved chemically by an increase in DIC concentration from evaporation and isotopically by equilibration of carbon in the DIC with atmospheric $CO_{2(g)}$.

The main difference in the chemical and isotopic evolution of the mixed and unmixed samples is related to the effects of the solution agitation. Both the mixed and unmixed $NaHCO_3$ samples undergo evaporation and the difference in DIC concentration is caused by the extent of sample agitation and the resulting enhanced evaporation (Fig. I-8). The agitation of the $NaHCO_3$ sample caused a faster rate of carbon isotopic equilibration between the DIC and atmospheric $CO_{2(g)}$ (Fig. I-3d). When the DIC concentration increases were due mainly to evaporation (model 2; Fig I-6a and b), a positive slope of 13.5 for the mixed $NaHCO_3$ sample and 25.7 for the unmixed $NaHCO_3$ sample are controlled by the rate of evaporation.

4.3.2 Groundwater samples

The DIC concentration in the mixed groundwater decreased by 32% in the first 96 hours of the experiment (Fig. I-3b). This decrease in the DIC concentration is accompanied by enrichment of the $\delta^{13}C_{DIC}$ (Fig. I-3e). The least square regression of the relationship between C_t/C_0 vs. $\delta^{13}C_{DIC}$ ($r^2 = 0.90$) and the behavior of DIC and $\delta^{13}C_{DIC}$ of the mixed groundwater during this time is characterized by model 1 with a negative slope of -9.1 (filled circles; Fig I-6c). The continuous decrease in DIC concentrations is due to CO_2 outgassing whereby $^{12}CO_{2(g)}$ is preferentially lost from the sample. Because of the initially high log pCO_2 ($10^{-1.7}$ atm.; Fig. I-7b) in the sample, there was a unidirectional transfer of $CO_{2(g)}$ from sample to the laboratory air. This trend of enriching $\delta^{13}C_{DIC}$ from CO_2 outgassing is described by kinetic isotopic fractionation (Mills and Urey, 1940; Usdowski and Hoefs, 1990). The final $\delta^{13}C_{DIC}$ in the sample will depend on the cumulative effect of the kinetic fractionation during $CO_{2(g)}$ loss.

The trend of decreasing DIC concentrations for the first 96 hours, characterized by model 1, reverses to one in which the DIC concentrations increase with enriching $\delta^{13}C_{DIC}$ and is depicted by model 2 with a positive slope of 19.4 (filled squares; Fig. I-6c). There were no external input of DIC into the reactor containing the groundwater sample, and the log pCO_2 ($10^{-2.9}$ to $10^{-3.4}$ atm.) of this time segment was still higher than atmospheric (log $pCO_2 > 10^{-3.5}$ atm.; Fig. I-7b). Therefore, the apparent increase in the DIC concentrations can be attributed to evaporation. The enrichment in the $\delta^{13}C_{DIC}$ is from carbon exchange (isotopic equilibration) between the carbon in DIC and atmospheric $CO_{2(g)}$ similar to the $NaHCO_3$ solutions (model 2; Figs. I-6a and b). Once isotopic equilibration of carbon between the DIC and the $CO_{2(g)}$ in the laboratory air was achieved, further evaporative concentration increased the DIC concentrations but did not result in an enrichment in the $\delta^{13}C_{DIC}$ shown by model 4 (open squares; Fig. I-6c).

The results for the unmixed groundwater are drastically different from the mixed groundwater sample. During the entire experiment of 980 hours, the unmixed groundwater lost about 16% of its DIC (Fig. 3b) with a corresponding enrichment in the $\delta^{13}C_{DIC}$ of about 7‰ (Fig. I-3e). The relationship between C_t/C_0 and $\delta^{13}C_{DIC}$ suggest continuous loss of DIC from the sample (filled circles; Fig I-6d). The least square regression of C_t/C_0 vs. $\delta^{13}C_{DIC}$ can be modeled as a single evolutionary behavior described by model 1 (filled circles; Fig. I-6d; $r^2 = 0.87$) in which the ^{12}C of the DIC is preferentially lost as $CO_{2(g)}$. In this case, the carbon isotopic fractionation is kinetic.

The behavior of the mixed groundwater characterized by model 1 has a negative slope of -9.1, while that of the unmixed groundwater is -40.8. We suggest that the difference in the slopes is due to enhancement of the evaporation and kinetic isotopic effect by agitation, with the slope controlled by the water and $^{12}CO_2$ loss rate.

4.3.3 Lake samples

The lake samples showed small but continuous increases in DIC concentrations in the first 400 hours (Fig. I-3b). This is accompanied by a continuous negative shift in the $\delta^{13}C_{DIC}$ (0.8‰) during this time (Fig. I-3f). The C_t/C_0 vs. $\delta^{13}C_{DIC}$ relationship should be described by model 5 (Fig. I-6e). Attempts to fit least squares regression equations resulted in negative slopes of -2.68 and -0.93 and poor correlation coefficients for the mixed ($r^2 = 0.2$) and unmixed ($r^2 = 0.1$) lake samples, respectively. The mixed and unmixed lake samples show a slow decrease in the pCO_2 over this time interval, which become nearly steady at a pCO_2 of $10^{-3.2}$ and ~$10^{-3.5}$ after 408 hours for the mixed and unmixed samples, respectively (Fig. I-7c). Because the pCO_2 in the lake samples are above atmospheric and the pH is below 9 in the first 400 hours, the negative shift in

the $\delta^{13}C_{DIC}$ cannot be explained by dissolution of $CO_{2(g)}$. In these experiments, we assume minimal biotic effects for the natural water samples. Thus, we speculate that respiration of organic carbon in the lake samples (e.g., Richey et al., 1998) could be responsible for the systematic negative shift in the $\delta^{13}C_{DIC}$ (e.g., Boutton, 1991) for the first 400 hours.

The results of the mixed $NaHCO_3$ and groundwater samples suggest that carbon isotopic equilibrium between DIC and atmospheric $CO_{2(g)}$ occurred around a $\delta^{13}C_{DIC}$ of ~4 $\pm$ 1‰ (Fig. I-3d and 3f). We observed that the $\delta^{13}C_{DIC}$ for the lake samples are within 1‰ of the equilibrium $\delta^{13}C$ value of DIC of ~4‰ observed for the $NaHCO_3$ and groundwater samples and suggest that the lake samples were near the chemical and isotopic equilibrium with atmospheric $CO_{2(g)}$ at the start of the experiments. The $\delta^{13}C$ of $CO_{2(g)}$ of the laboratory air to which the samples were exposed averaged -11.4 ± 1.5‰ (n=3; Appendix I). This $\delta^{13}C$ value for $CO_{2(g)}$ in the laboratory air could be affected by the $CO_{2(g)}$ from human breath with a $\delta^{13}C$ value of -22.3 ± 0.2‰ (Hagit and Eiler, 2006). Using the $\delta^{13}C$ value for $CO_{2(g)}$ in the laboratory air of -11.4 ± 1.5‰ and the temperature measured in samples over time, we estimate an equilibrium isotopic-enrichment of DIC of 8.5‰ to 7.9‰ ± 0.03 for samples in equilibrium with $CO_{2(g)}$ in the laboratory air (Mook et al., 1974; Clark and Fritz, 1977). We estimate that the $\delta^{13}C_{DIC}$ of samples in isotopic equilibrium with laboratory $CO_{2(g)}$ should range from -3.5 to -2.9‰. The assumed equilibrium value for the test samples of -4 $\pm$ 1 is higher but near the upper range of this estimate.

Additionally, evidence that the lake samples were chemically near equilibrium with respect to atmospheric $CO_{2(g)}$ is derived from the estimated log pCO_2 ($10^{-3.0}$ atm.) of the samples (Fig. I-7c). The lake samples did not show a clear trend in C_t/C_0 vs. $\delta^{13}C_{DIC}$ (Fig. 6f) which allows us to suggest that the lake samples were close to both chemical and carbon isotopic equilibrium with the $CO_{2(g)}$ of the laboratory air. The fluctuations observed in the DIC concentrations and the

$\delta^{13}C_{DIC}$ after 400 hrs (Fig. I-3f) could be due to variations in the concentrations and isotopic composition associated with anthropogenic perturbation of the $CO_{2(g)}$ in air within the laboratory.

4.4 Application of models to field scenarios

The DIC-$\delta^{13}C_{DIC}$ models generated from the results of our laboratory study were applied to field settings. Gray et al. (2011) studied carbon cycling in a floodplain ecosystem of the Hawdon Valley in New Zealand and showed from field experiments that outgassing of $CO_{2(g)}$ was the main process controlling carbon cycling in the water column. Their results showed that DIC in the water column originated from a groundwater source which was characterized by high initial pCO_2 upstream that decreased in the downstream direction. The downstream decrease in the DIC concentrations was accompanied by enrichment in the $\delta^{13}C_{DIC}$. To confirm $CO_{2(g)}$ outgassing as the main control of carbon cycling in the river, they exposed stream samples to the atmosphere in the laboratory for 20 hours and observed outgassing of $CO_{2(g)}$ accompanied by $\delta^{13}C_{DIC}$ enrichment. Gray et al. (2011) suggested that in-stream respiration and photosynthetic activities in the first 1,296 m of the stream was minor, and that carbon cycling was dominated by $CO_{2(g)}$ outgassing to the atmosphere. We assign the uppermost stream station the concentration of C_0 and subsequent downstream stations the DIC concentration C_t. When we plot the C_t/C_0 vs. $\delta^{13}C_{DIC}$ for the field data (Fig. I-9a) with an overall evolutionary direction shown by the arrow, the data can be explained by our model 1 (Fig. I-5a). The dominance of $CO_{2(g)}$ outgassing is consistent with the directional change in the DIC concentration. We therefore explain the $\delta^{13}C_{DIC}$ enrichment as a result of kinetic isotopic fractionation. Our interpretation is consistent with that of Gray et al. (2011) showing that groundwater feeding the streams in the Hawdon Valley has

high DIC concentrations and hence higher pCO_2 and that even though the streams flow in a highly vegetative floodplain, surface water DIC-atmospheric $CO_{2(g)}$ interaction surpasses the effects of organic matter respiration and photosynthesis in the water-column.

Doctor et al. (2008) sampled a headwater stream in the Sleepers River Research watershed during the summer months (June and July, 2004) after the growing season had begun and identified three distinct inflow seeps that were sampled downstream during the month of June. The seeps generally showed similar DIC concentrations to the stream but lower isotopic values due to a greater proportion of soil $CO_{2(g)}$ in the DIC. The stream DIC concentration in June decreased downstream as groundwater additions were low. The $\delta^{13}C_{DIC}$ was continuously enriched downstream. Since the groundwater additions were low and the DIC concentrations decreased downstream with enrichment in $\delta^{13}C_{DIC}$ during the month of June, the stream is therefore losing its DIC due to $CO_{2(g)}$ outgassing. The trend observed in the June sampling was also reflected during the much drier month of July. Plots of C_t/C_0 vs. $\delta^{13}C_{DIC}$ for the months of June (Fig. I-9b) and July (Fig. I-9c) with an overall DIC evolutionary direction indicated by the arrows are characterized by negative slopes and can be explained by our model 1 (Fig. I-5a). The results of the work by Doctor et al. (2008) is applicable to our model 1 since the dominant process controlling carbon cycling is stream water DIC-atmospheric $CO_{2(g)}$ interaction.

We present data from work performed in the Okavango Delta in semi-arid Botswana. The Okavango River forms a meandering and distributary system that flow for over 400 km in a pristine wetland developed on a large (>22,000 km^2) alluvial fan (Okavango Delta) (e.g., McCarthy and Ellery 1992). The hydrology of the Okavango River and distributaries is controlled by an annual flood pulse that inundates the floodplains and the wetlands and travels across the Delta in 4-6 months (Wilson and Dincer 1976; Gieske 1997). Groundwater discharge

to the river and distributaries is absent in this river system. The effect of long hydraulic residence time, variable hydrologic interaction between river-floodplain-wetland and evapotranspiration on carbon cycling has been previously reported by Akoko et al. (2013). Akoko et al. (2013) suggested that the increasing DIC concentration downriver is mostly due to evapo-concentration from transpiration and evaporation with increased transit time. They also suggest from the $\delta^{13}C_{DIC}$ enrichment downriver that river water atmospheric interaction was predominant over in-stream processes such as organic matter respiration and photosynthesis. We collected water samples from several stations across the Okavango Delta during the flood season of 2011 and analyzed them for DIC concentrations and $\delta^{13}C_{DIC}$ similar to the Akoko et al (2013) study. When we plot the C_t/C_0 vs. $\delta^{13}C_{DIC}$ (Fig. I-9d), the trend in increasing DIC concentrations with $\delta^{13}C_{DIC}$ enrichment as indicated by the arrow corresponds to our model 2 (Fig. I-5b). Similar to the interpretations of Akoko et al. (2013), we explain the increasing DIC concentrations to evapo-concentration by evaporation and transpiration. $\delta^{13}C_{DIC}$ enrichment based on our model 2 is controlled by carbon isotopic exchange between river water DIC and atmospheric $CO_{2(g)}$, and is consistent with the Akoko et al. (2013) interpretation that water column processes such as photosynthesis and respiration do not dominate carbon cycling in this semi-arid river system.

4.4.1 Caution on model application

Although we show that DIC-$\delta^{13}C_{DIC}$ evolution in surface waters dominated by DIC-atmospheric $CO_{2(g)}$ can be explained from graphical data, there may be situations where plots of C_t/C_0 vs. $\delta^{13}C_{DIC}$ may be wrongly interpreted. We use studies by Telmer and Veizer (1999) in the Ottawa River, Canada and by Doctor et al. (2008) in headwater stream in the Sleepers River Research watershed to illustrate this point. Telmer and Veizer (1999) investigated carbon cycling

in the 1160 km Ottawa River and tributaries. The results of this study showed that DIC concentration increased from the headwater to the mouth. There was an overall continuous enrichment of the $\delta^{13}C_{DIC}$ from the head waters dominated by silicate rocks to the mouth of the river where the lower catchment was carbonate rocks. Telmer and Veizer (1999) suggest that the increasing DIC concentrations result from carbonate weathering and that in-river respiration and photosynthesis were not significant processes that contribute to the cycling of DIC in the river. When we plot C_t/C_0 vs. $\delta^{13}C_{DIC}$ (Fig. I-10a), the data could be interpreted using model 2 (Fig. I-5b), owing to the positive relationship between C_t/C_0 and $\delta^{13}C_{DIC}$ for the DIC evolutionary direction indicated by the arrow. However, the continuous increase in the DIC (C_t/C_0) is the result of the discharge of increasing amounts of carbonate-rich groundwater to the river from the lower carbonate catchment. The increasing groundwater discharge to the river adds DIC with heavier $\delta^{13}C_{DIC}$ causing the positive relationship between C_t/C_0 and $\delta^{13}C_{DIC}$.

Doctor et al. (2008) sampled the same stream in the Sleepers River Research watershed described in section 4.4 on two separate dates in the spring of 2008; an earlier sampling (April 09) taken prior to an increase in the flux of snowmelt into the stream which occurred on April 17. Both data sets showed an increase in the DIC (C_t/C_0) concentration downstream. When we plot C_t/C_0 vs. $\delta^{13}C_{DIC}$ (Fig. I-10b), the data could be interpreted using model 5 based on the negative relationship between C_t/C_0 and $\delta^{13}C_{DIC}$ because the overall evolutionary behavior indicated by the arrow is described by DIC increase with depletion in $\delta^{13}C_{DIC}$. The increasing DIC concentration downstream was as a result of groundwater seepage into the stream. The excess pCO_2 ($epCO_2$) defined as the ratio of the pCO_2 of the sample calculated from the field pH and temperature to that of the atmosphere (Neal, 1988) was plotted against the $\delta^{13}C_{DIC}$ i.e., $epCO_2$ vs. $\delta^{13}C_{DIC}$ (Fig. I-10c). The relationship shows decreasing $epCO_2$ with enrichment in

$\delta^{13}C_{DIC}$ as indicated by the arrow, suggesting that $CO_{2(g)}$ is outgassing from the stream. The enrichment in the $\delta^{13}C_{DIC}$ that accompanies the increasing DIC downstream was due to $CO_{2(g)}$ loss as evidenced in the plots of $epCO_2$ vs. $\delta^{13}C_{DIC}$. Thus, the plots of the C_t/C_0 vs. $\delta^{13}C_{DIC}$ and $epCO_2$ vs. $\delta^{13}C_{DIC}$ show that two processes ($CO_{2(g)}$ loss and DIC addition by groundwater seepage) are occurring simultaneously to account for the change in the C_t/C_0 ratio, but the overall control on the isotopic composition is the fractionation due to $CO_{2(g)}$ loss from the stream surface. Thus, using our model 5 to interpret this relationship could be misleading. In catchments in humid environments, the relationship between C_t/C_0 and $\delta^{13}C_{DIC}$ may not necessarily indicate a surface water system dominated by surface water DIC-atmospheric $CO_{2(g)}$ interaction and to determine which process is dominant, a multi-tracer approach is useful for distinguishing between mixing of waters vs. atmospheric exchange.

5. Conclusions

The processes that control $CO_{2(g)}$ loss, $CO_{2(g)}$ gain and carbon exchange between DIC in surface waters and atmospheric $CO_{2(g)}$ is affected by multiple in-column processes (respiration, photosynthesis, photo-oxidation) and variable (short to long) residence time. This makes investigating the interaction of DIC to the point of chemical and isotopic equilibrium with atmospheric $CO_{2(g)}$ difficult. The continuum in the temporal behavior of DIC and $\square^{13}C_{DIC}$ in surface waters that interact with atmospheric $CO_{2(g)}$ is difficult to capture in natural experiments and was investigated in a laboratory setting. Time series sampling of artificial and natural samples exposed to atmospheric $CO_{2(g)}$ was performed to mimic samples in which (1) DIC concentrations were close to chemical equilibrium with atmospheric $CO_{2(g)}$ and $\delta^{13}C_{DIC}$ that was

far from isotopic equilibrium with atmospheric $CO_{2(g)}$, (2) DIC concentrations and the $\delta^{13}C_{DIC}$ were both far from chemical and isotopic equilibrium with atmospheric $CO_{2(g)}$ and (3) DIC concentrations and the $\delta^{13}C_{DIC}$ were near chemical and isotopic equilibrium with atmospheric $CO_{2(g)}$. These solutions allowed us to ascertain when only chemical or isotopic changes were occurring or when both chemical and isotopic changes were ongoing as the DIC in the water samples interacted with atmospheric $CO_{2(g)}$.

The results of the chemical and stable carbon isotopic analyses were modeled by combining one or more of the five DIC-$\delta^{13}C_{DIC}$ evolutionary pathways: (1) loss of $CO_{2(g)}$ to the atmosphere with enrichment in $\delta^{13}C_{DIC}$. The ratio of concentration at any time to that at the beginning (C_t/C_0) vs. $\delta^{13}C_{DIC}$ is characterized by a negative slope; (2) DIC gain from evaporative enrichment and exchange of carbon in DIC with the atmospheric $CO_{2(g)}$ to cause the $\delta^{13}C_{DIC}$ to increase. The C_t/C_0 vs. $\delta^{13}C_{DIC}$ has a positive slope; (3) no net gain or loss of DIC as carbon is exchanged between DIC and atmospheric $CO_{2(g)}$ which causes the $\delta^{13}C_{DIC}$ to increase. The C_t/C_0 vs. $\delta^{13}C_{DIC}$ shows no slope because of constant DIC concentrations along with increases in the $\delta^{13}C_{DIC}$; (4) increases in the DIC concentrations from evaporative enrichment accompanied by no change in the $\delta^{13}C_{DIC}$. The C_t/C_0 vs. $\delta^{13}C_{DIC}$ shows no slope because of the nearly steady state of the $\delta^{13}C_{DIC}$; (5) increases in the DIC concentrations accompanied by depletion in $\delta^{13}C_{DIC}$. The C_t/C_0 vs. $\delta^{13}C_{DIC}$ has a negative slope. In this study, the increase in DIC concentrations was due to respiration of organic carbon.

Our results show that mixing the solutions by agitation enhanced reaction rates. This agitation led to greater $CO_{2(g)}$ loss and carbon exchange between DIC and atmospheric $CO_{(2g)}$, thereby enriching the $\delta^{13}C_{DIC}$ to equilibrium isotopic values based on the isotopic value of the

$CO_{2(g)}$ in the laboratory atmosphere. In addition, agitation increased evaporative loss which caused an apparent increase in the DIC concentrations.

Models based on the DIC concentrations and $\delta^{13}C_{DIC}$ can be used to assess the temporary trajectory during carbon cycling in surface waters with variable residence time and are applicable in systems where the dominant carbon-cycling process is controlled by atmospheric $CO_{2(g)}$-surface water DIC interaction. We tested the models with field data and showed how changes in the DIC and the $\delta^{13}C_{DIC}$ can be explained in surface waters where the cycling of carbon is dominated by DIC-atmospheric $CO_{2(g)}$ interaction. However, the models developed in this study should not be applied to field scenarios in which the dominant carbon-cycling process is not controlled by surface water DIC-atmospheric $CO_{2(g)}$ interaction. These situations include those in which there is continuous supply or removal of DIC from the DIC pool in the water column due to rock-water interaction, photosynthesis and organic matter respiration activities or a continuous supply of DIC by recharging groundwater. In applying our models, one would want to investigate the DIC isotopic evolution as an indicator of DIC supply or removal, then cross-check the DIC data against data obtained from other tracers.

Acknowledgements

Partial funding for the work on the Okavango River Delta was provided by the US National Science Foundation (NSF grant # OISE-0927841) under the International Research Experience for Students (IRES) initiative. The University of Botswana provided logistical support for field sampling in the Okavango Delta and the government of Botswana (Ministry of Education) provided research permits for the Okavango Delta study. We thank D. Gray for providing us data

for the floodplain ecosystem of the Hawdon Valley in New Zealand and D. Doctor for provided us with data from the Sleepers River Research watershed. Laboratory assistance from E. Akoko, E. Guderian and N. Paizis is greatly appreciated. Critical reviews by S. Sharma and D. Doctor greatly improved this manuscript.

References

Ambrosetti, W., Barbanti, L., Sala, N., 2003. Residence time and physical processes in lakes. Journal of Limnology 62, 1-15.

Anderson, D.E., Striegel, R.G., Stannard, D.I., Michmerhuizen, M., 1999. Estimating lake-atmosphere CO_2 exchange. Limnology and Oceanography 44, 998-1001.

Atekwana, E.A., Krishnamurthy, R.V., 1998. Seasonal variations of dissolved inorganic carbon and $\delta^{13}C$ of surface waters: application of a modified gas evolution technique. Journal of Hydrology 205, 265-278.

Akoko, E., Atekwana, E.A., Cruse, A.M., Molwalefhe, L. Masamba, W.R.L., 2013. River-wetland interaction and carbon cycling in a semi-arid riverine system: The Okavango Delta, Botswana. Biogeochemistry. DOI 10.1007/s10533-012-9817-x

Basu, B.K., Pick, F.R., 1996. A large-scale comparison of factors influencing phytoplankton abundance in temperate rivers. Limnology and Oceanography 41, 1572-1577.

Boutton, T., 1991. Stable carbon isotope ratios of natural materials: II. Atmospheric, Terrestrial, Marine, Freshwater Environments. Academic Press, Inc., San Diego, California, 173-186.

Cartwright, I., 2010. The origins and behavior of carbon in a major semi-arid river, the Murray River, Australia, as constrained by carbon isotopes and hydrochemistry. Applied geochemistry 25, 1734-1745.

Clark, I.D., Fritz, P., 1997. Environmental Isotopes in Hydrogeology. CRC Press, 352 p.

Cole, J.J., Prairie, Y.T., Caraco, N.F., McDowell, W.H., Tranvik, L.J., Striegel, R.G., Duarte, C.M., Kortelainen, P., Downing, J.A., Middleburg, J.J., Melack, J., 2007. Plumbing the global carbon cycle: Integrating inland waters into the terrestrial carbon budget. Ecosystems 10, 171-184.

Dincer, T., Hutton L.G, Kupee, B.B.J., 1979. Study, using stableisotopes, of flow distribution, surface-groundwater relations and evapotranspiration in the Okavango Swamp, Botswana. Isotope Hydrology 1978, vol. 1. International Atomic Energy Agency, Vienna, pp 3–25

Doctor, H.D., Kendall, C., Sebestyen, S.D., Shanley, T.B., Ohte, N., Boyer, E.N., 2008. Carbon isotope fractionation of dissolved inorganic carbon (DIC) due to outgassing of carbon dioxide from a headwater stream. Hydrological Processes 22, 2410-2423.

Gray, D.P., Harding, J.S., Elberling, B., Horton, T., Clough, T.J., Winterbourn, M.J., 2011. Carbon cycling in floodplain ecosystems: Out-gassing and photosynthesis transmit soil $\delta^{13}C_{DIC}$ gradient through stream food webs. Ecosystems.

Emerson, S., 1975. Chemically enhanced carbon dioxide gas exchange in a eutrophic lake: a general model. Limnology and Oceanography 20, 743-753.

Gehre, M., Geilmann, H., Richter, J., Werner, R.A., Brand, W.A., 2004. Continuous flow $^{2}H/^{1}H$ and $^{18}O/^{16}O$ analysis of water samples with dual inlet precision. Rapid Communications in Mass Spectrometry 18, 2650-2660.

Hach Company, 1992. Water Analysis Handbook. Hach Company, Loveland, Co.

Hagit, P.A., Eiler, J.M., 2006. Abundance of mass 47 CO_2 in urban air, car exhaust, and human breath. Geochimica et Cosmochimica Acta 70, 1-12.

Hein, M., Sand-Jensen, K., 1997. CO_2 increases oceanic primary production. Nature 388, 526-527.

Houghton, R.A., Davidson, E.A., Woodwell, G.M., 1998. Missing sinks, feedbacks, and understanding the role of terrestrial ecosystems in the global carbon balance. Global Biogeochemical Cycles, 12, 25-34.

Ikeda, T., Tajika, E., 2002. Carbon cycling and climate change during the last glacial cycle inferred from isotope records using an ocean biogeochemical carbon cycle model. Global and Planetary Change 35, 131-141.

Jonsson, A., Karlsson, J.J., Jansson, M., 2003. Sources of carbon dioxide supersaturation in Clearwater and humic lakes in northern Sweden. Ecology 6, 224-235.

Lewis, W.K., Whitman, W.G., 1924. Principles of Gas Absorption. Industrial and Engineering Chemistry 16, 1215-1220.

McCarthy, T.S., Metcalfe, J., 1990. Chemical sedimentation in the semi-arid environment of the Okavango Delta, Botswana. Chemical Geology 89(1-2):157-178.

Mayorga, E., Aufdenkampe, A.K., Masiello, C.A., Krusche, A.V., Hedges, J.I., Quay, P.D., Richey, J.E., Brown, T.A., 2005. Young organic matter as a source of carbon dioxide outgassing from Amazonian rivers. Nature 436, 538-541.

Mills, A., Urey, H.C., 1940. The kinetics of isotope exchange between carbon dioxide, bicarbonate ion, carbonate ion, and water. Journal of American Chemistry Society 62, 1019-1026.

Mook, W.G., Bommerson, J.C., Staverman, W.H., 1974. Carbon isotope fractionation between dissolved bicarbonate and gaseous carbon dioxide. Earth and Planetary Science Letters 22, 169-176.

Neal, C., 1988. Determination of dissolved CO2 in upland streamwater. Journal of Hydrology 99: 127–142.

Parkhurst, D.L., Appelo, C.A.J., 1999. User's Guide to PHREEQC (Version 2.1)-A Computer Program for Speciation, Batch-Reactions, One-Dimensional Transport and Inverse Geochemical Calculations. U.S. Geological Survey, Water Resource Investigation Report, 99-4256.

Pawellek, F., Veizer, J., 1994. Carbon cycle in the upper Danube and its tributaries: $\delta^{13}C_{DIC}$ constraints. Isreal Journal of Earth Science 43, 187-194.

Quinn, F.H., 1992. Hydraulic residence times for the Laurentian Great Lakes. Journal of Great Lakes Research 18, 22-28.

Richey, J.E., Devol, A.H., Wofsy, S.C., Victoria, R., Ribeiro, M.N.G., 1988. Biogenic gases and the oxidation and reduction of carbon in Amazon River and floodplain waters. American Society of Limnology and Oceanography 33, 551-561.

Richey, J.E., Melack, J.M., Aufdenkampe, A.K., Ballester, V.M., Hess, L.L., 2002. Outgassing from Amazonian rivers and wetlands as a large tropical source of atmospheric carbon dioxide. Nature 416, 617-620.

Shin, W.J., Chung, G.S., Lee, D., Lee, K.S., 2011. Dissolved inorganic carbon export from carbonate and silicate catchments estimated from carbonate chemistry and $\delta^{13}C_{DIC}$. Hydrology and Earth System Sciences 15, 2551-2560.

Stiller, M., Rounick, J.S., Shasha, S., 1985. Extreme carbon-isotope enrichment in evaporating brines. Nature 316, 434-435.

Stumm, W., Morgan, J.J., 1981. Aquatic Chemistry: An Introduction Emphasizing Chemical Equilibria in Natural Waters, 2nd edition. Wiley Interscience: New York; 780 p.

Szaran, J., 1998. Carbon isotope fractionation between dissolved and gaseous carbon dioxide. Chemical Geology 150, 331-337.

Telmer, K., Veizer, J., 1999. Carbon fluxes, pCO2, and substrate weathering in a large northern river basin, Canada: carbon isotope perspectives. Chemical Geology 159, 61-86.

Tranvik, L.J., Downing, J.A., Cotner, J.B., et al., 2009. Lakes and reservoirs as regulators of carbon cycling and climate. American Society of Limnology and Oceanography 54, 2298-2314.

Usdowski, E., Hoefs, J., 1990. Kinetic $^{13}C/^{12}C$ and $^{18}O/^{16}O$ effects upon dissolution and outgassing of CO_2 in the system CO_2-H_2O. Chemical Geology: Isotope Geoscience Section, 80, 109-118.

Vogel, J.C., Grootes, P.M., Mook, W.G., 1970. Isotopic fractionation between gaseous and dissolved carbon dioxide. Zeitschrift fur Physik A (Atoms and Nuclei) 230, 225-238.

Vörösmarty, C.J., Fekete, B.M., Meybeck, M., Lammers, R., 2000. A simulated topological network representing the global system of rivers at 30-minute spatial resolution (STN-30). Global Biochemical Cycles 14, 599-621.

Wachniew, P., 2006. Isotopic composition of dissolved inorganic carbon in a large polluted river: the Vistula, Poland. Chemical Geology 233, 293-308.

Zeng, F-W., Masiello, C.A., 2011. Controls on the origin and cycling of riverine dissolved inorganic carbon in the Brazos River, Texas. Biogeochemistry 104, 275-291

Zhang, J., Quay, P.D., Wilbur, D.O., 1995. Carbon isotope fractionation during gas–water exchange and dissolution of CO_2. Geochimica et Cosmochimica Acta 59, 107-114.

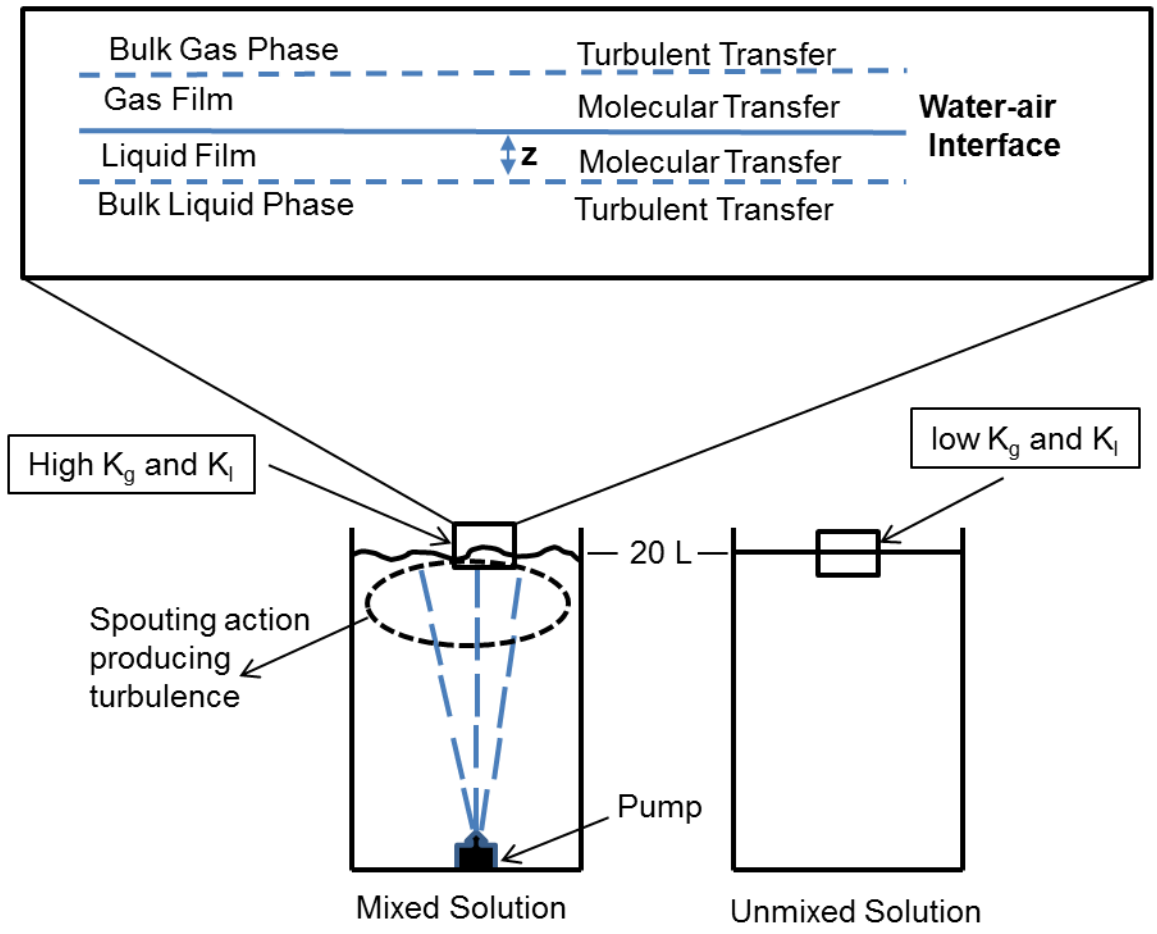

Figure I- 2. Schematic showing the arrangement of the mixed and unmixed samples in which maximizing and minimizing z could have an effect on the CO_2 transfer rate. Mixing was done by an aquarium pump by circulating water at a flow rate of ~ 10 l/min. The expanded section in the mixed solution shows the different gas and liquid phases at the gas-liquid interface. [K_g and K_l are the transfer coefficients or exchange constants (cm/sec) of the $CO_{2(g)}$ molecules across the gas film and liquid films respectively].

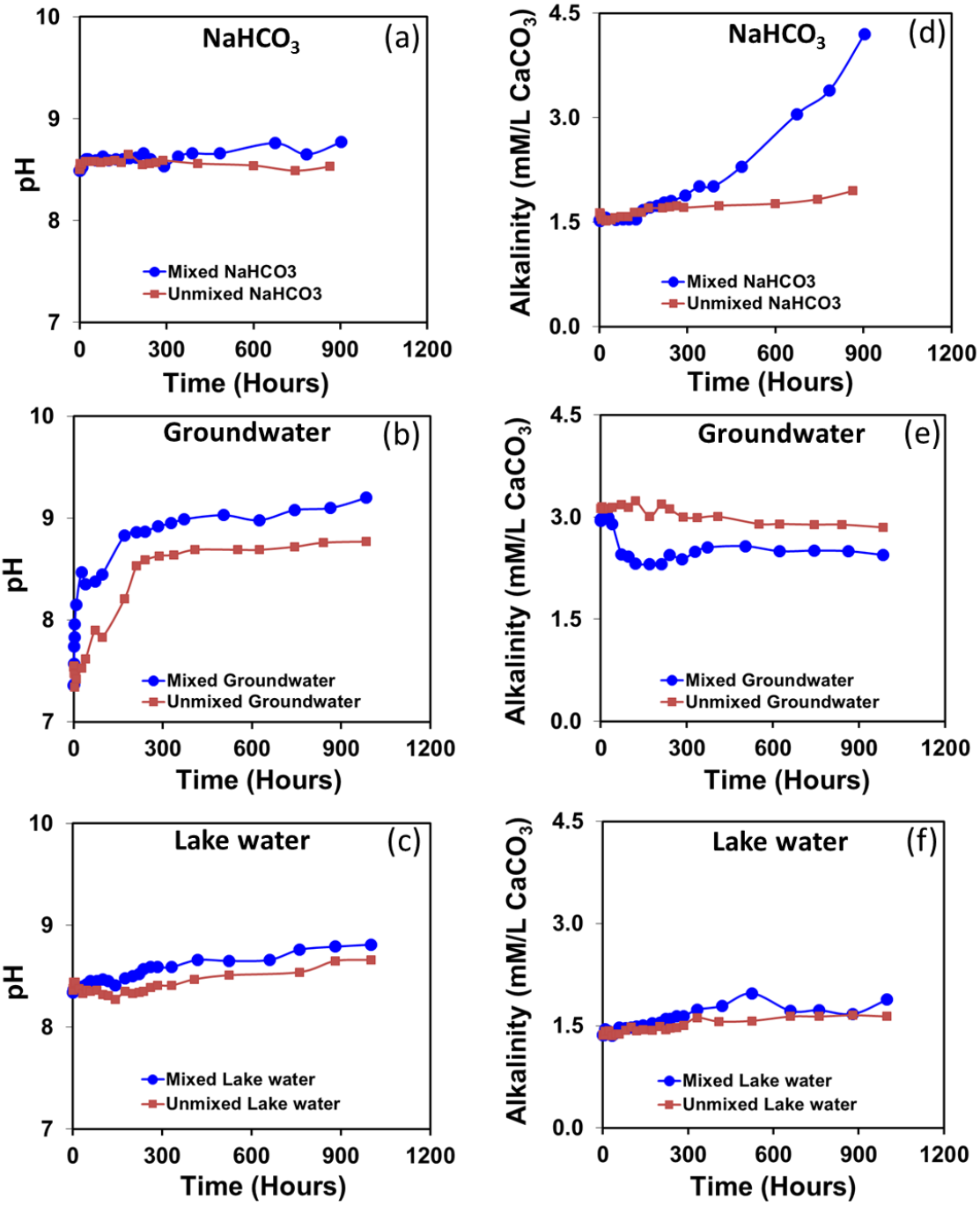

Figure 3. Temporal plots of dissolved inorganic carbon (DIC) concentrations and the stable carbon isotope composition of dissolved inorganic carbon ($\delta^{13}C_{DIC}$) for $NaHCO_3$ (a and d), groundwater (b and e) and lake water (c and f) samples exposed to the atmosphere in a laboratory setting.

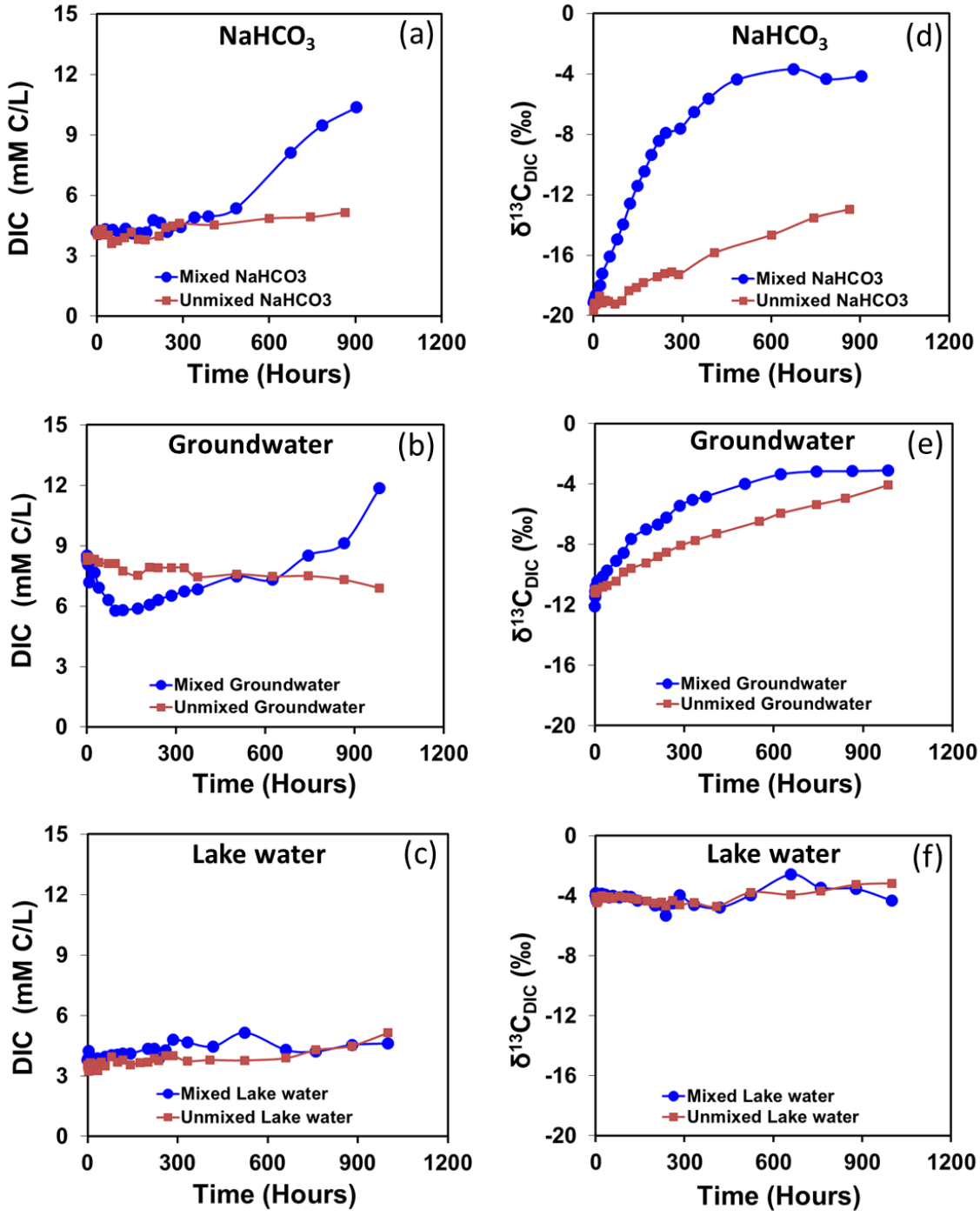

Figure I- 3. Temporal plots of dissolved inorganic carbon (DIC) concentrations and the stable carbon isotope composition of dissolved inorganic carbon ($\delta^{13}C_{DIC}$) for $NaHCO_3$ (a and d), groundwater (b and e) and lake water (c and f) samples exposed to the atmosphere in a laboratory setting.

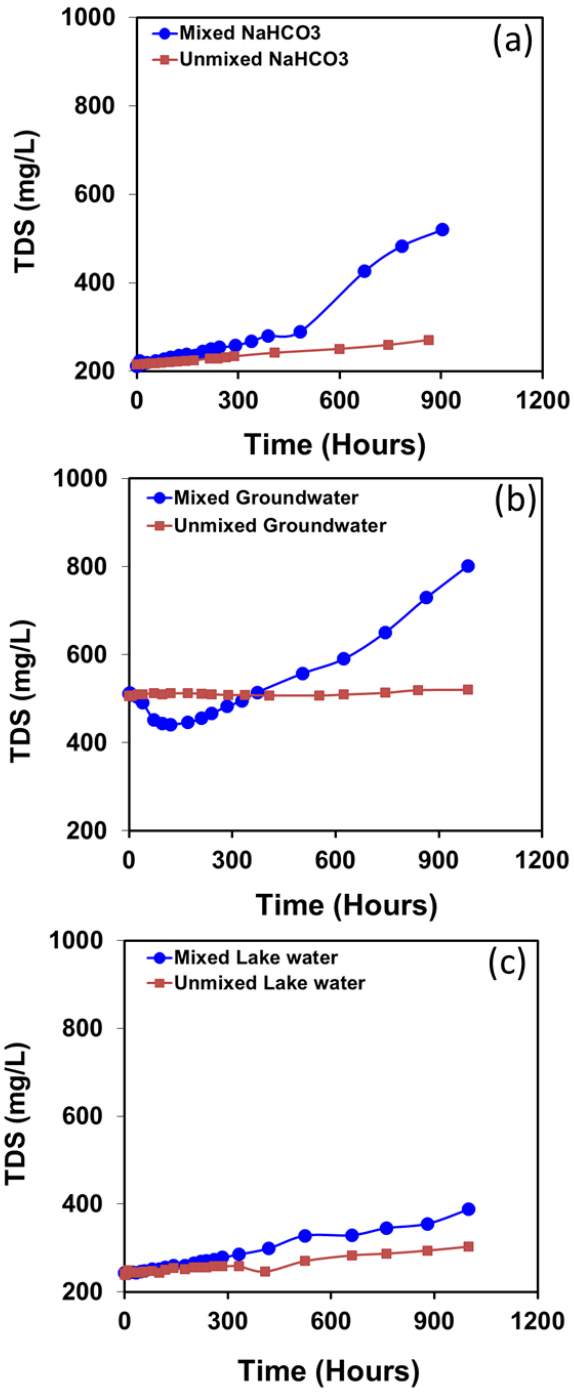

Figure I- 4. Temporal plots of total dissolved solids (TDS) for $NaHCO_3$ (a), groundwater (b) and lake water (c) samples exposed to the atmosphere in a laboratory setting.

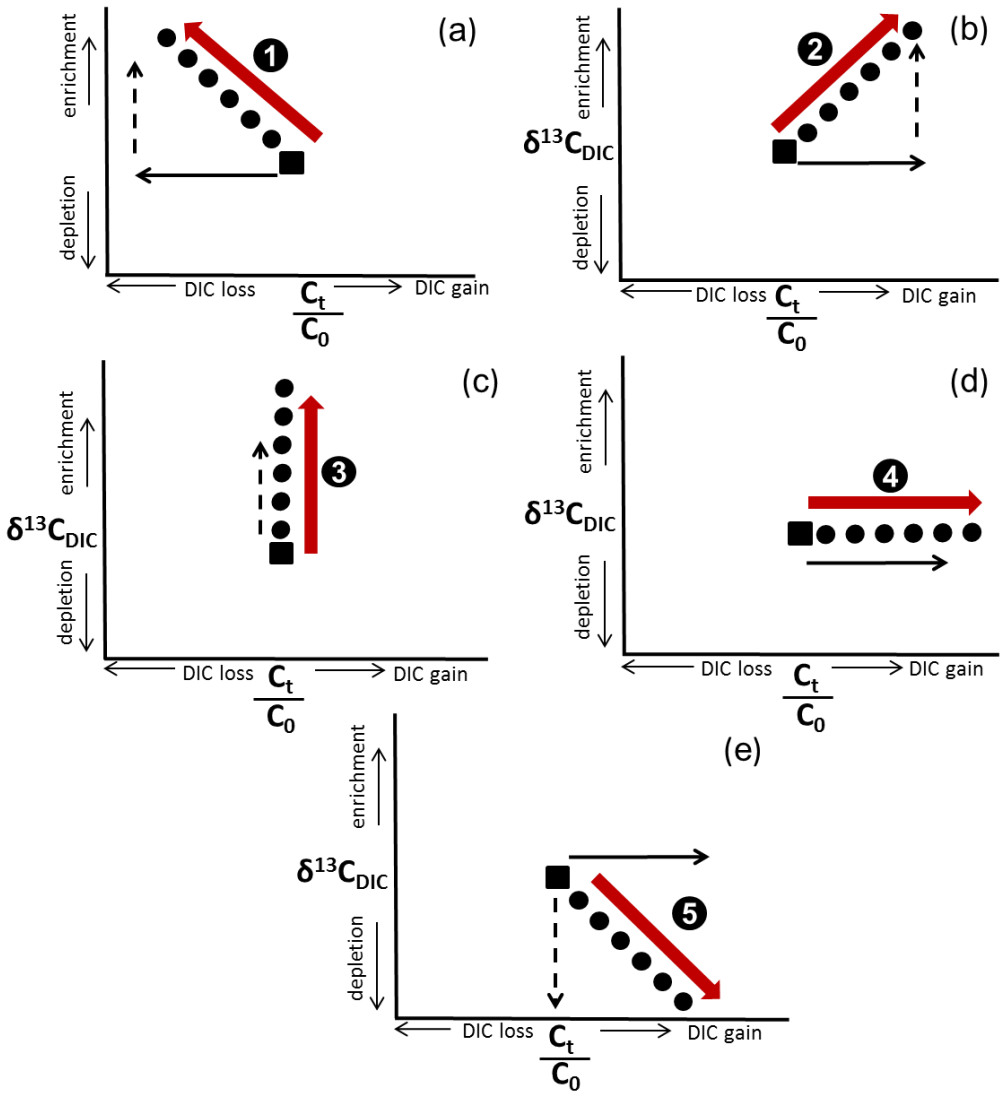

Figure I- 5. Conceptual models showing changes in the dissolved inorganic carbon (DIC) concentration and the stable carbon isotope composition of dissolved inorganic carbon ($\delta^{13}C_{DIC}$) for solutions interacting with atmospheric $CO_{2(g)}$. (a) Model 1 characterizes a decrease in DIC concentrations and an increase in the $\delta^{13}C_{DIC}$, (b) Model 2 characterizes an increase in DIC concentrations with an increase in the $\delta^{13}C_{DIC}$, (c) Model 3 characterizes no change in the DIC concentration but increase in $\delta^{13}C_{DIC}$, (d) Model 4 characterizes an increase in the DIC concentrations with no change in the $\delta^{13}C_{DIC}$, and (e) Model 5 characterizes an increase in DIC concentrations and a decrease in the $\delta^{13}C_{DIC}$. Initial concentration is represented by filled squares; temporal direction of evolution of DIC is shown by small solid arrows and temporal direction of evolution of $\delta^{13}C_{DIC}$ is shown by small dashed arrows. Overall evolution of both the samples DIC and $\delta^{13}C_{DIC}$ is shown by solid dots and the direction of evolution by the large solid arrows.

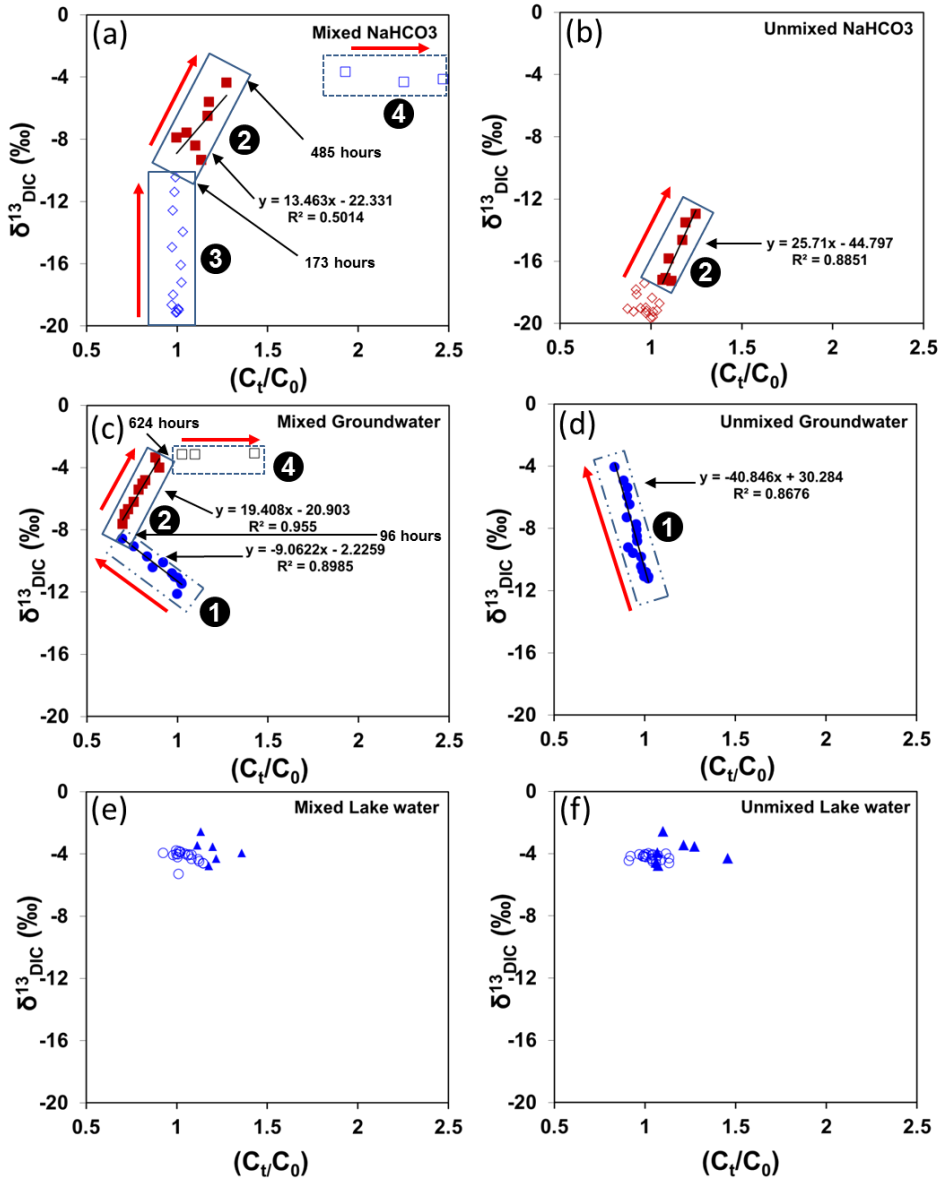

Figure I- 6. Change in the ratio of the concentration at any time (C_t) to the initial concentration (C_0) vs. the stable carbon isotope composition of dissolved inorganic carbon ($\delta^{13}C_{DIC}$) for $NaHCO_3$ (a and b), groundwater (c and d) and lake water (e and f) samples exposed to the atmosphere in a laboratory setting. Polygons and circles around select data delineate the models (see Fig. 5) that fit that time segment of the sample evolution. The time that each sample switches to a different model is noted.

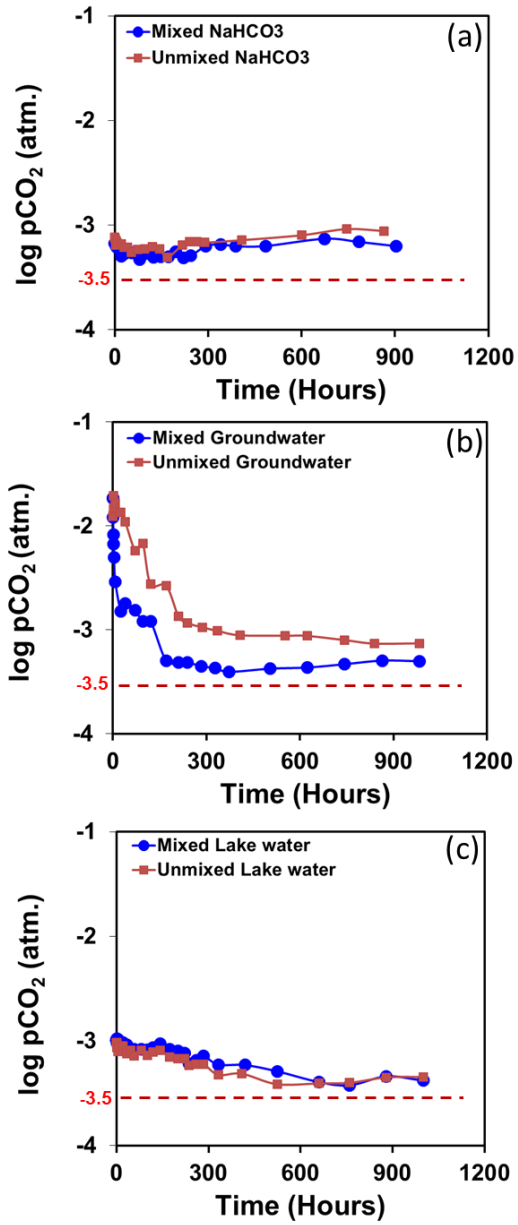

Figure I- 7. Temporal plots of the partial pressure of $CO_{2(g)}$ (pCO_2) for $NaHCO_3$ (a), groundwater (b) and lake water (c) samples exposed to the atmosphere in a laboratory setting. The dashed lines represent an atmospheric pCO_2 value of $10^{-3.5}$ atmosphere (the accepted average atmospheric pCO_2).

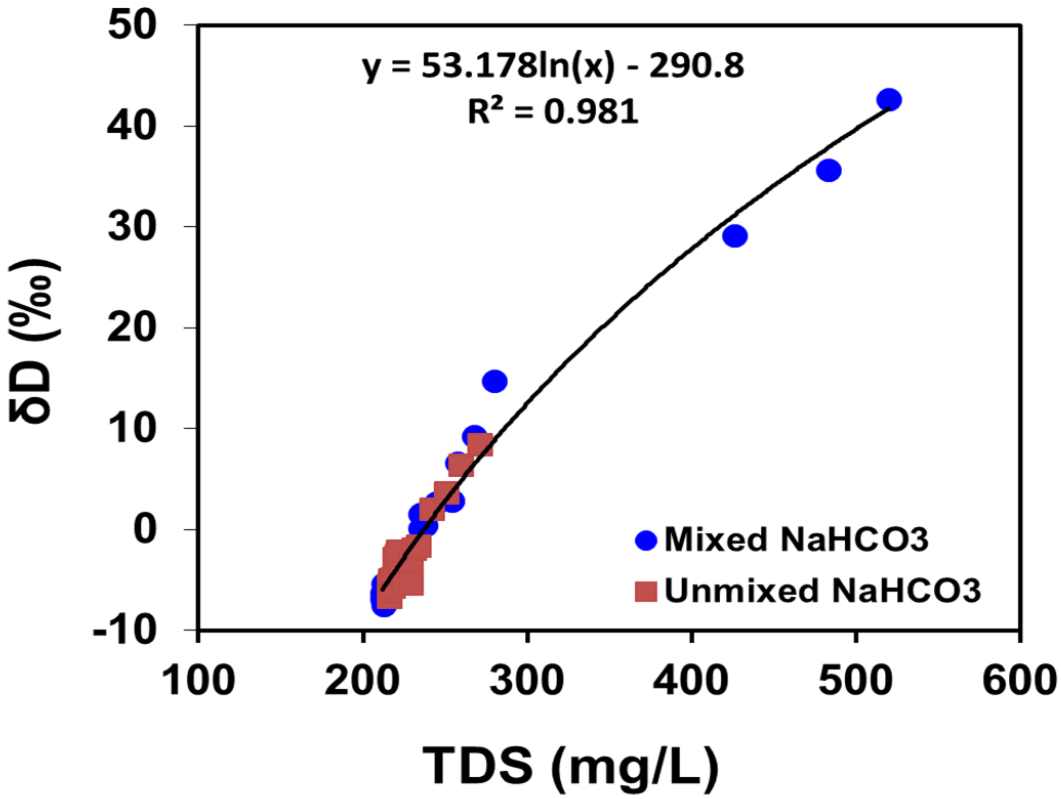

Figure I- 8. Cross plot of total dissolved solids (TDS) vs. the stable hydrogen isotopic composition (δD) in the mixed and unmixed $NaHCO_3$ samples exposed to the atmosphere in a laboratory setting. Increasing TDS with increasing $\delta^{13}C_{DIC}$ indicates the occurrence of evaporation since evaporation would result to increasing solute concentration and enrichment in δD over time.

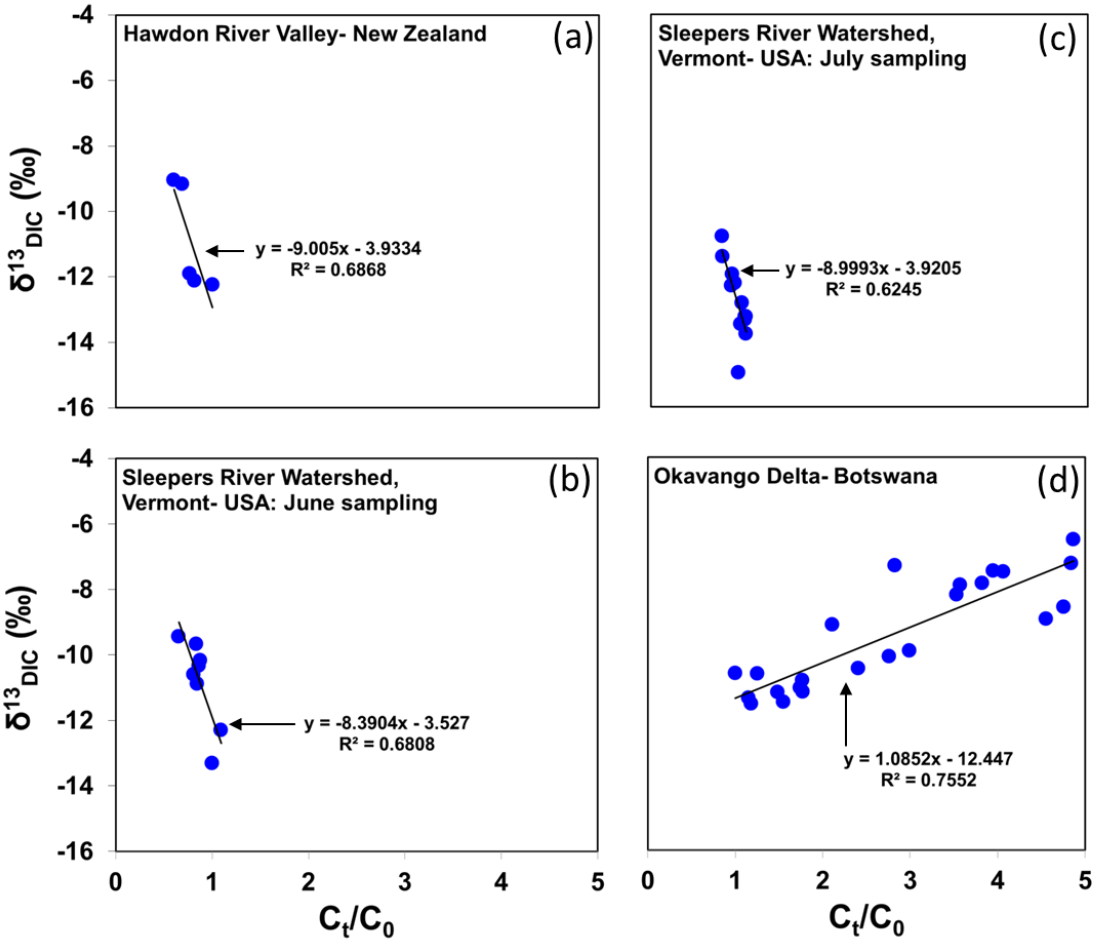

Figure I- 9. Change in the C_t/C_0 vs. $\delta^{13}C_{DIC}$ for field samples from (a) Hawdon River Valley, New Zealand (Duncan et al., 2011), (b) Sleepers River watershed, June sampling (Doctor et al., 2008), (c) Sleepers River watershed, July sampling (Doctor et al., 2008) and (d) Okavango Delta, Botswana (unpublished). The data sets fit into Model 1 depicting CO_2 outgassing and Model 2 representing the effect of evapo-concentration on DIC concentration. Arrows indicate direction of evolution.

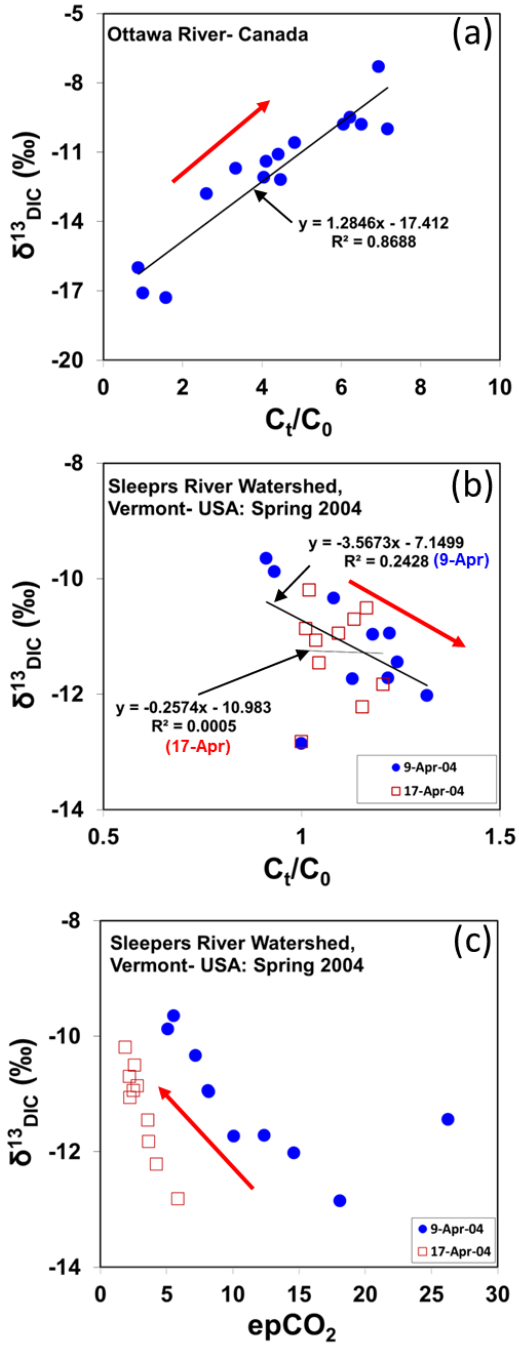

Figure I- 10. Change in the C_t/C_0 vs. $\delta^{13}C_{DIC}$ for field samples from (a) Ottawa River-Canada (Telmer and Veizer, 1999) and (b) Sleepers River watershed, spring 2004 sampling (Doctor et. al, 2008). (c) Plots of $epCO_2$ vs. $\delta^{13}C_{DIC}$ for the Sleepers River watershed, spring 2004 (Doctor et al., 2008). The results by Telmer and Veizer (1999) and spring sampling by Doctor et al. (2008) should not be interpreted using our model since it represents a carbon evolution process dominated by groundwater seepage into rivers and streams. Arrows indicate direction of evolution.

Table I- 1. Physical, chemical and stable carbon isotope results for mixed and unmixed $NaHCO_3$, groundwater and lake water samples exposed to laboratory

1

Sample ID	Time Hours	pH	Temp. (°C)	SPC (µs/cm)	TDS mg/L	Cl^- (mmol/L)	SO_4^{2-} (mmol/L)	NO_3^- (mmol/L)	K^+ (mmol/L)	Na+ (mmol/L)	Ca^+ (mmol/L)	Mg^+ (mmol/L)	Tot. Alk. as $CaCO_3$ (mmol/L)	DIC (mmol C /L)	$\delta^{13}C_{DIC}$ (‰)	$\delta^{18}O$ (‰)	δD (‰)	Log pCO_2 (atm)
Mixed $NaHCO_3$ solution																		
	0	8.49	21.8	328	213	-	-	-	-	1.12	-	-	1.55	4.20	-19.1	-1.9	-7.6	-3.2
	0.5	8.49	21.8	327	212	-	-	-	-	0.92	-	-	1.54	4.17	-19.2	-1.3	-6.9	-3.2
	2	8.49	21.8	327	212	-	-	-	-	1.01	-	-	1.53	4.24	-19.0	-1.1	-6.3	-3.2
	5	8.52	21.8	328	213	-	-	-	-	1.00	-	-	1.57	4.23	-18.9	-0.9	-5.4	-3.2
	8	8.52	21.8	330	224	-	-	-	-	1.04	-	-	1.55	4.08	-18.6	-0.9	-5.4	-3.2
	21.45	8.6	22.1	336	218	-	-	-	-	1.07	-	-	1.57	4.11	-18.0	-0.7	-4.7	-3.3
	29.45	8.6	22.4	336	219	-	-	-	-	1.05	-	-	1.55	4.30	-17.2	-0.5	-4.9	-3.3
	55.45	8.59	23	343	223	-	-	-	-	1.05	-	-	1.55	4.29	-16.1	-0.2	-4.0	-3.3
	80.15	8.63	22.1	351	228	-	-	-	-	1.10	-	-	1.55	4.09	-15.0	-0.6	-4.4	-3.3
	100	8.59	22.1	355	231	-	-	-	-	1.10	-	-	1.55	4.34	-14.0	0.0	-2.1	-3.3
	124	8.6	22.3	361	235	-	-	-	-	1.14	-	-	1.55	4.10	-12.6	0.5	0.0	-3.3
	148	8.6	22.3	366	238	-	-	-	-	1.13	-	-	1.68	4.14	-11.4	0.9	0.4	-3.3
	172	8.61	22.1	370	235	-	-	-	-	1.15	-	-	1.72	4.16	-10.4	1.0	1.5	-3.3
	196	8.62	22.3	379	245	-	-	-	-	1.15	-	-	1.75	4.76	-9.4	0.7	2.6	-3.3
	220	8.66	23	384	250	-	-	-	-	1.15	-	-	1.79	4.62	-8.4	0.6	3.2	-3.3
	244	8.6	22.4	390	254	-	-	-	-	1.24	-	-	1.81	4.18	-7.9	1.1	2.8	-3.2
	292	8.53	22.3	396	258	-	-	-	-	1.22	-	-	1.90	4.43	-7.6	1.7	6.6	-2.9
	340	8.63	21.1	412	268	-	-	-	-	1.25	-	-	2.03	4.91	-6.5	2.3	9.2	-3.1
	388	8.66	21.7	431	280	-	-	-	-	1.39	-	-	2.03	4.94	-5.6	3.0	14.7	-3.1
	484	8.66	21.9	450	290	-	-	-	-	1.53	-	-	2.31	5.35	-4.4	4.4	25.3	-3.1
	674	8.76	23.5	656	426	-	-	-	-	1.87	-	-	3.07	8.10	-3.7	5.4	29.1	-3.1
	784	8.65	23.5	743	483	-	-	-	-	2.00	-	-	3.41	9.46	-4.3	6.1	35.6	-3.0
	904	8.77	24	800	520	-	-	-	-	2.35	-	-	4.23	10.36	-4.2	8.7	42.6	-3.1
Unmixed $NaHCO_3$ solution																		
	0	8.5	22.1	332	216	-	-	-	-	3.64	-	-	1.65	4.13	-19.7	-1.8	-6.7	-3.2
	0.5	8.52	22.1	332	216	-	-	-	-	3.34	-	-	1.65	4.17	-19.6	-1.1	-6.2	-3.2
	2	8.56	21.8	332	216	-	-	-	-	3.39	-	-	1.64	4.02	-19.3	-0.9	-5.9	-3.2
	4	8.55	21.7	332	216	-	-	-	-	3.39	-	-	1.59	4.27	-19.2	-0.9	-6.2	-3.3
	7.5	8.56	21.21	333	216	-	-	-	-	3.45	-	-	1.55	4.18	-19.3	-0.7	-5.5	-3.3
	20.5	8.58	21.4	334	217	-	-	-	-	3.47	-	-	1.53	4.33	-18.7	-0.6	-5.1	-3.3
	29	8.58	21.3	334	217	-	-	-	-	3.49	-	-	1.55	4.03	-19.2	-0.4	-5.1	-3.3
	40	8.58	21.4	336	218	-	-	-	-	3.58	-	-	1.55	4.02	-19.0	-0.2	-4.9	-3.3
	52	8.58	21.3	336	218	-	-	-	-	3.62	-	-	1.57	3.60	-19.1	-0.7	-5.7	-3.3
	72	8.57	21.3	339	220	-	-	-	-	3.65	-	-	1.59	3.74	-19.2	-0.1	-2.9	-3.3
	96	8.58	21.4	340	221	-	-	-	-	3.82	-	-	1.59	3.90	-19.0	0.2	-2.6	-3.3
	120	8.59	21.9	341	222	-	-	-	-	3.80	-	-	1.66	4.15	-18.4	0.4	-2.1	-3.3
	144	8.57	21.5	343	223	-	-	-	-	3.83	-	-	1.66	3.81	-18.1	-0.4	-4.7	-3.3
	168	8.65	21.4	346	225	-	-	-	-	3.93	-	-	1.71	3.80	-17.8	-0.4	-5.4	-3.3
	216	8.55	20.5	352	229	-	-	-	-	3.96	-	-	1.71	3.98	-17.4	-0.4	-3.2	-3.2
	240	8.56	20.8	352	229	-	-	-	-	4.11	-	-	1.73	4.39	-17.2	-0.7	-5.4	-3.2
	264	8.57	21.2	356	231	-	-	-	-	4.17	-	-	1.75	4.46	-17.1	0.2	-1.9	-3.2
	288	8.59	21.2	360	234	-	-	-	-	4.25	-	-	1.72	4.60	-17.3	0.4	-1.7	-3.3
	408	8.56	21	373	242	-	-	-	-	4.80	-	-	1.75	4.54	-15.9	1.4	1.9	-3.2
	600	8.54	21	387	251	-	-	-	-	5.15	-	-	1.78	4.85	-14.7	2.0	3.6	-3.2
	744	8.49	21.3	399	260	-	-	-	-	6.56	-	-	1.84	4.92	-13.5	2.7	6.4	-3.1
	864	8.53	21.8	418	271	-	-	-	-	6.82	-	-	1.96	5.15	-13.0	3.1	8.4	-3.1
Mixed Groundwater sample																		
	0	7.36	18.11	786	511	0.17	0.08	0.45	0.013	2.66	0.98	1.51	2.94	8.30	-12.1	-	-	-1.8
	0.5	7.37	18.35	788	512	0.17	0.08	0.45	0.012	2.68	0.93	1.50	2.97	8.51	-11.5	-	-	-1.8
	1	7.57	18.62	788	512	0.17	0.08	0.45	0.013	2.74	0.93	1.53	2.95	8.49	-11.4	-	-	-2.0
	2	7.74	19.05	784	510	0.17	0.08	0.46	0.013	2.72	1.26	1.51	2.95	8.33	-11.1	-	-	-2.2

	3	7.83	19.44	787	512	0.17	0.08	0.46	0.014	2.68	1.21	1.53	2.96	8.20	-11.0	-	-	-2.3
	4	7.96	19.74	784	510	0.17	0.08	0.42	0.013	2.68	0.98	1.50	2.98	8.06	-10.8	-	-	-2.4
	8	8.15	20.81	782	508	0.17	0.09	0.47	0.014	2.68	1.20	1.51	2.98	7.18	-10.4	-	-	-2.6
	26	8.47	22.01	775	503	0.17	0.09	0.47	0.014	2.70	0.74	1.51	2.99	7.66	-10.1	-	-	-2.9
	40	8.35	22.30	754	490	0.16	0.09	0.47	0.017	2.70	0.61	1.48	2.90	6.93	-9.7	-	-	-2.8
	72	8.38	22.36	694	451	0.17	0.09	0.46	0.018	2.65	0.65	1.49	2.45	6.32	-9.1	-	-	-2.9
	96	8.45	22.17	682	443	0.16	0.09	0.49	0.034	3.47	0.73	1.96	2.41	5.78	-8.6	-	-	-3.0
	121	8.46	22.46	679	441	0.18	0.09	0.49	0.026	2.69	0.68	1.51	2.31	5.80	-7.6	-	-	-3.0
	171	8.83	22.23	686	446	0.19	0.09	0.49	0.032	3.01	0.56	1.68	2.30	5.90	-7.0	-	-	-3.4
	211	8.86	22.42	700	455	0.19	0.09	0.50	0.061	2.82	0.62	1.58	2.30	6.07	-6.7	-	-	-3.4
	240	8.87	22.16	717	466	0.18	0.10	0.53	0.102	3.19	0.68	1.90	2.44	6.32	-6.2	-	-	-3.4
	288	8.92	22.57	741	482	0.19	0.10	0.52	0.115	3.00	0.52	1.62	2.38	6.53	-5.4	-	-	-3.5
	336	8.95	22.55	761	495	0.20	0.10	0.55	0.122	3.01	0.60	1.72	2.49	6.72	-5.1	-	-	-3.5
	408	8.99	22.62	791	514	0.22	0.10	0.55	0.132	3.42	0.57	1.84	2.55	6.85	-4.9	-	-	-3.5
	552	9.03	22.89	857	557	0.23	0.12	0.63	0.163	3.55	0.57	1.94	2.57	7.30	-4.0	-	-	-3.6
	624	8.98	22.31	908	590	0.23	0.14	0.71	0.178	3.85	0.55	2.05	2.50	7.48	-3.4	-	-	-3.5
	744	9.08	22.28	1000	650	0.24	0.15	0.81	0.219	4.76	0.44	2.41	2.51	8.52	-3.2	-	-	-3.6
	840	9.10	22.29	1121	729	0.25	0.18	0.94	0.256	5.27	0.40	2.68	2.50	9.12	-3.2	-	-	-3.6
	984	9.20	21.30	1376	801	0.26	0.26	1.33	0.349	7.21	0.31	3.47	2.44	11.85	-3.1	-	-	-3.8
Unmixed Groundwater sample																		
	0	7.54	17.42	778	506	0.17	0.09	0.49	0.006	2.49	0.87	1.36	3.13	8.26	-11.1	-	-	-2.0
	0.5	7.54	17.28	778	505	0.17	0.09	0.50	0.006	2.46	0.96	1.37	3.13	8.36	-11.0	-	-	-2.0
	1	7.55	17.48	777	505	0.17	0.09	0.48	0.017	2.79	0.89	1.62	3.13	8.44	-11.2	-	-	-2.0
	2	7.48	17.91	779	507	0.17	0.09	0.49	0.006	2.50	0.68	1.35	3.13	8.44	-11.1	-	-	-1.9
	3	7.34	18.21	778	506	0.17	0.09	0.49	0.006	2.45	0.74	1.32	3.15	8.41	-11.1	-	-	-1.8
	4	7.47	18.49	779	506	0.17	0.09	0.49	0.006	2.41	0.84	1.31	3.15	8.38	-11.2	-	-	-1.9
	8	7.42	19.34	780	507	0.17	0.09	0.50	0.005	2.43	0.90	1.26	3.12	8.35	-11.0	-	-	-1.9
	26	7.53	20.78	785	510	0.17	0.09	0.49	0.011	2.62	0.90	1.50	3.13	8.34	-10.8	-	-	-2.0
	40	7.62	21.24	785	510	0.16	0.08	0.47	0.010	2.58	0.86	1.40	3.14	8.17	-10.7	-	-	-2.1
	72	7.90	21.33	787	512	0.17	0.09	0.49	0.016	2.57	1.04	1.41	3.18	8.11	-10.4	-	-	-2.3
	96	7.83	21.24	784	510	0.16	0.08	0.46	0.022	2.80	1.07	1.58	3.14	8.11	-9.9	-	-	-2.3
	121	7.88	21.37	788	512	0.18	0.09	0.50	0.021	2.54	1.10	1.42	3.24	7.74	-9.6	-	-	-2.6
	171	8.21	21.25	788	512	0.19	0.09	0.51	0.041	2.55	0.89	1.38	3.01	7.53	-9.2	-	-	-2.7
	211	8.53	21.47	786	511	0.19	0.09	0.51	0.046	2.56	0.94	1.38	3.19	7.93	-8.8	-	-	-3.0
	240	8.59	21.29	784	510	0.18	0.09	0.51	0.047	2.55	0.92	1.45	3.12	7.91	-8.5	-	-	-3.0
	288	8.63	21.44	781	508	0.19	0.09	0.51	0.058	2.60	0.87	1.42	3.00	7.91	-8.1	-	-	-3.1
	336	8.64	21.57	781	508	0.20	0.09	0.53	0.066	2.37	0.59	1.29	2.99	7.89	-7.7	-	-	-3.1
	408	8.69	21.73	781	507	0.22	0.10	0.54	0.141	3.19	0.92	1.78	3.01	7.45	-7.3	-	-	-3.2
	552	8.69	22.05	779	507	0.23	0.10	0.55	0.114	2.46	0.84	1.39	2.90	7.58	-6.5	-	-	-3.2
	624	8.69	21.49	783	509	0.23	0.10	0.59	0.142	3.13	1.02	1.73	2.90	7.48	-6.0	-	-	-3.2
	744	8.72	21.70	789	513	0.24	0.10	0.57	0.174	3.46	1.09	1.93	2.89	7.50	-5.4	-	-	-3.2
	840	8.76	21.64	799	519	0.25	0.11	0.60	0.155	3.07	0.89	1.73	2.89	7.31	-4.9	-	-	-3.3
	984	8.77	21.52	800	520	0.26	0.11	0.61	0.152	3.08	0.78	1.67	2.85	6.90	-4.1	-	-	-3.3
Mixed Lake water sample																		
	0	8.34	22.33	372	242	0.15	0.05	0.00	0.089	0.72	0.77	0.65	1.38	3.78	-4.0	-	-	-3.1
	0.5	8.34	22.33	373	243	0.14	0.05	0.00	0.087	0.71	0.76	0.64	1.37	3.78	-3.8	-	-	-3.1
	1	8.34	22.33	373	243	0.14	0.04	0.00	0.085	0.69	0.73	0.61	1.37	3.87	-3.9	-	-	-3.1
	2	8.37	22.33	374	243	0.14	0.05	0.00	0.087	0.71	0.74	0.63	1.38	3.80	-4.2	-	-	-3.1
	3	8.38	22.28	374	242	0.15	0.05	0.00	0.088	0.72	0.74	0.62	1.37	3.82	-4.0	-	-	-3.1
	4	8.38	22.23	374	243	0.14	0.05	0.00	0.089	0.72	0.75	0.64	1.37	4.24	-4.4	-	-	-3.1
	8	8.39	22.14	374	243	0.15	0.05	0.00	0.093	0.72	0.76	0.68	1.46	3.50	-4.0	-	-	-3.1
	21	8.37	22.43	376	245	0.15	0.05	0.00	0.095	0.72	0.77	0.64	1.42	3.84	-3.9	-	-	-3.1
	33	8.4	22.22	377	244	0.15	0.05	0.00	0.102	0.72	0.77	0.65	1.36	3.86	-3.9	-	-	-3.1
	46	8.42	22.23	379	246	0.15	0.05	0.00	0.104	0.73	0.77	0.66	1.41	3.72	-4.1	-	-	-3.2
	58	8.45	21.98	381	248	0.15	0.05	0.00	0.095	0.70	0.74	0.63	1.48	3.96	-4.0	-	-	-3.2
	80	8.45	21.98	385	251	0.15	0.05	0.00	0.111	0.82	0.86	0.73	1.47	4.02	-4.1	-	-	-3.2
	100	8.47	22.26	388	252	0.16	0.05	0.00	0.103	0.74	0.79	0.67	1.48	4.04	-4.1	-	-	-3.2
	118	8.45	22.56	393	256	0.15	0.05	0.00	0.120	0.88	0.94	0.79	1.50	4.09	-4.1	-	-	-3.2

19

	142	8.41	22.83	398	259	0.16	0.05	0.00	0.103	0.76	0.81	0.68	1.52	4.10	-4.3	-	-	-3.1
	174	8.48	22	397	260	0.16	0.05	0.00	0.108	0.80	0.83	0.70	1.55	4.11	-4.4	-	-	-3.2
	201	8.5	22.18	408	265	0.16	0.05	0.00	0.118	0.86	0.89	0.78	1.55	4.35	-4.6	-	-	-3.2
	222	8.52	22.5	414	269	0.17	0.05	0.00	0.132	0.96	1.01	0.86	1.61	4.34	-4.6	-	-	-3.2
	237	8.57	22.42	416	270	0.17	0.05	0.00	0.137	1.04	1.06	0.91	1.61	3.83	-5.3	-	-	-3.3
	260	8.59	22.47	421	273	0.17	0.05	0.00	0.158	1.16	0.66	1.01	1.65	4.26	-4.5	-	-	-3.3
	284	8.59	22.68	427	278	0.18	0.06	0.00	0.165	1.18	0.70	1.08	1.65	4.79	-4.0	-	-	-3.3
	332	8.59	22.01	438	285	0.19	0.06	0.00	0.183	1.21	0.70	1.11	1.75	4.67	-4.6	-	-	-3.4
	419	8.66	21.58	460	299	0.21	0.07	0.02	0.185	1.24	0.67	1.13	1.80	4.46	-4.8	-	-	-3.3
	524	8.65	21.5	504	328	0.22	0.07	0.00	0.198	1.42	0.65	1.27	1.99	5.14	-4.0	-	-	-3.4
	660	8.7	22.19	491	329	0.24	0.08	0.00	0.199	1.42	0.65	1.26	1.73	4.29	-2.6	-	-	-3.4
	760	8.76	22.15	515	345	0.28	0.09	0.00	0.191	1.41	0.62	1.19	1.74	4.21	-3.5	-	-	-3.5
	880	8.79	22.97	546	355	0.30	0.09	0.01	0.191	1.42	0.61	1.20	1.68	4.53	-3.5	-	-	-3.4
	1000	8.81	23.22	597	388	0.35	0.11	0.01	0.266	1.86	0.61	1.27	1.90	4.61	-4.3	-	-	-3.4
Unmixed Lake water sample																		
	0	8.38	22.84	370	241	0.15	0.05	0.00	0.086	0.71	0.74	0.64	1.38	3.53	-4.1	-	-	-3.1
	0.5	8.38	22.68	370	240	0.15	0.05	0.00	0.088	0.73	0.76	0.66	1.37	3.51	-4.2	-	-	-3.1
	1	8.36	22.54	368	239	0.14	0.05	0.00	0.084	0.69	0.72	0.62	1.37	3.53	-4.2	-	-	-3.1
	2	8.44	22.35	371	241	0.15	0.05	0.00	0.079	0.65	0.68	0.58	1.37	3.42	-4.1	-	-	-3.1
	3	8.42	22.08	366	238	0.14	0.05	0.00	0.098	0.79	0.83	0.70	1.37	3.56	-4.1	-	-	-3.1
	4	8.43	21.93	372	242	0.15	0.05	0.00	0.077	0.60	0.61	0.53	1.37	3.22	-4.5	-	-	-3.1
	8	8.44	21.48	371	249	0.15	0.05	0.00	0.084	0.65	0.67	0.58	1.42	3.66	-4.4	-	-	-3.1
	21	8.38	21.47	375	244	0.15	0.05	0.00	0.096	0.73	0.76	0.65	1.43	3.60	-4.0	-	-	-3.1
	33	8.33	21.33	376	245	0.15	0.05	0.00	0.097	0.73	0.86	0.65	1.36	3.25	-4.2	-	-	-3.2
	46	8.36	21.29	373	243	0.15	0.05	0.00	0.107	0.83	0.77	0.73	1.39	3.68	-4.1	-	-	-3.2
	58	8.35	21.06	378	246	0.15	0.05	0.00	0.094	0.73	0.73	0.65	1.39	3.49	-4.2	-	-	-3.2
	80	8.36	21.11	380	247	0.15	0.05	0.00	0.095	0.72	0.73	0.63	1.44	3.94	-4.0	-	-	-3.2
	100	8.32	21.41	373	243	0.16	0.05	0.00	0.105	0.70	0.72	0.63	1.49	3.68	-4.1	-	-	-3.2
	118	8.31	21.61	384	250	0.16	0.05	0.00	0.105	0.70	0.86	0.62	1.43	3.78	-4.1	-	-	-3.2
	142	8.27	21.83	390	254	0.16	0.05	0.00	0.127	0.82	0.78	0.62	1.45	3.55	-4.2	-	-	-3.1
	174	8.35	21.05	387	252	0.16	0.05	0.00	0.117	0.76	0.79	0.73	1.44	3.66	-4.3	-	-	-3.2
	201	8.33	21.23	393	256	0.16	0.05	0.00	0.119	0.77	0.84	0.66	1.50	3.68	-4.5	-	-	-3.2
	222	8.34	21.38	392	255	0.17	0.05	0.00	0.125	0.81	0.69	0.69	1.45	3.85	-4.4	-	-	-3.3
	237	8.35	21.43	394	256	0.16	0.05	0.00	0.103	0.67	0.71	0.72	1.47	3.75	-4.7	-	-	-3.3
	260	8.39	21.65	396	258	0.16	0.05	0.00	0.106	0.68	0.81	0.59	1.48	4.00	-4.3	-	-	-3.3
	284	8.41	21.95	397	258	0.17	0.05	0.00	0.121	0.78	0.80	0.70	1.52	4.00	-4.6	-	-	-3.3
	332	8.41	21.33	398	258	0.17	0.05	0.00	0.123	0.79	0.86	0.62	1.63	3.74	-4.5	-	-	-3.4
	408	8.47	20.97	406	246	0.17	0.05	0.00	0.127	0.81	0.86	0.69	1.57	3.78	-4.7	-	-	-3.4
	524	8.51	20.79	415	270	0.17	0.05	0.00	0.130	0.84	0.88	0.73	1.58	3.77	-3.8	-	-	-3.5
	660	8.52	21.38	435	283	0.18	0.06	0.00	0.134	0.87	0.88	0.74	1.65	3.88	-3.9	-	-	-3.5
	760	8.54	21.44	441	287	0.18	0.05	0.01	0.135	0.88	0.88	0.76	1.65	4.28	-3.7	-	-	-3.5
	880	8.65	21.32	452	294	0.19	0.06	0.00	0.148	0.93	0.91	0.85	1.67	4.49	-3.3	-	-	-3.5
	1000	8.66	21.39	466	303	0.19	0.06	0.00	0.141	0.77	0.90	0.82	1.65	5.13	-3.2	-	-	-3.5

SPC = specific conductance

= Not applicable

CHAPTER II

CONTROLS ON THE CHEMICAL AND ISOTOPIC COMPOSITION OF CARBONATE SPRINGS DURING EVOLUTION TO SATURATION WITH RESPECT TO CALCITE

Submitted for review (Chemical Geology)

Pride T. Abongwa and Eliot A. Atekwana

Boone Pickens School of Geology, 105 Noble Research Center, Oklahoma State University, Stillwater OK, 74078, USA.

Summary

We investigated the stable carbon isotopic composition ($\delta^{13}C$) of dissolved inorganic carbon (DIC) in carbonate springs that evolve chemically to supersaturation with respect to calcite and to isotopic equilibrium with atmospheric $CO_{2(g)}$. Carbonate spring–atmospheric $CO_{2(g)}$ interaction is complex because the saturation state with respect to calcite and the evolution to isotopic equilibrium with respect to atmospheric $CO_{2(g)}$ depends on carbon transformation between $CO_{2(g)} \leftrightarrow H_2CO_3 \leftrightarrow HCO_3^- \leftrightarrow CO_3^{2-} \leftrightarrow CaCO_{3(s)}$. The $\delta^{13}C$ of DIC ($\delta^{13}C_{DIC}$) will track isotopic fractionation accompanying carbon loss to the atmosphere, precipitation of calcite or carbon exchange with atmospheric $CO_{2(g)}$. We assessed the DIC and $\delta^{13}C_{DIC}$ evolution along the

flow paths of springs in the field. Since chemical equilibrium is a precondition for isotopic equilibrium, and, because it is difficult to follow the evolution of carbonate springs to isotopic equilibrium with atmospheric $CO_{2(g)}$ in field settings, three sets of spring samples were exposed to laboratory atmospheric $CO_{2(g)}$ and allowed to evolve to equilibrium. One subset of the experimental sample was agitated to simulate mixing in the field. The physical, chemical and carbon isotopic changes in the field and laboratory experiments were complex and varied. Chemical speciation and isotopic mass balance modeling showed that the evolution to calcite supersaturation can be conceptualized in 4 discrete steps each characterized by kinetic fractionation, equilibrium fractionation or carbon isotopic exchange with atmospheric $CO_{2(g)}$. These steps sequentially are (1) undersaturation to supersaturation where DIC decreases from $CO_{2(g)}$ loss from solution and small increases in the $\delta^{13}C_{DIC}$ (1-2‰) is from kinetic fractionation, (2) saturation to supersaturation where relatively no DIC is lost and small increases in the $\delta^{13}C_{DIC}$ (~1‰) is likely due to carbon isotopic exchange between DIC and atmospheric $CO_{2(g)}$, (3) decreasing supersaturation where DIC concentration decreases and larger enrichment in the $\delta^{13}C_{DIC}$ (~5‰) is from equilibrium isotopic fractionation and (4) increasing saturation where the previous decreasing supersaturation and DIC concentration decreases reverse and increase because of evaporation and the continued increase in the $\delta^{13}C_{DIC}$ (~2‰) is from equilibrium isotopic fractionation. The unmixed laboratory samples evolved through steps 1, 2 and 3 while the mixed laboratory sample evolved through steps 1, 2, 3 and 4 because agitation of the solution increased the reaction rates and enhanced DIC atmospheric $CO_{2(g)}$ interaction. The chemical and isotopic evolution of the field samples were limited to steps 1 and 2 because of the relatively short length of flowing springs which limit carbonate evolution to calcite saturation. Our findings suggest that for carbonate springs in contact with atmospheric $CO_{2(g)}$, significant $\delta^{13}C_{DIC}$

enrichment that occurs after calcite supersaturation is dominated by equilibrium isotopic effect, despite conditions conducive for calcite precipitation. We hypothesize that the chemical and isotopic behavior observed for the field and laboratory experiments may characterize other carbonate-rich waters (streams and lakes) evolving in contact with the atmosphere.

Keywords: Carbonate springs; Dissolved inorganic carbon; Stable carbon isotopes; Calcite supersaturation; Isotopic fractionation

1. Introduction

Springs issuing from a carbonate aquifer (carbonate springs) with high concentrations of dissolved inorganic carbon (DIC) and high partial pressure of CO_2 (pCO_2) will lose $CO_{2(g)}$ as they evolve towards chemical equilibrium with atmospheric $CO_{2(g)}$. As $CO_{2(g)}$ is lost from solution, the equilibrium solubility of calcite ($CaCO_3$) decreases to the point of calcite saturation and $CaCO_3$ can precipitate from solution (e.g., Jacobson and Usdowski, 1975; Herman and Lorah, 1986; 1988; Dreybrodt et al., 1992; Pentecost, 1995; Liu et al., 2000). The carbonate spring–atmospheric $CO_{2(g)}$ interaction is complex because both the saturation state with respect to calcite and the evolution to chemical equilibrium with respect to atmospheric $CO_{2(g)}$ depends on carbon transformation between $CO_{2(g)} \leftrightarrow H_2CO_3 \leftrightarrow HCO_3^- \leftrightarrow CO_3^{2-} \leftrightarrow CaCO_{3(s)}$ (Stumm and Morgan, 1981). The carbon isotopic composition of DIC ($\delta^{13}C_{DIC}$) in the evolving carbonate spring will change because of isotopic fractionation accompanying carbon loss to the atmosphere, carbon loss from the precipitation of carbonate or carbon exchange with atmospheric $CO_{2(g)}$ (e.g., Clark and Fritz, 1997). Several studies have investigated the behavior

of DIC and $\delta^{13}C_{DIC}$ of carbonate springs (e.g., Pentecost, 1995; Lu, 2000; Marfia et al., 2004; Li et al., 2010). However, the DIC and $\delta^{13}C_{DIC}$ behavior has not been examined in the context of (1) evolution of the carbonate system to saturation where carbon ($CO_{2(g)}$) is lost from the DIC pool, (2) chemical evolution at saturation with respect to calcite when carbon ($CaCO_3$) is removed from the DIC pool and (3) concomitant evolution of the DIC towards chemical equilibrium with atmospheric $CO_{2(g)}$. Moreover, measurements of $\delta^{13}C$ of calcite that precipitates during the evolution of carbonate-rich waters were conducted with the aim of determining the chemical and isotopic kinetics controlling calcite precipitation (e.g., Dandurand et al., 1982).

Knowledge of the behavior of $\delta^{13}C_{DIC}$ in carbonate springs evolving towards and at calcite saturation conditions, as well as during DIC equilibration with atmospheric $CO_{2(g)}$ is lacking. Chemical equilibrium is a precondition for isotopic equilibrium and in field settings, it is difficult to follow the chemical evolution of springs towards isotopic equilibrium with atmospheric $CO_{2(g)}$. This is because over relatively short distances, springs flow into streams, are intercepted by tributaries or disappear underground, thus limiting the flow pathway along which carbonate evolution can be evaluated. Additionally, even if carbonate springs have long flow pathways that could be followed, assessing the chemical and isotopic evolution can be problematic due to the addition of carbon from organic matter decomposition (Wicks and Engeln, 1997). Furthermore, when the material lining the channels are carbonates, weathering may introduce DIC into the water column (e.g., Hess and White, 1988; Hoffer-French and Herman, 1989; Groves, 1992) thereby affecting $\delta^{13}C_{DIC}$ (e.g., Doctor et al., 1999). Laboratory experiments provide a near ideal way to assess how the DIC and $\delta^{13}C_{DIC}$ for carbonate springs behave during the chemical evolution to calcite saturation and to equilibrium with atmospheric $CO_{2(g)}$. Results from the near-

ideal behavior in laboratory experiments aid in the interpretation of processes that affect the $\delta^{13}C_{DIC}$ behavior in carbonate springs in field settings.

In this study, we assessed the behavior of $\delta^{13}C_{DIC}$ associated with DIC evolution in field and laboratory experiments with waters from carbonate springs. We aimed to use the temporal and spatial DIC concentrations and the $\delta^{13}C_{DIC}$ to generate DIC-$\delta^{13}C_{DIC}$ models that characterize carbonate springs that evolve to calcite saturation and to chemical and isotopic equilibrium with atmospheric $CO_{2(g)}$.

2. Study area

The springs used in this study are Antelope Spring ($34^0 30' 7.32'' N$, $96^0 56' 29.05'' W$), Buffalo Spring ($34^0 30' 14.32'' N$, $96^0 56' 16.05'' W$) and Byrds Mill Spring ($34^0 35' 40.47'' N$, $96^0 39' 55.33'' W$) which issue from the Arbuckle-Simpson aquifer in Oklahoma, USA (Fig. II-1). The rocks which make up the Arbuckle-Simpson aquifer crop out in south central Oklahoma and underlay parts of Carter, Coal, Johnston, Murray and Pontotoc Counties (Fig. II-1). The Arbuckle-Simpson aquifer is highly folded, faulted and fractured and is made up of the Arbuckle and the Simpson Groups (Ham, 1955; Fairchild et al., 1990; Donovan, 1991; Campbell and Weber, 2006). The Arbuckle Group consists of Late Cambrian to Middle Ordovician limestones and dolomites (e.g., Ham, 1955; Donovan, 1991). The Simpson Group is Ordovician and consists of basal sandstone, middle shale and an upper limestone (e.g., Fairchild et al., 1990). The Arbuckle-Simpson aquifer is overlain by Pennsylvanian limestones, conglomerates, shales and sandstones and is underlain by Cambrian and Precambrian rhyolite and granite basement (e.g., Hanson and Cates, 1994).

The study area is a moist, sub-humid zone (Fairchild et al., 1990) where precipitation occurs mostly as rainfall, with occasional snow during the winter. The mean annual precipitation from

1960 to 2010 is ~1000 mm measured in Ada, Oklahoma (Fig. II-1), ~40 km northeast of Antelope and Buffalo Springs and ~20 km north of Byrds Mill Spring (National Climatic Data Center, 2013). Antelope Spring discharges about 56 l/s and is located in the Chickasaw National Recreation Area (CNRA) near Sulfur, Oklahoma. Buffalo Spring discharges from several points into a rock-bound pool and flows from the pool at a discharge rate of about 65 l/s. Buffalo Spring is located 270 m SE of Antelope Spring and flows for about 365 m before joining Antelope Spring 150 m downstream from its source. Byrds Mill Spring, which discharges at approximately 527 l/s, is the largest spring in Oklahoma and is the drinking water source for the city of Ada (Christenson et al., 2009).

3. Materials and Methods

3.1 Field and Laboratory experiments

In the field experiment, we made measurements and collected grab samples of water from the source and along the flow paths of Antelope Spring, Buffalo Spring and Byrds Mill Spring at 5 to 10 m increments for the first 50 m, after which the sampling distances were increased to 100 m and finally to 200 m increments for a total distance of 895 m for Antelope Spring, 365 m for Buffalo Spring and 1000 m for Byrds Mill Spring. Measurements were made along Buffalo Spring up to its confluence with Antelope Spring. For this study, we ascribe water downstream of the confluence to Antelope Spring. The damming of Antelope Spring to form a pool used for recreation ~895 m from its source and a fish farm located 1000 m from the Byrds Mill Spring source served as the spatial limit for the collection of field samples. We terminated sampling where Antelope Spring is dammed and at the Byrds Mill Spring fish farm, because the natural

properties of the springs would be compromised by recreational activities and the fish farming. At the time of sample collection, water depths averaged 0.15 m for the Antelope Spring and 0.5 m for Byrds Mill Spring. The air temperature measured at nearby Ada and Sulfur, Oklahoma averaged 18 ^{0}C and the wind speed averaged 18 km/h (Oklahoma Climatological Survey, 2012).

In the field, the efflux of $CO_{2(g)}$ to the atmosphere which depends on water-air gas transfer rates is controlled by wind speed, water depth, turbulence and temperature. The discharge rates of the springs varied (e.g., Antelope Spring, 65 l/sec and Byrds Mill Spring, 527 l/sec). It is difficult to simulated field conditions in out laboratory experiment. Our laboratory experimental design did not exactly match field conditions. We used 20 L of sample in 25 L plastic reactors. The water in the reactors were 0.4 m high and the surface area exposed to the atmosphere was 0.32 m in diameter. The experiment was conducted ambient temperatures of ~23^{0} C. To simulate mixing and turbulence in the field, one set of the reactor samples were circulated at ~10 l/min with an aquarium pump (ViaAqua Powerhead, VA 360-906060; Foster and Smith Aquatics). The ~10 l/min water circulation in the reactor can be considered as a fast flowing spring. Comparing the results from a well-mixed reactor with the non-agitated (unmixed) sample should allow for better assessment how DIC behavior is influenced by water exposure to the atmosphere.

The laboratory experiment consisted of collecting duplicate 20 L of unfiltered water from the source of Antelope Spring and Byrds Mill Spring in 25 L plastic reactors. The samples were exposed to the atmosphere and sampling and analyses were conducted at 0, 0.25, 0.5, 1 and 24 h followed by every 24 h for a week and once every 3 to 4 days to the end of the experiment. One set of the reactor samples of Antelope Spring and Byrds Mill Spring were circulated at ~10 l/min with an aquarium pump (ViaAqua Powerhead, VA 360-906060; Foster and Smith Aquatics while the duplicate set of the Byrds Mill Spring was not agitated. The laboratory experiment

commenced in the field where the samples were exposed to the atmosphere and samples were collected for the first 1 h. Although the reactors could have been filled with no headspace and transported to the laboratory before starting the experiment, we wanted the early time interaction to be closer to field observations. After 1 h, water circulation by pumping was stopped in the mixed samples and the reactors were tightly sealed with lids and transported for a 2 h journey to the laboratory. Once in the laboratory, the lids were removed, the samples exposed to the laboratory atmosphere and sampling continued. The 2 h of sample transportation to the laboratory was included in the temporal evolution of the samples which was between 425 to 500 h. This exposure time was determined to be sufficient for the spring samples to evolve to chemical and isotopic equilibrium with $CO_{2(g)}$ in the laboratory atmosphere (e.g., Abongwa and Atekwana, 2013).

3.2 Sampling and analyses

Prior to collecting samples in the field and laboratory experiments, measurements of temperature, pH and total dissolved solids (TDS) were made using a Yellow Springs Instrument (YSI) multi-parameter probe calibrated to manufacturer's specifications. Water samples collected during the field experiment and from each laboratory reactor for chemical and isotopic analyses were filtered through 0.45 µM nylon syringe filters. Alkalinity was measured immediately after filtering by acid titration (Hach Company, 1992). Samples for anions and cations were collected in high density polyethylene (HDP) bottles; the cation samples were acidified to a pH <2.0 using high purity HNO_3. Major cations (Ca^{2+}, Mg^{2+}, K^+ and Na^+) and anions (SO_4^{2-} and Cl^-) were measured by ion chromatography using a Dionex ICS 3000. Samples

were measure in triplicate and the results averaged. The averages agreed to within 3%. Repeated measurement of standards gave an overall precision of better that 1%.

Samples for DIC analysis were collected in pre-acidified (1 mL of 85% H_3PO_4) vaccutainer tubes as described by Atekwana and Krishnamurthy (1998). DIC was extracted as $CO_{2(g)}$ from the vaccutainer tubes. The DIC concentrations were calculated from extracted $CO_{2(g)}$ and then the $CO_{2(g)}$ was sealed in Pyrex tubes. Our measured concentrations were better than 1% based on duplicate samples and dissolved $NaHCO_3$ standards (Atekwana and Krishnamurthy 1998). We collected laboratory air and outside air periodically in pre-evacuated 1.5 L glass ampoules and used a vacuum line to purify the $CO_{2(g)}$ which we sealed in Pyrex tubes. Although, air was not collected in the field where the spring samples were collected, we assumed that since this region of Oklahoma is rural, the $CO_{2(g)}$ in the atmosphere is well mixed and the pCO_2 and $\delta^{13}C$ are similar to outside air in Stillwater Oklahoma. The $CO_{2(g)}$ from DIC and the purified $CO_{2(g)}$ from laboratory and outside air were analyzed for $\delta^{13}C$ using a Finnigan Delta Plus XL isotope ratio mass spectrometer. The stable isotope ratios are reported in the delta (δ) notation in per mil (‰):

$$\delta(‰) = \left(\left(R_{sample}/R_{standard}\right) - 1\right) x\ 1000$$

where R is $^{13}C/^{12}C$. The δ values are reported relative to VPDB international standard. Routine $\delta^{13}C$ measurements of in-house standards and replicate samples have an overall precision (1-sigma) of better than 0.1‰.

The computer program PHREEQC Version 2.8 (Parkhurst and Appelo, 1999) was used to calculate the pCO_2 using pH, temperature and DIC and to calculate the equilibrium temporal concentrations in the carbonate species H_2CO_3, HCO_3^- and CO_3^{2-} during DIC evolution. We also used the computer program PHREEQC to calculate the saturation state with respect to calcite using pH, temperature, alkalinity and Ca^{2+} concentrations. The computer program NETHPATH

(Plummer et al., 1994) was used to compute $\delta^{13}C_{DIC}$ values based on isotope mass balance calculations.

4. Results

The physical, chemical and stable carbon isotope results for the field experiment are listed in Table 1 and laboratory experiments are listed in Table 2.

4.1 pH, alkalinity and DIC

The pH of the field samples increased from 6.8 to 7.8 over 875 m for Antelope Spring, 6.8 to 7.2 over 365 m for Buffalo Spring and 6.8 to 7.6 over 1000 m for Byrds Mill Spring (Fig. II-2a). The pH values were nearly constant for the first 50 m and then increased steadily to the end of the sampling distance. In the laboratory experiments, the pH of the unmixed Byrds Mill Spring sample behaved similar to field samples which was nearly constant for the first hour and increasing steeply from 6.8 to 8.0 to 50 h and then gently to 8.6 to the end of the experiment (Fig. II-2b). In contrast, the pH of the mixed samples of Byrds Mill Spring and Antelope Spring increased steeply from 6.8 to 8. for the first 8 h and gently to 8.8 for Byrds Mill Spring and 8.6 for Antelope Spring to the end of the experiment (Fig. II-2b). The increases in pH for samples from the laboratory experiment were higher than those of the field samples, and for the laboratory experiments, the increase in the pH for the mixed samples were higher than those of the unmixed samples (Fig. II-2a and b).

For the field samples, the alkalinity concentrations of Antelope Spring, Buffalo Spring and Byrds Mill Spring ranged from 5.8 to 5.5 mM/L. Overall the alkalinity concentrations decreased

steadily from the source to ~5.5 about 500 m where the alkalinity concentrations increased to 5.8 mM/L to the end of the sampling distances (Fig. II-2c). In the laboratory experiment, the alkalinity concentrations for the unmixed sample of Byrds Mill Spring decreased slowly from 5.7 to 5.4 mM/L for the first ~100 h and then decreased sharply to 4.2 mM/L to the end of the experiment (Fig. 3d). In contrast, the alkalinity concentrations of the mixed samples of Byrds Mill Spring and Antelope Spring decreased gradually from ~5.5 to 5.2 mM/L for the first 7 h, decreased sharply from 5.2 to 3.1 mM/L from 7 h to 78 h, then decreases slowly to 3.5 -3.0 mM/L at 2013 h, after which the alkalinity concentrations increased continuously to 4.1-4.6 to mM/L the end of the experiment (Fig. II-2d). The behavior of the alkalinity in the early stages of the laboratory experiment was similar to those of the field samples. The marked decrease in alkalinity concentrations occurred earlier in the mixed samples compared to the unmixed sample and the increase in alkalinity near the end of the experiment was not observed in the unmixed sample.

In the field, the DIC concentrations for Antelope Spring, Byrds Mill Spring and Buffalo Spring showed a continuous decrease from ~8.8 -8.4 to ~7.0 mM/L throughout the sampling distance (Fig. II-2e). In the laboratory experiment, the DIC concentrations of the unmixed sample of Byrds Mill Spring decreased gradually from 8.8 to 6.5 mM/L for the first 148 h and then decreased sharply to 4.8 mM/L to the end of the experiment. In contrast, the DIC concentrations of the mixed samples of Byrds Mill Spring and Antelope Spring decreased steadily from ~8.4 to 3.2 mM/L for 214 h and then increased continuously to 4.6 mM/L to the end of the experiment (Fig. II-2f). The behavior in the DIC concentrations in unmixed Byrds Mill Spring for the first 148 h was similar to those of the field samples. The mixed laboratory samples showed a continuous decrease in DIC concentrations similar to the unmixed sample but

of a greater magnitude and the increase in DIC concentrations near the end of the experiment was not observed in the unmixed samples (Fig. II-2f). Unlike the alkalinity concentrations that decreased very slowly at the beginning of the experiments (Fig. II-2c and d), the DIC concentrations (Fig. II-2e and f) clearly show steady continuous decreases throughout the experiment.

4.2 Ca^{2+}, Mg^{2+} and TDS

For the field samples, the Ca^{2+} concentrations from Antelope Spring decreased from ~2.0 to 1.8 mM/L for the first two sampling stations (first 10 m) and then remained nearly constant at ~1.8 mM/L to the end of the sampling distance (Fig. II-3a). In contrast, the Ca^{2+} concentrations stayed at ~ 1.8 mM/L for the Buffalo Spring and increased from 1.9 to 2.0 mM/L for the Byrds Mill Spring over the entire sampling distance (Fig. II-3a).

In the laboratory experiment, the Ca^{2+} concentrations of the unmixed sample of Byrds Mill Spring showed an overall decrease from 1.9 to 0.7 throughout the experiment (Fig. II-3b). The Ca^{2+} concentration of the mixed sample from Byrds Mill Spring decreased sharply from 1.8 to 0.5 mM/L for the first 52 h, after which, the Ca^{2+} concentrations showed a gradual and continuous decrease to 0.2 mM/L to the end of the experiment (Fig. II-3b). For the mixed samples of Antelope Spring, the Ca^{2+} concentrations decreased from 1.9 to 0.2 mM/L to the end of the experiment (Fig. II-3b). The behavior of Ca^{2+} concentrations in the initial hours of the laboratory experiment was similar to those of the field samples. Between the mixed and unmixed laboratory samples, the marked decrease in Ca^{2+} concentrations occurred much earlier in the mixed samples compared to that of the unmixed samples (Fig. II-3a and b).

In the field, the Mg^{2+} concentrations of Antelope Spring showed a general decrease from 1.6 to 1.5 mM/L throughout the sampling distance. In contrast, the Mg^{2+} concentration stayed at ~1.6 mM/L for Buffalo Spring and increased from 1.7 to 2.1 mM/L for Byrds Mill Spring over the entire sampling distance (Fig. II-3c).

In the laboratory experiment, Mg^{2+} concentrations of the unmixed sample from Byrds Mill Spring decreased from 1.8 to 1.6 mM/L for the first 3 h and then increased continuously from 1.6 to 1.9 mM/L to the end of the experiment (Fig. II-3d). The Mg^{2+} concentrations of the mixed sample from Byrds Mill Spring increased from 1.5 to 2.5 mM/L throughout the experiment (Fig. II-3d). The Mg^{2+} concentrations of the mixed sample from Antelope Spring stayed almost constant at 1.4 mM/L for the first 72 h, after which it increased sharply from 1.4 to 2.8 mM/L to the end of the experiment (Fig. II-3d). The behavior of the Mg^{2+} concentrations in the initial hours of the laboratory experiment was similar to Byrds Mill spring which increased and different from Antelope Spring and Buffalo Spring in which Mg^{2+} concentrations were nearly constant. The mixed laboratory samples showed marked increases in the Mg^{2+} concentrations after 100 hrs to the end of the experiment compared to the unmixed sample (Fig. II-3c and d).

The TDS concentrations for the field samples showed an overall decrease from 396 to 389 mg/L for Antelope Spring and stayed nearly constant at 391 mg/L for Buffalo Spring over the entire distance (Fig. II-3e). The TDS concentrations for Byrds Mill Spring decreased from 415 to 396 mg/L for the entire sampling distance (Fig. II-4e).

In the laboratory experiment, the TDS concentrations for the unmixed Byrds Mill Spring showed an overall decrease from 389 to 280 mg/L during the experiment (Fig. II-3f). The TDS of the mixed sample from Byrds Mill Spring decreased from 389 to 238 from 0 to 213 h before increasing markedly to 290 mg/L to the end of the experiment (Fig. II-3f). The TDS

concentration of the mixed sample from Antelope Spring decreased from 415 to 263 mg/L from 0 to 117 h, after which it increased sharply to 321 mg/L to the end of the experiment (Fig. II-3f). The TDS concentrations decreases in the initial hours of the laboratory experiment were similar to those of the field samples. The marked decrease in TDS concentrations occurred much earlier compared to the unmixed samples and the increase in TDS concentrations near the end of the experiment was not observed in the unmixed sample (Fig. II-3f).

4.3 $\delta^{13}C_{DIC}$

In the field, the $\delta^{13}C_{DIC}$ for samples from Antelope Spring showed an increase of 0.5‰ from -8.4 to -7.9‰ in the first 32 m and then were increased gradually from -7.9 to -7.4‰ (0.5‰ increase) for the rest of the sampling distance. The $\delta^{13}C_{DIC}$ of the Buffalo Spring increased slowly by 0.7‰ from -8.5 to -7.8‰ throughout the sampling distance (Fig. II-4a). The $\delta^{13}C_{DIC}$ for Byrds Mill Spring increased by 1.4‰ from -8.8 to -7.4‰ for the first 15 m, after which it increased gradually to -6.5‰ (0.9‰ shift) to the end of the sampling distance (Fig. II-5b).

In the laboratory experiment, the $\delta^{13}C_{DIC}$ of the unmixed samples of Byrds Mill Spring increased slowly from -8.8 to -8.2‰ (0.6‰ shift) for the first 7 h then sharply increased to 2.2‰ (6‰ shift) to end of experiment (Fig. II-4b). The $\delta^{13}C_{DIC}$ of the mixed sample from Byrds Mill Spring increased sharply from -8.8 to -1.1‰ (7.7‰ shift) for the first 317 h and stayed constant at -1.1‰ to the end of the experiment (Fig. II-5c). The $\delta^{13}C_{DIC}$ of the mixed sample from Antelope Spring increased gradually from -8.4 to -7.1‰ (1.3‰) for the first 4.5 h and then sharply to -3.0‰ (4.1‰) to end of the experiment (Fig. II-5d). The $\delta^{13}C_{DIC}$ of the field samples increased by 1.0 to 2.3‰ while those for the laboratory experiments increased by 6.0 to7.7‰. The slow increase in the $\delta^{13}C_{DIC}$ of the field samples appear to be captured in the early time of

the laboratory samples. Beyond the slow increase in the $\delta^{13}C_{DIC}$ in the early times, there are increases in the $\delta^{13}C_{DIC}$ evolutionary trajectory at about 1 h, 10 h and 100 h (Fig. II-4b, c and d).

5. Discussion

5.1 DIC evolution and calcite saturation

To understand the behavior of $\delta^{13}C_{DIC}$ during the chemical evolution of DIC in carbonate springs, we need to determine how and when carbon is removed from the DIC pool. Studies of carbonate-rich waters have shown that removal of carbon from the DIC pool is either by $CO_{2(g)}$ outgassing and/or carbonate precipitation (e.g., Dandurand et al., 1982; Herman and Lorah, 1987; 1988; Pentecost, 1995). As $CO_{2(g)}$ is removed from the DIC pool in the field and laboratory experiments, the pH increases (Fig. 2a and b) while DIC concentrations decrease (Fig. II-2e and f). Continuous loss of $CO_{2(g)}$ causes the DIC to evolve towards saturation with respect to calcite (Stumm and Morgan 1981). The modeled distribution of carbonate species (H_2CO_3, HCO_3^-, and CO_3^{2-}) can be used to describe the behavior of DIC during the chemical evolution from undersaturation with respect to calcite to saturation under field conditions (Fig. II-5) and in the laboratory experiments (Fig. II-6). We do not show the results of Buffalo Spring in Figure II-5 because it mimics the behavior of the Antelope Spring. In addition, Buffalo Spring was sampled for 365 m and distance beyond that was assigned to the Antelope Spring. We have devised a schematic representation of the DIC evolutionary stages by compiling the modeled H_2CO_3, HCO_3^- and CO_3^{2-} species from both the field (Fig. II-5) and laboratory (Fig. II-6) experiments and the measured $\delta^{13}C_{DIC}$ (Fig. II-7). We define four stages of the chemical

evolution of DIC evolution from the results shown in Figures II-5 and II-6 as (1) increasing saturation indicated ending at the dashed vertical lines, (2) increasing supersaturation ending at the dash-dot vertical lines, (3) decreasing supersaturation ending at the dotted lines and (4) increasing supersaturation to the end of the experiments. These four stages are represented in Figure 7 and will be used to characterize the chemical evolution of DIC.

As DIC chemically evolves towards saturation in the field and laboratory experiments (dashed vertical lines in Fig. II-5 and Fig. II-6; region 1 of increasing saturation, Fig. II-7), the decrease in the H_2CO_3 concentrations (Fig. II-5c and d; Fig. II-6d, e and f) is accompanied by a brief decrease and subsequent increase in HCO_3^- (Fig. II-5e and f; Fig. II-6g, h and i), and only small increases in the CO_3^{2-} concentrations (Fig. II-5g and h; Fig. II-6j, k and l). After saturation with respect to calcite, the saturation state continues to increase toward greater supersaturation (Fig. II-5a and b; Fig. II-6a, b and c; region 2 of increasing supersaturation, Fig. II-7), while the concentration of H_2CO_3 continues to decrease (Fig. II-5c and d; Fig. II-6d, e and f), HCO_3^- concentrations are nearly at steady state (Fig. II-5e and f; Fig. II-6g, h and i) and sharp increases are observed in the CO_3^{2-} concentrations (Fig. II-5g and h; Fig. II-6j, k and l). The chemical evolution of DIC in the field only goes through stages 1 and 2 (Fig. II-5).

The results of the temporal chemical saturation state with respect to calcite and speciation of DIC in the laboratory reactors are shown in Figure II-6. In the panels in Figure II-6, saturation is indicated by the dashed vertical lines, the end of increased supersaturation by the dash-dot vertical lines, while the dotted lines indicate the time period when decreasing supersaturation reverses (Fig. II-6a, b and c). The laboratory samples evolved to saturation with respect to calcite by $CO_{2(g)}$ loss from the DIC pool. As the samples evolved from undersaturation to saturation (Fig. II-6a, b and c; region 1 of increasing saturation, Fig. II-7), decreases in H_2CO_3

concentrations (Fig. II-6d, e and f) was accompanied by an overall decrease followed by a modest increase in the HCO_3^- concentrations (Fig. II-6g, h, and i) and virtually no change in the CO_3^{2-} concentration (Fig. II-6j, k and l). At saturation (dash line, Fig. II-6), the samples continued to evolve to greater supersaturation (dash-dot line, Fig II-6; region 2 of increasing supersaturation, Fig. II-7) with continued decreases in H_2CO_3 concentrations (Fig. II-6d, e and f) accompanied by nearly constant HCO_3^- concentrations seen mainly in the unmixed sample (Fig. II-6g) and increasing CO_3^{2-} concentrations (Fig. II-6j, k and l). Note that the nearly constant concentration of HCO_3^- is seen in the field samples (Fig. II-5e and f) and mainly in the unmixed sample (Fig. II-6g).

After the laboratory samples reach the highest supersaturation, the degree of supersaturation begins to decrease to a point where it reverses and increases (Fig. 6b and c; region 3 of decreasing supersaturation, Fig. II-7). During DIC evolution as supersaturation decreases, all the H_2CO_3 has been consumed (Fig. II-6d, e and f), HCO_3^- concentrations decrease markedly (Fig. II-6g, h and i) and CO_3^{2-} concentrations increase markedly (Fig. II-6j, k and l). When the decrease in supersaturation reverses and increases (dotted line, Fig. II-6b and c; region 4 of increasing supersaturation, Fig. II-7), the concentration of the HCO_3^- suddenly increases (Fig. II-6h and i) and the concentration of CO_3^{2-} increases even more sharply (Fig. II-6j, k and l). We attribute this increase in the HCO_3^- and CO_3^{2-} concentrations during supersaturation to evaporation from the open reactors (e.g., Abongwa and Atekwana, 2013).

We did not measure Ca^{2+} and Mg^{2+} of precipitates in the field and laboratory experiments. We are therefore unable to calculate the partition coefficient of Mg (D_{Mg}) = $[(Mg/Ca)_{calcite}/(Mg/Ca)_{solution}]$ which should provide addition chemical support for carbonate precipitation in the field and laboratory experiments (e.g., Morse and Bender, 1990; Burton and

Walter, 1991; Huang and Fairchild, 2000). However, we use the marked decrease in the DIC (Fig. II-8a, b and c) and Ca^{2+} (Fig. II-8d, e and f) concentrations with increasing Mg^{2+}/Ca^{2+} ratio to suggest that during stage 1 and stage 2, decrease in DIC can be accounted for by both $CO_{2(g)}$ loss and calcite precipitation and that during decreasing supersaturation (stage 3) followed by increasing supersaturation (stage 4) very little carbon was lost from the DIC pool. Infact, although the DIC and Ca^{2+} concentrations stays mostly constant relative to the Mg^{2+}/Ca^{2+}, the concentrations of Mg^{2+} increase most rapidly during decreasing saturation followed by increasing saturation (Fig. II-8g, h and i). The effect of evaporation, although occurring throughout the experiment, is magnified over time and is characterized by reversal of decreasing concentrations of HCO_3^- (Fig. II-2d), DIC (Fig. II-2f) and TDS (Fig. II-3f) in the mixed samples shortly after 100 h. This evapoconcentration is also characterized by rapidly increasing Mg^{2+} concentrations in the mixed samples (Fig. II-3d) shortly after 100 h (Fig. II-3f).

5.2 Changes in the $\delta^{13}C_{DIC}$ during the chemical evolution of carbonate springs

Our results show that although DIC evolution for the carbonate springs is a continuum, the field samples only evolved from undersaturation to supersaturation (e.g., Fig. II-5). The results of the laboratory experiments demonstrated how the continued evolution of the field samples would proceed in a state of supersaturation and under the effects of evaporation at supersaturation (Fig. II-6). We modeled the $\delta^{13}C_{DIC}$ changes that accompany $CO_{2(g)}$ loss and calcite precipitation as the samples evolved through increasing saturation, increasing supersaturation, decreasing supersaturation and increasing supersaturation by isotopic and mass balance using NETHPATH (Plummer et al., 1994). The $\delta^{13}C_{DIC}$ associated with $CO_{2(g)}$ ranged from 0.01 to 0.1‰ and that for $CaCO_3$ ranged from 0.01 to 0.1‰ for the evolutionary time steps (Fig. II-9a, b and c). The

isotope mass balance model suggested that the isotopic composition of the DIC appears to be markedly unrelated to the chemical evolution through the different stages of saturation (Fig. II-9). The difference between the [($\delta^{13}C_{DIC}CO_{2(g)}$ + $\delta^{13}C_{DIC}CaCO_3$) - $\delta^{13}C_{DIC}$ measured] represents the $\delta^{13}C_{DIC}$ from DIC equilibration with atmospheric $CO_{2(g)}$ and ^{13}C exchange between DIC and atmospheric $CO_{2(g)}$ (Fig. II-9a, b and c). The $\delta^{13}C_{DIC}$ from DIC equilibration with atmospheric $CO_{2(g)}$ is very close to our measured $\delta^{13}C_{DIC}$ (Fig.II- 9a, b and c). This suggest that the bulk of the fractionation associated with the isotopic evolution of the carbonate spring samples is from equilibration of carbon in the DIC with carbon in atmospheric $CO_{2(g)}$.

The isotopic mass balance suggests that speciation results do not provide greater insights into the $\delta^{13}C_{DIC}$ behavior (Fig. II-9). Since the DIC is a bulk parameter the DIC behavior should be directly compared with the $\delta^{13}C_{DIC}$ to elucidate the main control on the isotopic behavior. The four tier DIC evolutionary behavior (Fig. II-7) is observed when the log pCO_2 is plotted vs. DIC concentrations (Fig. II-10a-d). In the panels of Figure II-10a-d, the vertical dashed lines represent the log pCO_2 of the atmosphere (log $10^{-3.5}$ atm.). The arrows in each of the panel show the direction of the chemical evolution and the circled numbers represent the different evolutionary steps represented in Figure II-7. We plot the concentration of the DIC at any time (C_t) divided by the concentration of the DIC at discharge points of the spring or the start of the laboratory experiments (C_0) (i.e., C_t/C_0 vs. $\delta^{13}C_{DIC}$) to characterize the $\delta^{13}C_{DIC}$ changes during DC evolution (Fig. II-10e, f, g, h). This relationship is used to demonstrate how DIC concentrations and $\delta^{13}C_{DIC}$ in a continuously evolving water sample will change in a DIC-$\delta^{13}C$ space (Abongwa and Atekwana, 2013).

As the spring and reactor samples evolve from undersaturation to saturation, the decreases in DIC and increase in pH is caused by the outgassing of excess $CO_{2(g)}$ due to the initial high $CO_{2(g)}$

concentration in solution (e.g., Worrall and Lancaster, 2005; Doctor et al., 2008). We observe a rapid decrease in the DIC concentrations with relatively no change in the pCO_2 shown by the arrow labeled 1 in Fig. II-10a-d. Since the pCO_2 is computed using the alkalinity, the loss of the excess $CO_{2(g)}$ has little effect on the alkalinity. The decrease in DIC results in a less than 1.2‰ increase in the $\delta^{13}C_{DIC}$ (Fig. II-10e-h).

As the samples progress from a saturated to increased supersaturated state, it appears that very little DIC is lost from solution (arrow labeled 2; Fig II-10 a-d). This is best characterized by the unmixed Byrds Mill Spring reactor sample (Fig. II-10b) which shows virtually no change in the DIC concentrations despite the fact that there is a significant decrease in the pCO_2. For the DIC to remain constant, this step must be a DIC species redistribution step. The decreases in the H_2CO_3 concentrations (increasing supersaturation, Fig. II-7) was accompanied by nearly constant HCO_3^- concentrations seen mainly in the unmixed sample (Fig. II-6g) and increasing CO_3^{2-} concentrations (Fig. II-6j, k and l). The large increase in the pH during this step resulted from DIC species shift from H_2CO_3 to CO_3^{2-}. The $\delta^{13}C_{DIC}$ increase during this stage by about 1‰ (Fig. II-10 e-h) suggesting that isotopic fractionation may still be kinetic. However, with no decrease in DIC concentrations, there should be no isotopic fractionation. We hypothesize that although no DIC is lost, the difference in the $\delta^{13}C_{DIC}$ and the expected equilibrium value with respect to atmospheric $CO_{2(g)}$ might cause the enrichment observed. In other words, with no DIC loss, ^{13}C enrichment occurs by isotopic exchange of carbon between DIC and atmospheric $CO_{2(g)}$ (e.g., Abongwa and Atekwana, 2013).

After the reactor samples reached maximum supersaturation, the supersaturation state begins to decrease, characterized by a marked decrease in HCO_3^- concentrations (Fig. II-6g, h and i) and increases in CO_3^{2-} (Fig. II-6j, k and l) concentrations (region of decreasing supersaturation, Fig.

II-7). There is concomitant decrease in the pCO_2 and in the DIC concentrations (Arrow labeled II-3; Fig. II-10b, c and d). The $\delta^{13}C_{DIC}$ increases as the DIC concentrations and pCO_2 decrease (Fig. II-10f, g and h). The decrease in the DIC concentrations during this step is from $CO_{2(g)}$ loss induced by chemical equilibration of C in DIC with atmospheric $CO_{2(g)}$. The ^{13}C enrichment due to equilibration enriches the ^{13}C of DIC by ~7.9‰ at 25^0C (Mook et al., 1974). The $\delta^{13}C_{DIC}$ during the period of decreasing saturation increased by up to 5.9‰ in the laboratory samples, indicating that the $\delta^{13}C_{DIC}$ of the solutions are not in isotopic equilibrium with atmospheric $CO_{2(g)}$. Measured $\delta^{13}C$ values of $CO_{2(g)}$ for the laboratory and outside air during the experiments ranged from -9.5 to -12.0‰ (n=5). Using a fractionation factor of 8.5 to 7.9‰ at 25 ^0C and pH above 6.4 (Mook et al., 1974; Clark and Fritz, 1997), DIC in the samples that achieve equilibrium with $CO_{2(g)}$ in the laboratory and outside air will have $\delta^{13}C_{DIC}$ values ranging between -1.0 and -3.5‰. The DIC in the reactor samples did not reached isotopic equilibrium with the laboratory or outside atmospheric $CO_{2(g)}$.

The increase in the DIC concentrations during the period when the decreasing supersaturation reverses to increasing supersaturation near the end of the experiment (region of increasing supersaturation, Fig. II-7; Fig. II-10b, c and d) is attributed to evaporation (Abongwa and Atekwana, 2013). The isotopic enrichment of 2-3‰ during this period could be a continuation of the equilibrium isotopic enrichment of DIC towards the laboratory or outside atmospheric $CO_{2(g)}$. Because the DIC concentrations increased during the increased supersaturation phase, the isotopic evolution can be described by ^{13}C enrichment from C exchange between DIC and atmospheric $CO_{2(g)}$. The $\delta^{13}C_{DIC}$ values at the end of the laboratory experiment were -2.0‰ for the unmixed Byrds Mill Spring, -1.1‰ for the mixed Byrds Mill Spring and -2.5‰ for mixed Antelope Spring samples. At the end of the laboratory experiment,

the DIC of samples were at or near equilibrium with $CO_{2(g)}$ in the laboratory or outside atmosphere as the $\delta^{13}C_{DIC}$ values were between -1.0‰ and -3.5‰ modelled for the $\delta^{13}C_{DIC}$ of samples in isotopic equilibrium with atmospheric $CO_{2(g)}$ in the laboratory or outside.

6. Conclusions

We performed field and laboratory experiments on carbonate springs that evolved to saturation with respect to calcite and to equilibrium with atmospheric $CO_{2(g)}$. We modeled the distribution of carbonate species (H_2CO_3, HCO_3^-, CO_3^{2-}) during this evolution. High initial pCO_2 causes CO_2 outgassing that drives DIC evolution towards calcite supersaturation and to equilibrium with atmospheric $CO_{2(g)}$. We define four evolutionary phases during this evolution: increasing saturation, increasing supersaturation, decreasing supersaturation and increasing supersaturation. The $\delta^{13}C$ during the evolution of DIC increased throughout. During increasing saturation the fractionation of the 1-2‰ increase in the $\delta^{13}C_{DIC}$ was by kinetic isotopic fractionation. During the increasing supersaturation, the 1‰ increase in the $\delta^{13}C_{DIC}$ was from carbon isotopic exchange with atmospheric $CO_{2(g)}$ since no C was lost from the DIC pool. During decreasing supersaturation the ~5‰ increase in the $\delta^{13}C_{DIC}$ was from C equilibration with atmospheric $CO_{2(g)}$. Although the final phase of increasing saturation was driven by evapoconcentration, ~2‰ the isotopic enrichment was controlled by C exchange with atmospheric CO2 as C was not lost from the DIC pool. Isotopic and mass balance calculations revealed that $\delta^{13}C_{DIC}$ change accompanying the $CO_{2(g)}$ outgassing and calcite precipitation at each sampling interval in the laboratory experiment was about 0.01 to 0.1‰. Estimated $\delta^{13}C_{DIC}$ for the samples suggest that the bulk of the fractionation associated with the evolution of the

spring samples evolving chemically and isotopically in contact with $CO_{2(g)}$ in the atmosphere is from equilibration of DIC in the samples and carbon in atmospheric $CO_{2(g)}$.

Our results showed that sample agitation enhanced $CO_{2(g)}$ loss rate as well as carbon exchange between the springs DIC and atmospheric $CO_{2(g)}$. Evaporative loss rate was also increased by agitation resulting in increases in DIC concentrations. Based on our results, field samples only evolved to the stage of increasing supersaturation and thus its $\delta^{13}C$ was controlled mainly by kinetic isotopic fractionation from $CO_{2(g)}$ loss from the samples. Our study shows that significant enrichment of the $\delta^{13}C$ of carbonate springs only occur in the decreasing calcite supersaturation state. This state is not commonly achieved in field settings because of the limited flow distance which hampers investigation of carbonate evolution beyond calcite saturation. The results of this study could be applied to any highly charged $CO_{2(g)}$ system that evolve to calcite supersaturation conditions such as flowing rivers or lakes that are fed by $CO_{2(g)}$ dominated groundwater.

Acknowledgements

We thank R. Ross of US EPA, Ada, OK, T. Halihan, J. Puckette and staff of the Chickasaw National Recreation Area, Sulfur, OK, for logistic assistance. We also thank L. Guidry, C. Luckett, E. Akoko and K. Flinton for assistance in the field. We thank the two anonymous reviewers for their insightful comments and suggestions that help improve this manuscript.

References

Abongwa, P.T., Atekwana, E.A., 2013. Assessing the temporal evolution of dissolved inorganic carbon in waters exposed to atmospheric $CO_{2(g)}$: A Laboratory Approach. Journal of Hydrology 505, 250-265.

Akoko, E., Atekwana, E.A., Cruse, A.M., Molwalefhe, L. Masamba, W.R.L., 2013. River-wetland interaction and carbon cycling in a semi-arid riverine system: The Okavango Delta, Botswana. Biogeochemistry 114, 359-380.

Atekwana, E.A., Krishnamurthy, R.V., 1998. Seasonal variations of dissolved inorganic carbon and $\delta^{13}C$ of surface waters: application of a modified gas evolution technique. Journal of Hydrology 205, 265-278.

Burton, E.A., Walter, L.M., 1991. The effects of P_{CO2} and temperature on magnesium incorporation in calcite in seawater and $MgCl_2$-$CaCl_2$ solutions. Geochimica et Cosmochimica Acta 55, 777-785.

Campbell, J.A., Weber, J.L., 2006. Wells drilled to basement in Oklahoma: Oklahoma geological Survey Special Publication 2006-1.

Christenson, S., Hunt, A.G. and Parkhurst, D.L., 2009. Geochemical investigation of the Arbuckle-Simpson aquifer, south-central Oklahoma, 2004-06: U.S. Geological Survey: Scientific Investigations report 2009-5036, 50 p.

Clark, I.D., Fritz, P., 1997. Environmental Isotopes in Hydrogeology. CRC Press, 352 p.

Dandurand, J.L., Gout, R., Hoefs, J., Menschel, G., Schott, J., Usd owski, E., 1982. Kinetically controlled variations of major components and carbon isotopes in a calcite-precipitating spring. Chemical Geology 36, 299-315.

Doctor, H.D., Kendall, C., Sebestyen, S.D., Shanley, T.B., Ohte, N., Boyer, E.N., 2008. Carbon isotope fractionation of dissolved inorganic carbon (DIC) due to outgassing of carbon dioxide from a headwater stream. Hydrological Processes 22, 2410-2423.

Donovan, R.N., 1991. The Arbuckle group – An aid de memoire, *in* Johnson, K.S., ed., Arbuckle Group Core Workshop and field Trip: Oklahoma Geological Survey. Special Publication 91-3, 199-208.

Dreybrodt, W., Buhmann, D., Michaelis, J. and Usdowski, E., 1992. Geochemically controlled calcite precipitation by CO_2 outgassing: Field measurements of precipitation rates in comparison to theoretical predictions. Chemical Geology 97, 285-294.

Fairchild, R.W., Hanson, R.L. and Davis, R.E., 1990. Hydrology of the Arbuckle Mountains area, south-central Oklahoma: Oklahoma Geological Survey Circular 91, 112 p., 2 plates, scale 1:100,000.

Groves, C.G., 1992. Geochemical and kinetic evolution of a karst flow system: Laurel Creek, West Virginia. Ground Water 30, 186-191.

Hach Company, 1992. Water Analysis Handbook. Hach Company, Loveland, Co.

Ham, W.E., 1955. Field conference on the geology of the Arbuckle Mountain region: Oklahoma Geological Survey Guide Book III, 61 p.

Hanson, R.L., Cates, S.W., 1994. Hydrology of the Chickasaw National Recreation Area, Murray County, Oklahoma: U.S. Geological Survey Water-Resources Investigations Report 94-4102, 86 p., 2 plates, scale 1:24,000.

Herman, J.S. and Lorah, M.M., 1986. Groundwater geochemistry in Warm River Cave, Virginia. National Society of Speleotherm Bulletin 48, 54-61.

Herman, J.S. and Lorah, M.M., 1987. CO_2 outgassing and calcite precipitation in Falling Spring creek, Virginia, U.S.A. Chemical. Geology 62, 251-262.

Hess, J.W., White, W.B., 1988. Storm response of the karstic carbonate aquifer of southcentral Kentucky. Journal of Hydrology 99, 235-252.

Hoffer-French, K.J., Herman, J.S., 1989. Evaluation of hydrological and biological influences on CO_2 fluxes from a karst stream. Journal of Hydrology 108, 189-212.

Huang, Y. and Fairchild, I.J., 2000. Partioning of Sr^{2+} and Mg^{2+} into calcite under karst-analogue experimental conditions. Geochimica et Cosmochimica Acta 65, 47-62.

Jacobson, R. and Usdowski, E., 1975. Geochemical controls on a calcite precipitating spring. Contributions to Mineralogy and Petrology 51, 65-74.

Lu, G., Zheng, C., Donahoe, R.J. and Lyons, W.B., 2000. Controlling processes in $CaCO_3$ precipitating stream in Huanglong Natural Science District, Sichuan, China. Journal of Hydrology 230, 34-54.

Marfia, A.M., Krishnamurthy, R.V., Atekwana, E.A., Panton, W.F., 2004. Isotopic and geochemical evolution of ground and surface waters in a karst dominated geological setting: a case study from Belize, Central America. Applied Geochemistry 19, 937-946.

Mills, A., Urey, H.C., 1940. The kinetics of isotope exchange between carbon dioxide, bicarbonate ion, carbonate ion, and water. Journal of American Chemistry Society 62, 1019-1026.

Mook, W.G., Bommerson, J.C., Staverman, W.H., 1974. Carbon isotope fractionation between dissolved bicarbonate and gaseous carbon dioxide. Earth and Planetary Science Letters 22, 169-176.

Morse, J,W., Bender, M.L., 1990. Partition coefficientsin calcite: Examination of factors influencing the validity of experimental results and their application to natural systems. Chemical Geology 82, 265-277.National Climatic Data Center, 2013. Climatography of the United States: Station # COOP: 340017, 1960-2010: Ada, Oklahoma, USA, Precipitation Totals, accessed September 13, 2013, at *http:/www1.ncdc.noaa.gov/pub/orders/cdo/205233.csv.*

Oklahoma Climatological Survey, 2012: Accessed for the towns of Sulphur and Fittstown, OK, April and September 2012 at *http:/www.climate.ok.gov.*

Parkhurst, D.L. and Appelo, C.A.J., 1999. User's Guide to PHREEQC (Version 2.1)-A Computer Program for Speciation, Batch-Reactions, One-Dimensional Transport and Inverse Geochemical Calculations. U.S. Geological Survey, Water Resource Investigation Report, 99-4256.

Pentecost, A., 1995. Geochemistry of carbon dioxide in six travertine-depositing waters in Italy. Journal of Hydrology 167, 263-278.

Plummer, L.N., Prestemon, E.C., and Parkhurst, D.L., 1994. *An interactive code (NETPATH) for modeling net geochemical reactions along a flow path Version 2.0*. Water-Resources *Investigations Report 94-4169. Reston, Virginia: U.S. Geological Survey.http//wwwbrr.cr.usgs.gov/projects/GWC_coupled/nethpath.*Li, S.L., Liu, C.Q., Li, J., Lang, Y.C., Ding, H., Li, L., 2010. Geochemistry of dissolved inorganic carbon and carbonate weathering in a small typical karstic catchment of southwest China: Isotopic and chemical constraints. Chemical Geology 277, 301-309.

Stiller, M., Rounick, J.S., Shasha, S., 1985. Extreme carbon-isotope enrichment in evaporating brines. Nature 316, 434-435.

Stumm, W., Morgan, J.J., 1981. Aquatic Chemistry: An Introduction Emphasizing Chemical Equilibria in Natural Waters, 2nd edition. Wiley Interscience: New York; 780 p.

Usdowski, E. and Hoefs, J., 1990. Kinetic $^{13}C/^{12}C$ and $^{18}O/^{16}O$ effects upon dissolution and outgassing of CO_2 in the system CO_2-H_2O. Chemical Geology: Isotope Geoscience Section, 80, 109-118.

Usdowski, E., Hoefs, J., Menschel, G., 1979. Relationship between ^{13}C and ^{18}O fractionation and changes in major element composition in recent calcite-depositing spring- A model of chemical variations with inorganic $CaCO_3$ precipitation. Earth and Planetary Science letters 42, 267.

Wicks, C.M. and Engeln, J., 1997. Geochemical evolution of a karst stream in Devils Icebox Cave, Missouri, USA. Journal of Hydrology 198, 30-41.

Worrall, F., Lancaster, A., 2005. The release of excess CO_2 from river waters – the contribution of excess CO_2 from groundwater. Biogeochemistry 76, 299-317.

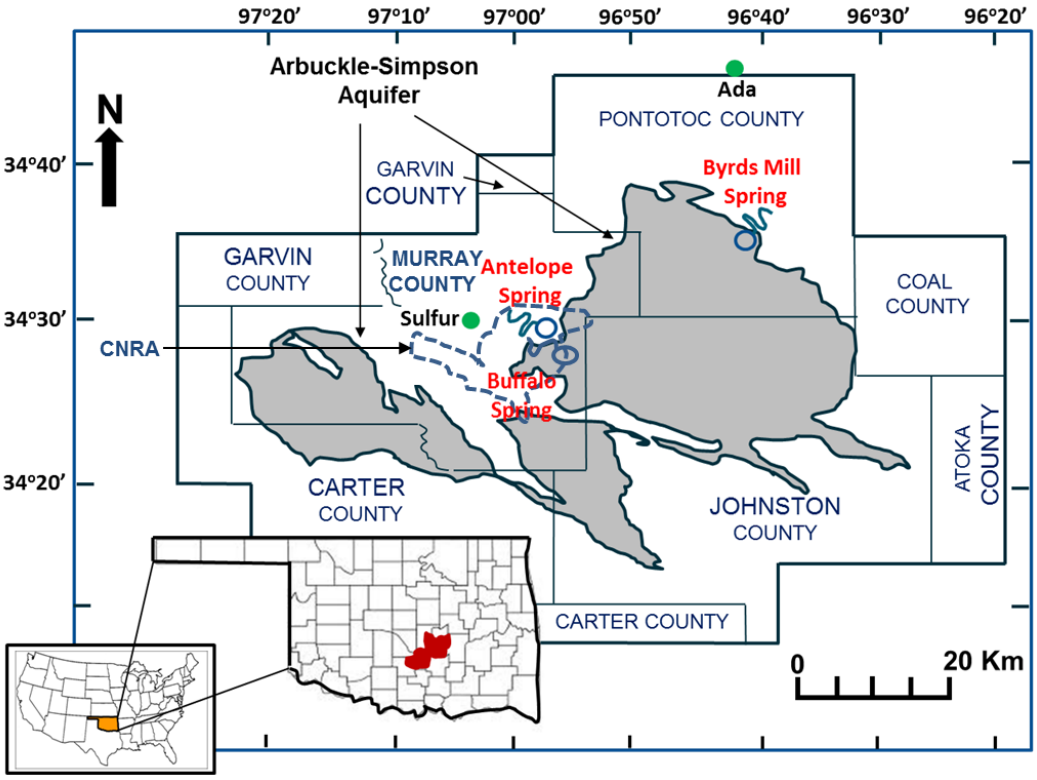

Figure II- 1. Map showing the location of Antelope Spring, Byrds Mill Spring and Buffalo Spring and the aerial extent of the Arbuckle-Simpson Aquifer (Modified from Christenson et al., 2009). Insert shows location of Oklahoma in the USA and counties in south-central Oklahoma where Arbuckle-Simpson aquifer underlies. CNRA = Chickasaw National Recreation Area.

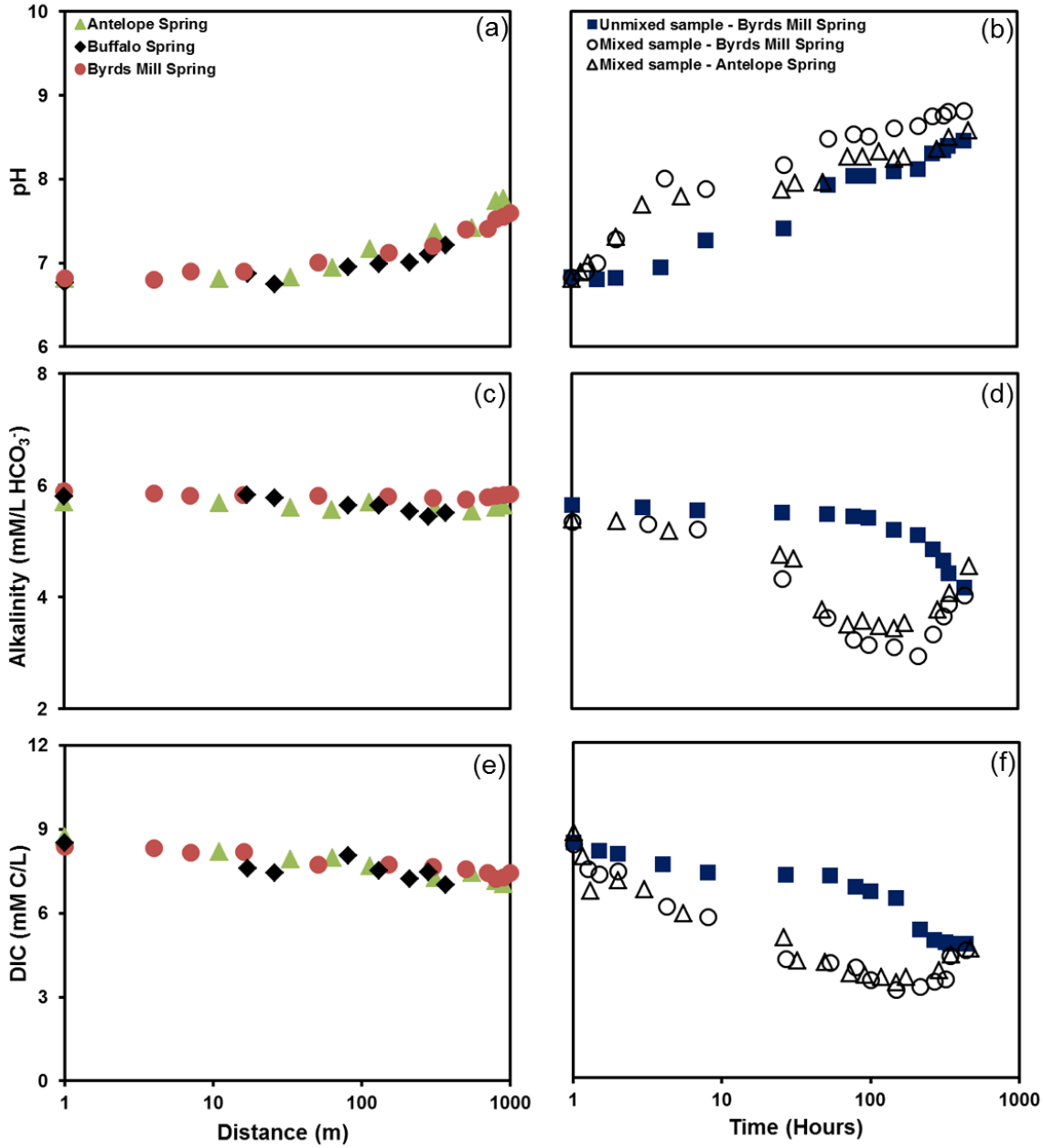

Figure II- 2. Plots of spatial and temporal variation in pH (a and b), of the concentrations of alkalinity (c and d) and the concentrations of dissolved inorganic carbon (DIC) (e and f) for field samples from Antelope, Buffalo and Byrds Mill Springs and mixed samples from Antelope Spring and mixed and unmixed samples from Byrds Mill Spring exposed to the atmosphere in the laboratory. [The first sampling points are at distance 0 m and time 0 hour but we arbitrary started the x-axis at 1 on the log scale.]

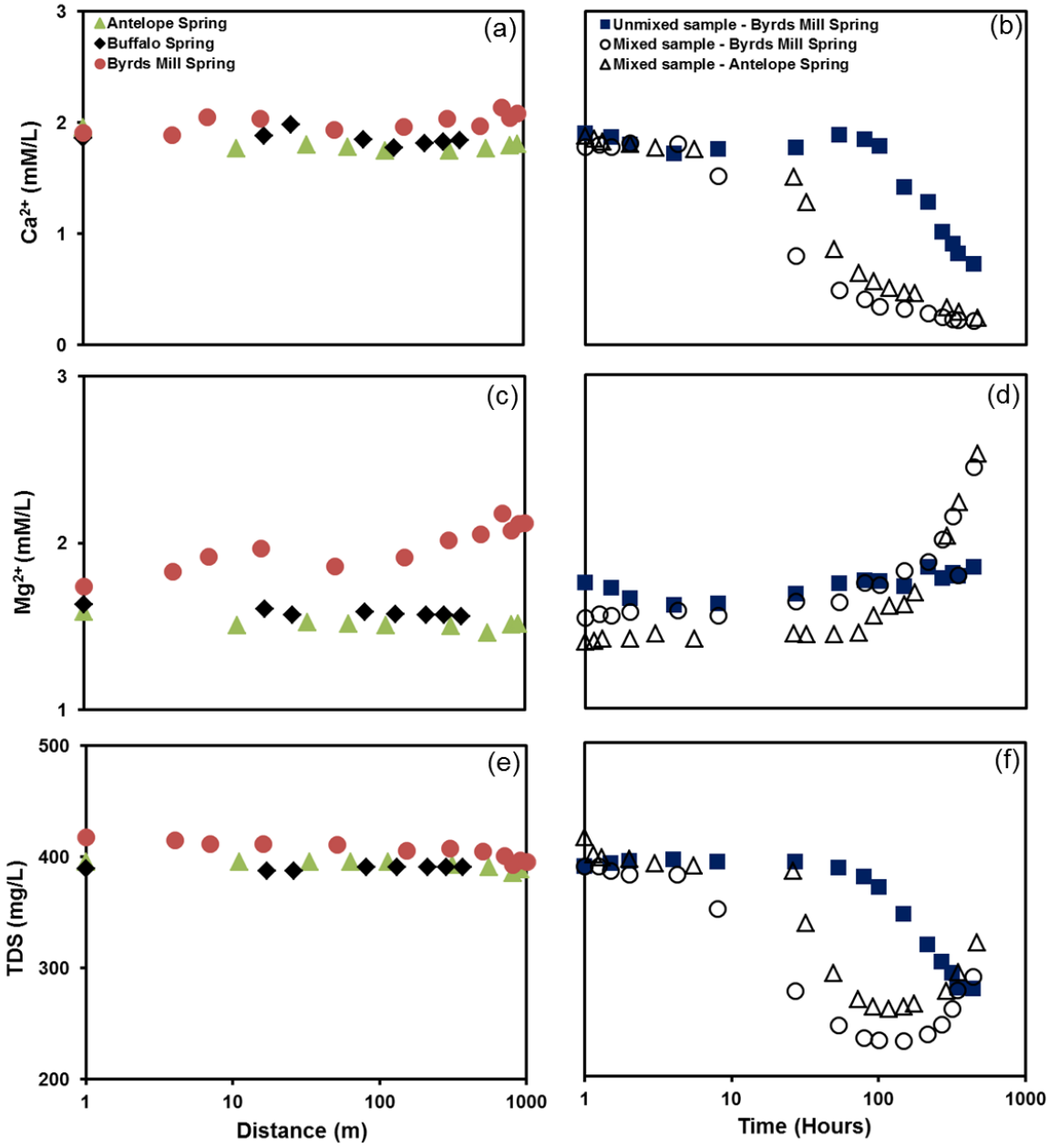

Figure II- 3. Plots of spatial and temporal concentrations of Ca^{2+} (a and b), Mg^{2+} (c and d) and total dissolved solids (TDS) (e and f) for field samples from Antelope, Buffalo and Byrds Mill Springs and mixed samples from Antelope Spring and mixed and unmixed samples from Byrds Mill Spring exposed to the atmosphere in the laboratory. [The first sampling points are at distance 0 m and time 0 hour but we arbitrary started the x-axis at 1 on the log scale.]

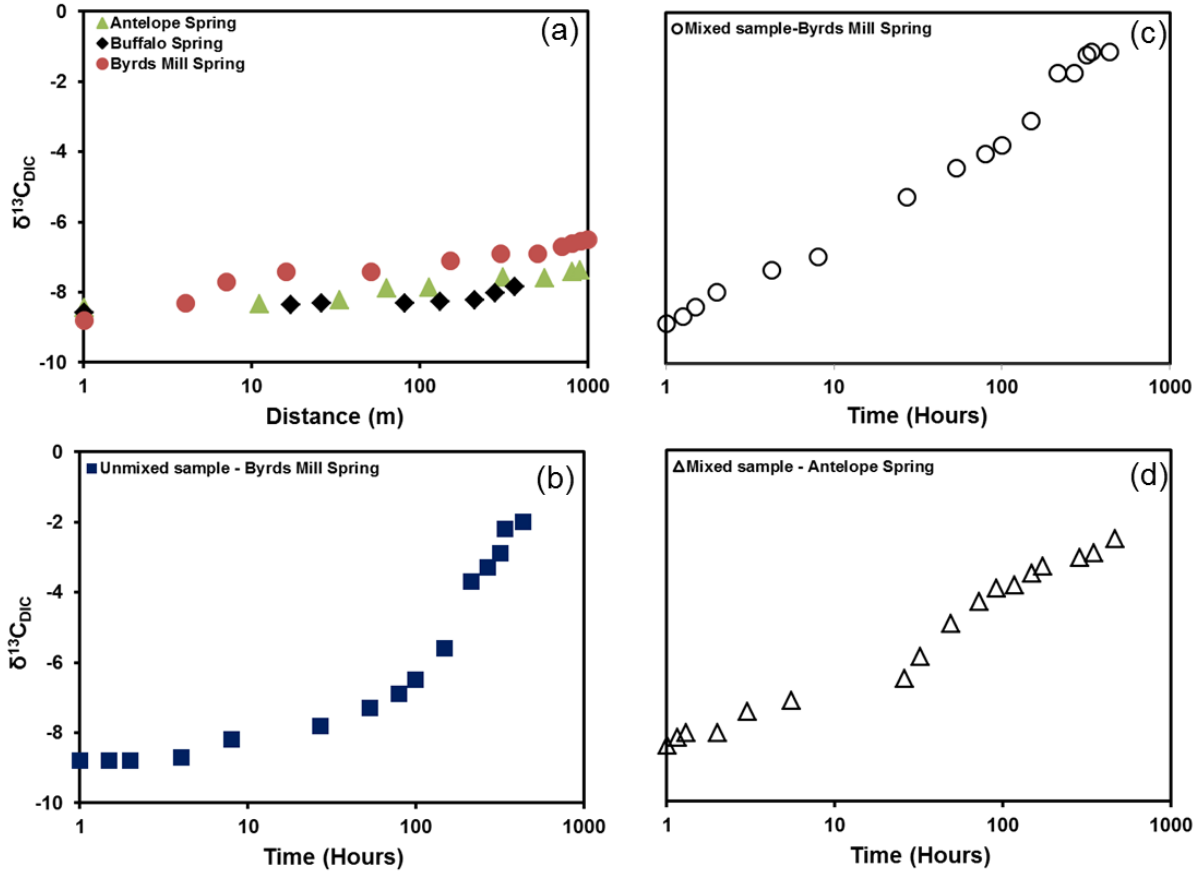

Figure II- 4. Plots of spatial stable carbon isotope composition of dissolved inorganic carbon ($\delta^{13}C_{DIC}$) for the field samples from Antelope Spring, Buffalo Spring and Byrds Mill Spring (a) and plots of the temporal $\delta^{13}C_{DIC}$ for the unmixed sample of the Byrds Mill Spring (b), mixed sample of the Byrds Mill Spring (c) and mixed sample of the Antelope Spring (d) exposed to the atmosphere in the laboratory. [The first sampling points are at distance 0 m and time 0 hour but we arbitrary started the x-axis at 1 on the log scale.]

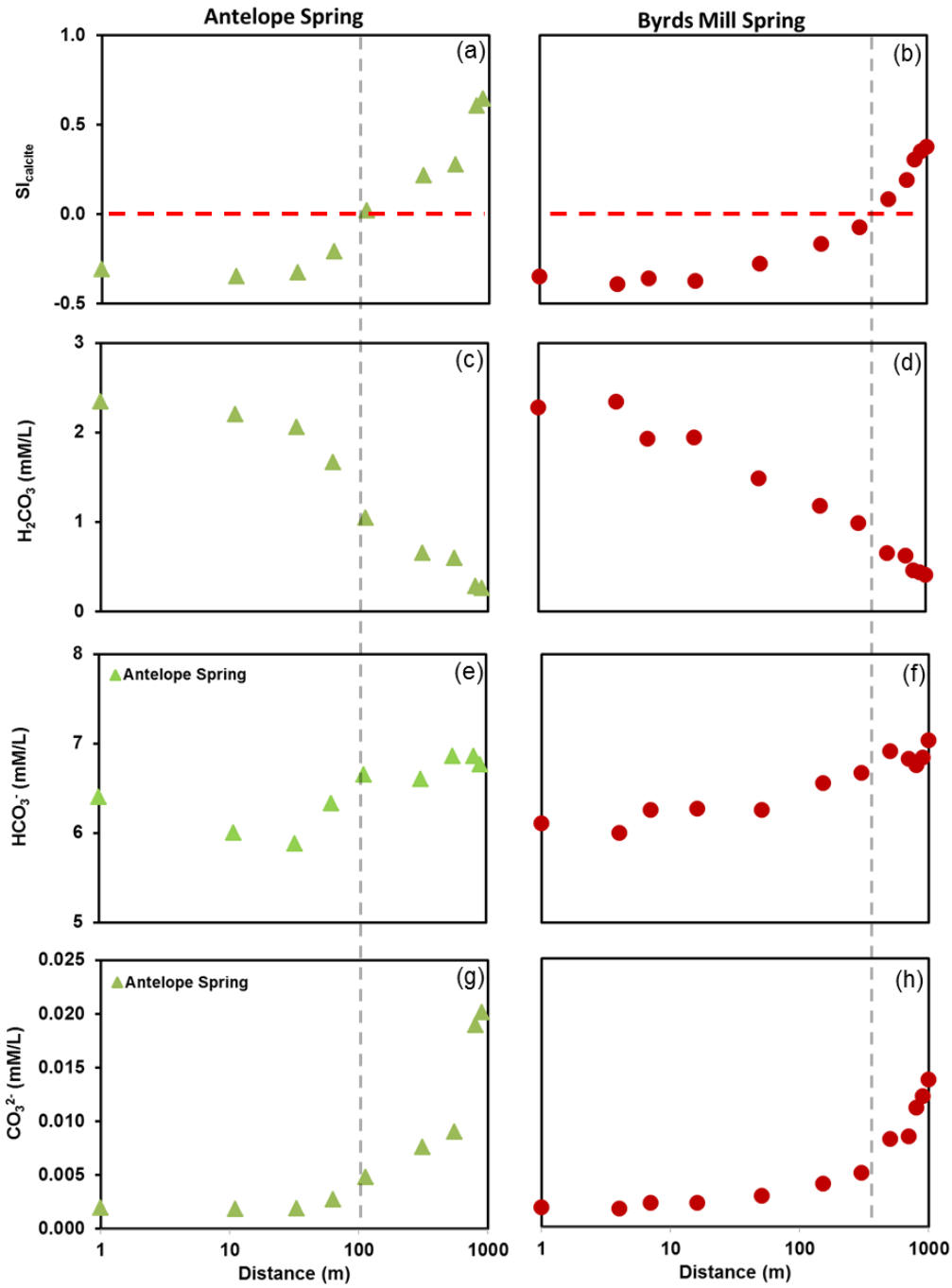

Figure II- 5. Spatial plots of the saturation indices with respect calcite ($SI_{calcite}$) for Antelope Spring (a) and Byrds Mill Spring (b) and modeled carbonate species H_2CO_3 (c and d), HCO_3^- (e and f) and CO_3^{2-} (g and h) for Antelope and Byrds Mill Springs. The dashed horizontal line in panel a and b is the equilibrium saturation line of calcite, i.e., at $SI_{calcite}$ = 0. The dashed vertical lines in panels c-h represent the distance at which the springs achieve saturation with respect to calcite. [The first sampling points are at distance 0 m and time 0 hour but we arbitrary started the x-axis at 1 on the log scale.]

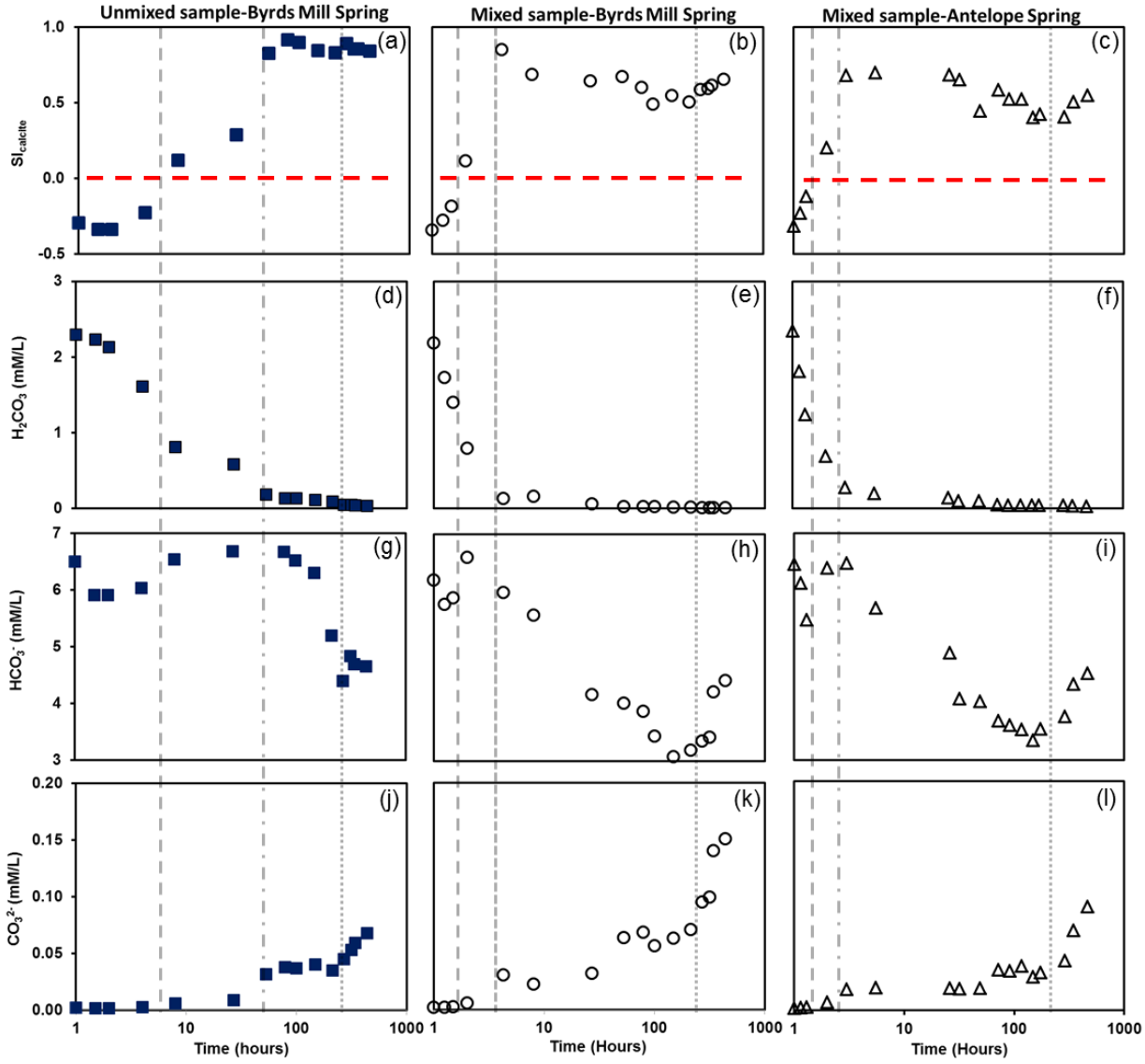

Figure II- 6. Temporal plots of the saturation indices with respect to calcite ($SI_{calcite}$) for unmixed Byrds Mill Spring (a), mixed Byrds Mill Spring (b) and mixed Antelope Spring (c) exposed to the atmosphere in the laboratory. The modeled carbonate specie of H_2CO_3 (d, e and f), HCO_3^- (g, h and i) and CO_3^{2-} (j, k and l) are for unmixed Byrds Mill Spring, mixed Byrds Mill Spring and mixed Antelope Spring, respectively. The dashed horizontal line consistent with previous in panel a, b and c is the equilibrium saturation line of calcite, i.e., at $SI_{calcite}$ = 0 and the vertical lines represent different stages of calcite saturation; the dashed lines represent undersaturation with respect to calcite; the dash-dot lines represent calcite supersaturation and the dotted lines represent the time period when the $SI_{calcite}$ direction reverses from decrease to increase. [The first sampling points are at distance 0 m and time 0 hour but we arbitrary started the x-axis at 1 on the log scale.]

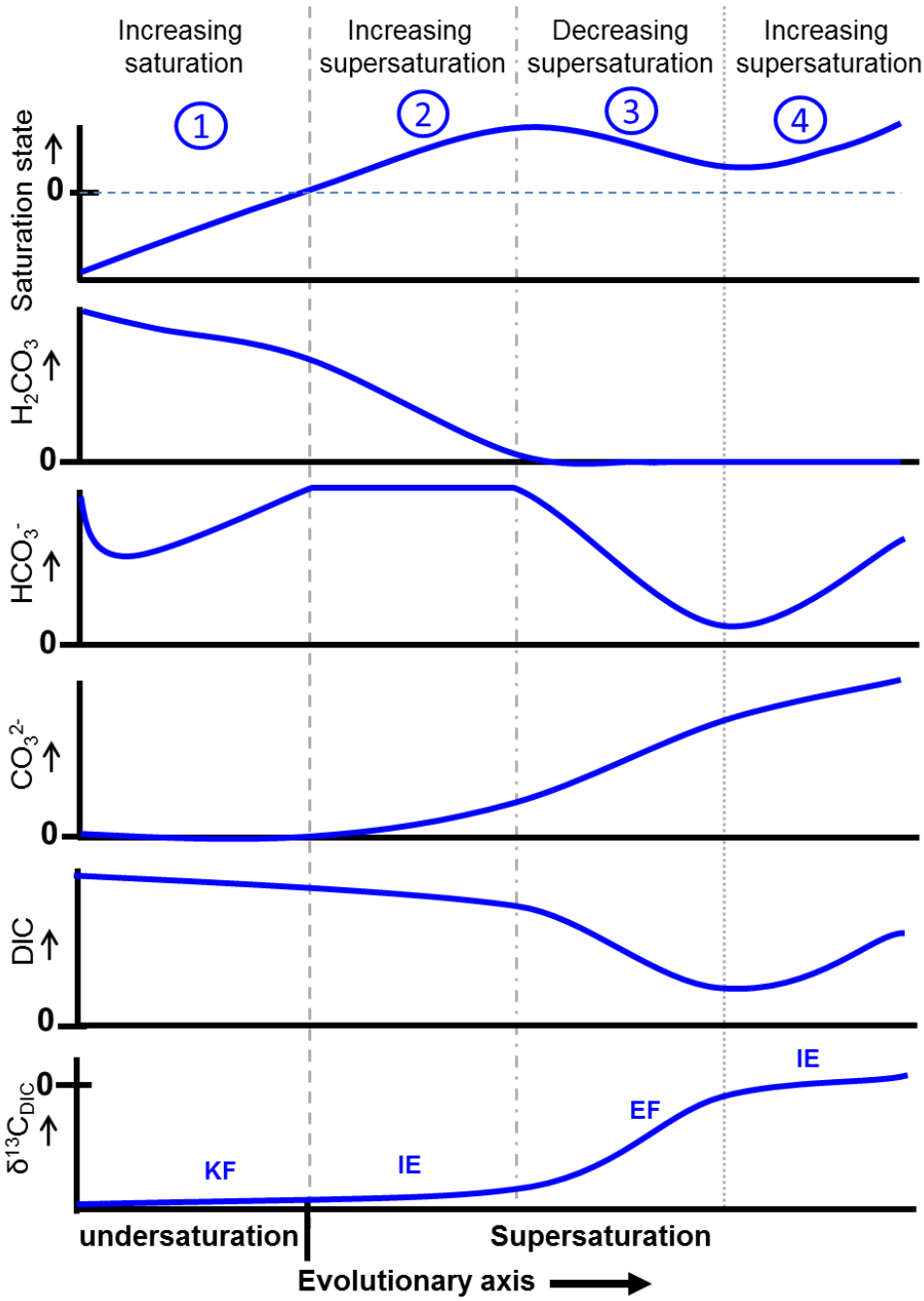

Figure II- 7. Generalized schematic of the saturation state and the behavior of H_2CO_3, HCO_3^-, CO_3^{2-}, dissolved inorganic carbon (DIC) and carbon isotope ratio of DIC ($\delta^{13}C_{DIC}$) distribution during the evolution from undersaturation to supersaturation with respect to calcite. The state of saturation is indicated by: segment (1) undersaturation, (2) increasing supersaturation, (3) decreasing supersaturation and (4) increasing supersaturation. The dashed horizontal line in the panel of saturation state is the equilibrium saturation line of calcite, i.e., at $SI_{calcite} = 0$. The $\delta^{13}C$ increase is caused by kinetic isotopic fractionation (KF in 1), isotopic exchange (IE in 2), equilibrium fractionation (EF in 3) and isotopic exchange (IE in 4).

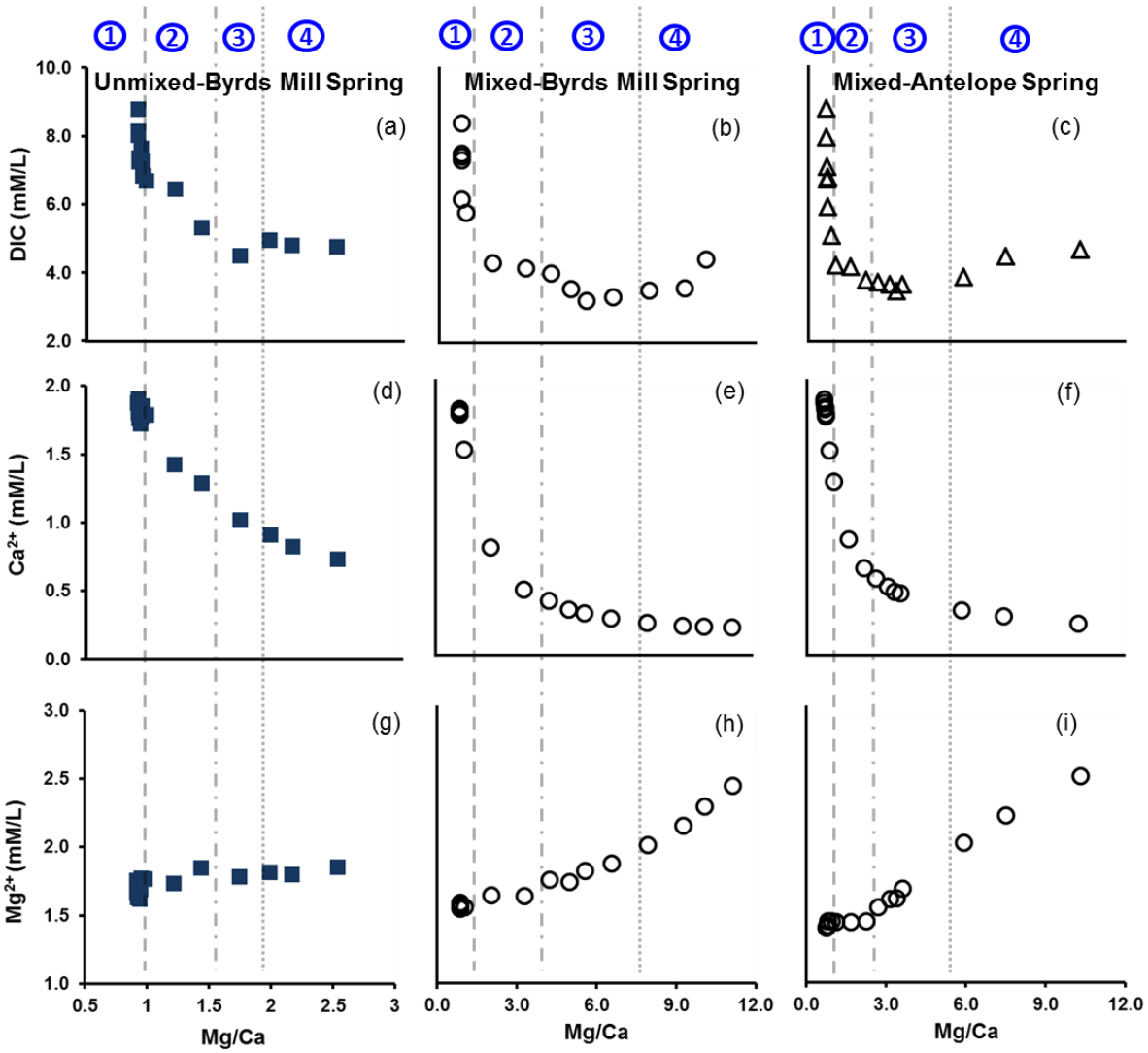

Figure II- 8. Plots of Mg^{2+}/Ca^{2+} ratio vs. DIC concentrations for the unmixed and mixed Byrds Mill Spring and Antelope Spring (a, b and c), Mg^{2+}/Ca^{2+} ratio vs. Ca^{2+} concentrations for the unmixed Byrds Mill Spring, mixed Byrds Mill Spring and Antelope Spring (d, e and f) and Mg^{2+}/Ca^{2+} ratio vs. Mg^{2+} concentrations for the unmixed Byrds Mill Spring, mixed Byrds Mill Spring and Antelope Spring (g, h and i). Segments 1 to 4 represent evolution from undersaturated to supersaturated conditions with respect to calcite as depicted in Fig. 7.

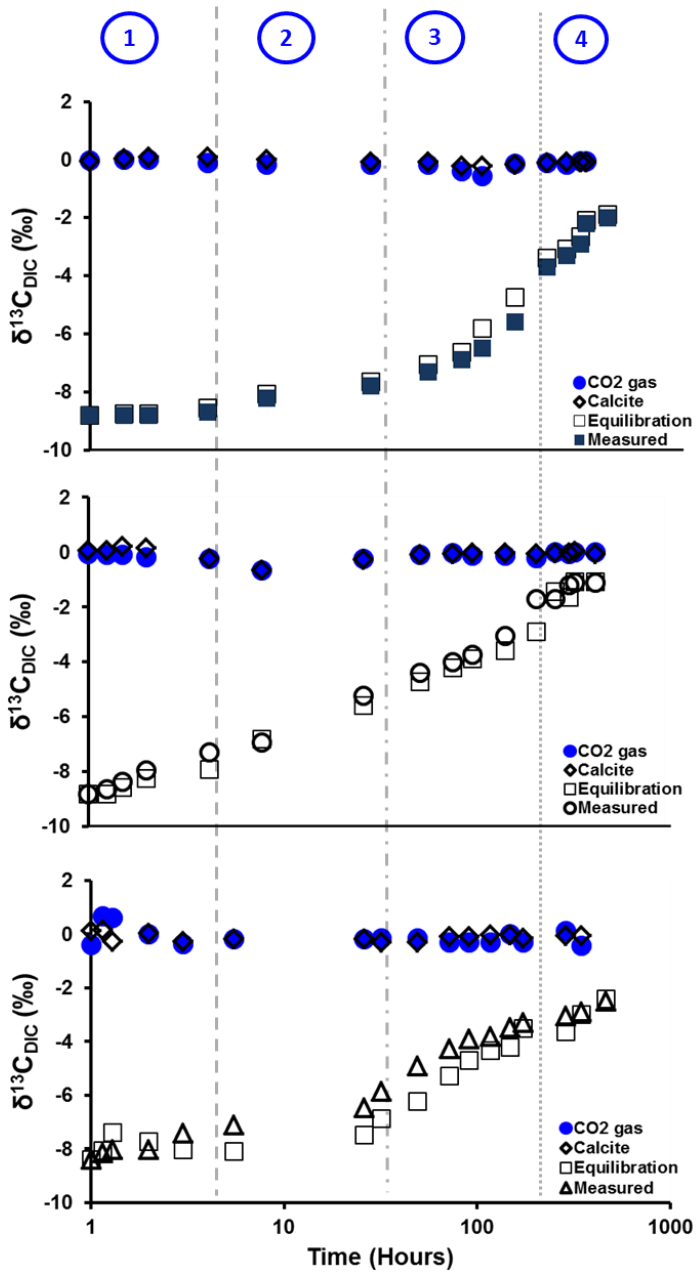

Figure II- 9. Temporal plots of modeled $\delta^{13}C_{DIC}$ using NETHPATH (Plummer et al., 1994) showing isotopic exchange associated with $CO_{2(g)}$ outgassing and calcite precipitating phase, the isotopic exchange associated with equilibration with atmospheric $CO_{2(g)}$ (equilibration) and the measured $\delta^{13}C_{DIC}$ for the laboratory experiments. Segments 1 – 4 shown in the top panel are explained in Fig. 7. [The first sampling point is at time 0 hour but we arbitrary started the x-axis at 1 on the log scale.]

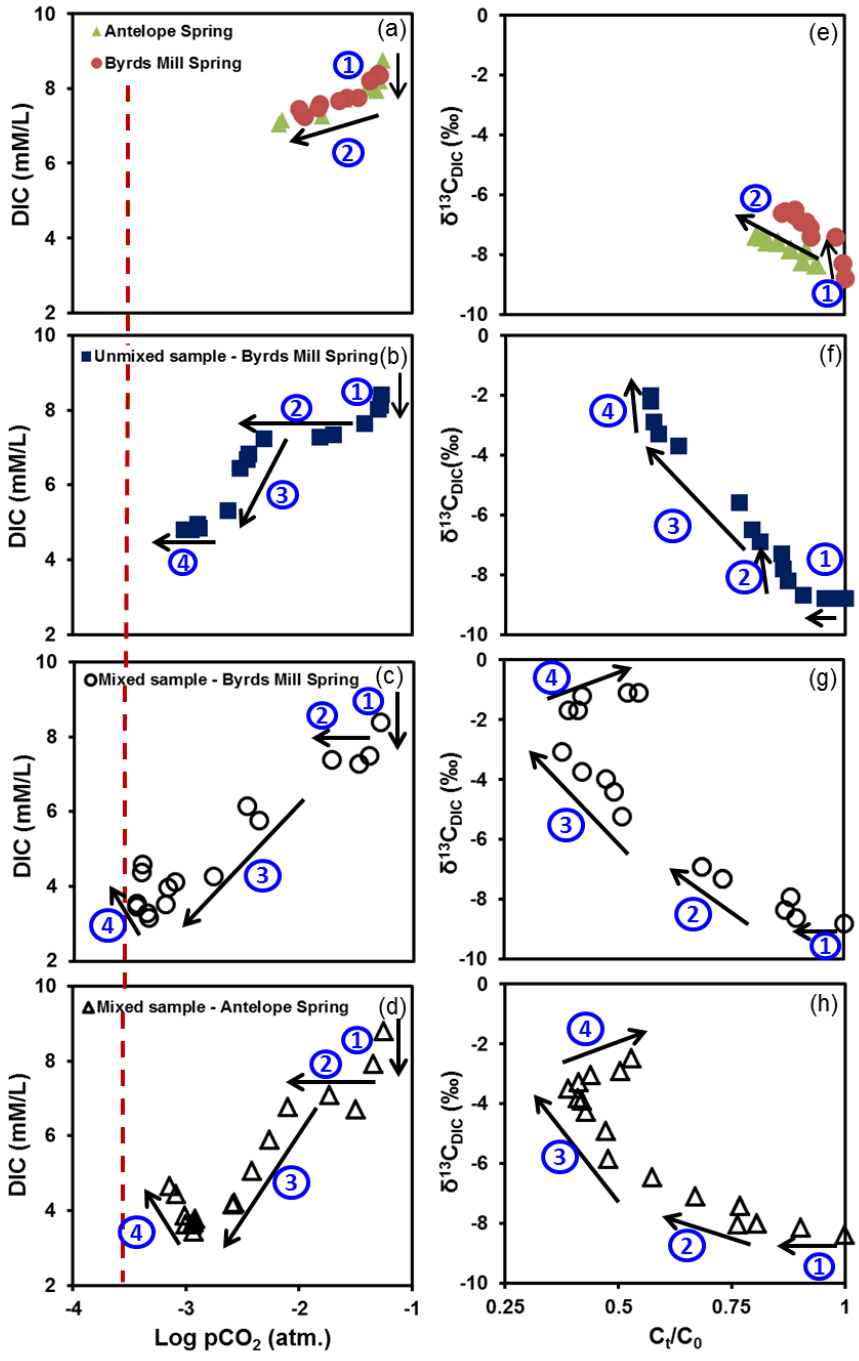

Figure II- 10. Plots of the log of the partial pressure of $CO_{2(g)}$ (log pCO_2) vs. dissolved inorganic carbon (DIC) for the field (a) and laboratory (b – d) samples and plots of the concentrations of the DIC at any time (C_t) divided by the concentration of the DIC at the discharge point or start of the laboratory experiments (C_0) i.e., C_t/C_0 versus the carbon isotope ratio of the DIC ($\delta^{13}C_{DIC}$) for field (e) and laboratory (f – h) samples. The arrows indicate the direction of the chemical and isotopic evolution of the samples with segments (1) to (4) representing the evolution from undersaturated to supersaturated conditions with respect to calcite as depicted in Fig. 7. The vertical dashed lines in panels a - d represent atmospheric equilibrium concentration of $CO_{2(g)}$ i.e. log pCO_2 = -3.5 atm.

Table II- 1. Physical, chemical and carbon isotope results for the field samples of Antelope and Byrds Mill Springs

	Distance (meters)	pH	Temp (°C)	SPC µs/cm	TDS mg/L	Cl^- (mmol/L)	SO_4^{2-} (mmol/L)	K^+ (mmol/L)	Na^+ (mmol/L)	Mg^{2+} (mmol/L)	Ca^{2+} (mmol/L)	Alkalinity (mmol/L HCO_3^-)	DIC (mmol C/L)	$\delta^{13}C_{DIC}$ (‰)	Log pCO_2 (atm.)	SIc
Antelope Spring	0	6.8	17.4	610	396	0.10	0.19	0.11	0.34	1.96	1.59	5.70	8.75	-8.43	-1.34	-0.25
	10	6.8	17.4	610	396	0.10	0.19	0.03	0.15	1.77	1.51	5.69	8.20	-8.33	-1.33	-0.39
	32	6.8	17.5	610	396	0.12	0.18	0.04	0.15	1.80	1.53	5.61	7.94	-8.22	-1.35	-0.36
	62	7.0	17.8	610	396	0.10	0.18	0.06	0.18	1.78	1.52	5.57	8.00	-7.87	-1.48	-0.25
	112	7.2	18.4	609	396	0.10	0.18	0.03	0.15	1.75	1.51	5.70	7.70	-7.85	-1.68	-0.02
	310	7.4	18.6	605	393	0.10	0.18	0.04	0.16	1.75	1.50	5.61	7.26	-7.57	-1.89	0.18
	550	7.4	19.3	602	391	0.11	0.18	0.04	0.15	1.77	1.47	5.55	7.46	-7.58	-1.94	0.24
	800	7.7	19.7	565	386	0.10	0.18	0.03	0.15	1.80	1.51	5.61	7.16	-7.41	-2.26	0.57
	895	7.8	20.0	599	389	0.10	0.18	0.03	0.14	1.81	1.52	5.65	7.04	-7.37	-2.28	0.61
Buffalo Spring	0	6.8	17.4	600	390	0.08	0.16	0.03	0.12	1.63	1.87	5.80	8.52	-8.57	-1.24	-0.36
	16	6.9	17.3	596	388	0.06	0.15	0.02	0.13	1.61	1.88	5.84	7.61	-8.34	-1.37	-0.25
	25	6.8	17.4	515	388	0.08	0.16	0.02	0.13	1.57	1.98	5.78	7.45	-8.31	-1.28	-0.36
	80	7.0	17.5	601	391	0.08	0.16	0.02	0.12	1.59	1.85	5.65	8.06	-8.29	-1.41	-0.18
	130	7.0	17.6	601	391	0.08	0.16	0.01	0.08	1.58	1.78	5.65	7.53	-8.25	-1.46	-0.17
	210	7.0	17.7	601	391	0.07	0.16	0.02	0.12	1.57	1.81	5.55	7.25	-8.21	-1.49	-0.14
	280	7.1	18.0	602	391	0.08	0.16	0.02	0.13	1.57	1.83	5.45	7.49	-8.02	-1.56	-0.04
	365	7.2	18.2	601	391	0.10	0.16	0.02	0.13	1.56	1.84	5.51	7.03	-7.84	-1.68	0.07
Byrds Mill Spring	0	6.8	15.2	633	418	0.08	0.03	0.04	0.22	1.74	1.91	5.59	8.39	-8.80	-1.30	-0.35
	3	6.8	15.2	633	415	0.08	0.09	0.04	0.22	1.83	1.89	5.31	8.34	-8.30	-1.29	-0.39
	6	6.9	15.5	633	412	0.08	0.09	0.05	0.24	1.92	2.05	4.09	8.19	-7.70	-1.37	-0.36
	15	6.9	15.2	633	412	0.08	0.09	0.07	0.25	1.97	2.04	4.03	8.22	-7.40	-1.37	-0.37
	50	7.0	15.8	633	411	0.09	0.09	0.06	0.23	1.86	1.94	4.01	7.75	-7.40	-1.47	-0.28
	150	7.1	15.9	625	406	0.08	0.09	0.05	0.07	1.92	1.97	3.84	7.74	-7.10	-1.57	-0.17

300	7.2	16.4	628	408	0.08	0.09	0.05	0.25	2.02	2.04	3.78	7.66	-6.90	-1.64	-0.07
500	7.4	16.8	625	405	0.09	0.09	0.05	0.23	2.06	1.97	3.54	7.58	-6.90	-1.82	0.08
700	7.4	17.8	616	401	0.09	0.09	0.05	0.25	2.18	2.14	4.01	7.46	-6.70	-1.83	0.19
800	7.5	18.2	613	393	0.09	0.09	0.05	0.23	2.08	2.05	4.09	7.23	-6.60	-1.95	0.30
900	7.6	18.5	611	397	0.09	0.09	0.05	0.25	2.12	2.09	4.15	7.29	-6.54	-1.97	0.35
1000	7.6	18.4	609	396	0.12	0.10	0.06	0.26	2.12	2.09	4.01	7.46	-6.50	-2.00	0.38

SPC = specific conductance

TDS = total dissolved solids

SIc= saturation index of calcite

Table II- 2. Physical, chemical and carbon isotope results for the laboratory samples of Antelope and Byrds Mill Springs

	Time (Hours)	pH	Temp (°C)	SPC µs/cm	TDS mg/L	Cl^- (mmol/L)	SO_4^{2-} (mmol/L)	K^+ (mmol/L)	Na^+ (mmol/L)	Mg^{2+} (mmol/L)	Ca^{2+} (mmol/L)	Alkalinity (mmol/L HCO_3^-)	DIC (mmol C/L)	$\delta^{13}C_{DIC}$ (‰)	Log pCO_2 (atm.)	SIc
Unmixed sample- Byrds Mill Spring	0	6.83	16.90	604	389	0.08	0.08	0.04	0.21	1.75	1.91	5.57	8.79	-8.80	-1.27	-0.29
	0.5	6.80	17.10	603	392	0.08	0.08	0.04	0.21	1.72	1.87	5.57	8.13	-8.80	-1.28	-0.34
	1	6.82	17.10	607	394	0.08	0.08	0.04	0.21	1.66	1.80	5.55	8.03	-8.80	-1.30	-0.34
	3	6.95	17.21	608	395	0.08	0.08	0.04	0.20	1.62	1.72	5.53	7.64	-8.70	-1.42	-0.23
	7	7.27	18.85	605	393	0.08	0.08	0.04	0.20	1.63	1.76	5.51	7.35	-8.20	-1.70	0.12
	26	7.41	20.85	604	393	0.08	0.09	0.04	0.20	1.69	1.78	5.47	7.27	-7.80	-1.82	0.29
	52	7.93	21.62	596	388	0.08	0.09	0.05	0.21	1.75	1.89	5.45	7.24	-7.30	-2.31	0.83
	78	8.04	21.19	585	380	0.08	0.08	0.04	0.21	1.77	1.85	5.41	6.84	-6.90	-2.45	0.92
	99	8.04	20.98	574	370	0.08	0.09	0.04	0.21	1.77	1.79	5.37	6.68	-6.50	-2.46	0.90
	147	8.09	21.16	532	346	0.09	0.09	0.04	0.21	1.73	1.42	4.80	6.45	-5.60	-2.52	0.84
	213	8.12	21.52	491	319	0.09	0.09	0.05	0.22	1.85	1.29	4.56	5.31	-3.70	-2.63	0.83
	268	8.31	20.90	466	303	0.09	0.09	0.04	0.22	1.78	1.02	4.23	4.49	-3.30	-2.90	0.89
	316	8.34	20.83	450	293	0.09	0.09	0.06	0.22	1.81	0.91	4.43	4.94	-2.90	-2.89	0.86
	340	8.40	20.99	435	280	0.09	0.09	0.05	0.22	1.80	0.83	4.33	4.79	-2.20	-2.96	0.86
	436	8.46	21.10	429	279	0.14	0.13	0.05	0.22	1.85	0.73	2.86	4.76	-2.00	-3.02	0.84
Mixed sample- Byrds Mill Spring	0	6.83	16.93	588	389	0.08	0.09	0.04	0.20	1.54	1.79	5.57	8.38	-8.83	-1.29	-0.34
	0.25	6.90	17.01	584	389	0.08	0.09	0.04	0.20	1.57	1.81	5.39	7.49	-8.64	-1.39	-0.28
	0.5	7.00	17.11	587	385	0.08	0.08	0.04	0.20	1.56	1.78	5.37	7.28	-8.37	-1.48	-0.18
	1	7.29	17.45	605	382	0.08	0.09	0.04	0.21	1.58	1.82	5.35	7.39	-7.95	-1.72	0.12
	3.25	8.01	19.91	604	382	0.08	0.08	0.04	0.20	1.59	1.81	5.31	6.14	-7.32	-2.47	0.85
	7	7.89	21.79	540	351	0.08	0.08	0.04	0.21	1.56	1.52	5.21	5.76	-6.93	-2.37	0.69
	26	8.17	22.63	427	277	0.09	0.09	0.04	0.21	1.65	0.81	4.33	4.27	-5.24	-2.77	0.65

	52	8.49	22.02	378	246	0.09	0.09	0.04	0.21	1.64	0.50	3.64	4.12	-4.40	-3.11	0.67
	78	8.54	21.92	361	235	0.09	0.09	0.04	0.22	1.76	0.42	3.25	3.97	-4.00	-3.17	0.60
	99	8.51	21.85	357	233	0.09	0.09	0.04	0.22	1.74	0.35	3.15	3.53	-3.76	-3.19	0.49
	147	8.61	21.86	356	232	0.09	0.09	0.05	0.23	1.83	0.33	3.11	3.16	-3.07	-3.34	0.55
	213	8.64	22.21	367	238	0.10	0.10	0.05	0.23	1.88	0.29	2.95	3.28	-1.70	-3.35	0.51
	268	8.75	21.64	379	247	0.11	0.10	0.05	0.25	2.01	0.25	3.34	3.46	-1.70	-3.45	0.59
	316	8.76	21.77	401	261	0.12	0.12	0.06	0.27	2.15	0.23	3.66	3.53	-1.20	-3.45	0.59
	340	8.81	21.86	420	278	0.09	0.09	0.04	0.22	1.80	0.23	3.88	4.38	-1.10	-3.41	0.62
	436	8.82	21.94	446	290	0.09	0.09	0.06	0.30	2.45	0.22	4.03	4.58	-1.10	-3.40	0.66
Mixed sample-	0	6.81	17.79	640	415	0.10	0.18	0.04	0.16	1.40	1.89	5.76	8.79	-8.40	-1.25	-0.32
Antelope Spring	0.15	6.89	19.29	632	400	0.10	0.18	0.04	0.16	1.41	1.86	5.61	7.93	-8.16	-1.34	-0.23
	0.3	7.00	20.25	619	397	0.10	0.18	0.04	0.16	1.42	1.83	5.49	6.71	-8.04	-1.50	-0.12
	1	7.31	21.97	611	396	0.10	0.18	0.04	0.16	1.42	1.81	5.39	7.08	-8.02	-1.73	0.20
	2	7.70	24.87	617	392	0.10	0.18	0.04	0.17	1.45	1.78	5.37	6.76	-7.42	-2.10	0.68
	4.5	7.80	23.93	609	390	0.13	0.19	0.05	0.19	1.42	1.76	5.19	5.89	-7.11	-2.26	0.70
	25	7.88	22.00	550	385	0.13	0.19	0.05	0.19	1.45	1.51	4.76	5.05	-6.48	-2.41	0.68
	31	7.96	21.77	520	338	0.13	0.19	0.05	0.19	1.45	1.29	4.70	4.01	-5.86	-2.57	0.65
	48	7.97	21.63	451	293	0.13	0.19	0.05	0.20	1.44	0.86	3.78	4.15	-4.93	-2.59	0.45
	71	8.27	22.41	416	270	0.13	0.19	0.05	0.20	1.45	0.65	3.52	3.77	-4.29	-2.92	0.59
	90	8.27	22.09	404	263	0.14	0.20	0.05	0.20	1.56	0.57	3.58	3.69	-3.92	-2.93	0.52
	116	8.33	22.04	402	261	0.14	0.21	0.06	0.20	1.62	0.51	3.48	3.62	-3.84	-3.00	0.52
	147	8.24	21.84	405	263	0.14	0.21	0.06	0.19	1.62	0.48	3.44	3.42	-3.50	-2.93	0.40
	172	8.27	21.25	410	266	0.15	0.21	0.06	0.20	1.70	0.47	3.54	3.62	-3.30	-2.94	0.42
	286	8.36	21.38	427	277	0.17	0.25	0.07	0.26	2.04	0.34	3.78	3.85	-3.06	-3.01	0.41
	345	8.50	21.43	452	294	0.19	0.28	0.08	0.28	2.24	0.30	4.07	4.44	-2.91	-3.09	0.50
	465	8.58	22.75	494	321	0.22	0.32	0.09	0.32	2.53	0.24	4.56	4.65	-2.50	-3.14	0.55

SPC = specific conductance

DS = total dissolved solids

SIc = saturation index of calcite

CHAPTER III

INVESTIGATING THE EFFECTS OF DILUTION BY PRECIPITATION ON DISSOLVED INORGANIC CARBON AND STABLE ISOTOPE EVOLUTION IN SURFACE WATERS

Abstract

Addition of precipitation to surface water dilutes solutes and dissolved inorganic carbon (DIC) according to the dilution proportion causing differential evolution of the carbon isotopic composition of DIC ($\delta^{13}C_{DIC}$). Assessing the effect of precipitation on the chemical and isotopic evolution of DIC is important in understanding carbon behavior in surface water affected by precipitation. Because of multiple water-column processes such as respiration, photosynthesis and water-rock interaction that could add or remove carbon from the DIC pool, tracing the behavior of DIC and $\delta^{13}C_{DIC}$ becomes difficult to conduct in natural settings. Thus, laboratory simulations provide an alternative in which the processes and mechanisms that affect DIC evolution in surface water could be studied. The laboratory experiments though might not replicate the exact results in natural settings, it could, however, help as a step in learning about processes and mechanisms accompanying the DIC and $\delta^{13}C_{DIC}$ evolution in surface water affected by precipitation. In this study, we prepared undiluted (100%) and snow-melt diluted 25,

50 and 75% solutions of $NaHCO_3$, lake and river water and exposed them to laboratory atmosphere for up to 1000 hour. We aim to determine how dilution by snow-melt affects DIC and $\delta^{13}C_{DIC}$ evolution in surface waters.

Differential dilution resulted to decreased solutes and DIC concentrations and decreased pH according to the dilution proportion. There were steep pH increases in the $NaHCO_3$ and lake samples and decreases in the river samples within the first 10 hour with the most diluted samples having the steepest slope. The DIC concentration stayed almost constant for the first ~100 hour and increased thereafter. The $\delta^{13}C_{DIC}$ shift towards that of precipitation and immediately after dilution, there were differences in the initial evolution of $\delta^{13}C_{DIC}$ but over time, there was an ultimate convergence of the different $\delta^{13}C_{DIC}$ at -4.0‰ for the $NaHCO_3$ and lake samples and -2.0‰ for the river samples. With no change in the DIC concentrations for about 100 hours and continuous pH increase coupled with pCO_2 greater than atmospheric ($>10^{-3.5}$ atm), we define the $NaHCO_3$ and lake samples as 'closed systems' in which there was conservation of carbon mass. We ascribed the pH increases to the transformation of bicarbonate to carbonate ion. For the river samples with no change in DIC for about 100 hour and pH decreases for the first 10 hour with pCO_2 less than atmospheric ($<10^{-3.5}$ atm), we describe it as an 'open system.' Continuous invasion of $CO_{2(g)}$ into river samples forms H_2CO_3 which increases the acidity of surface water and the preferential incorporation of the heavier $^{13}CO_2$ into the liquid phase causes the $\delta^{13}C_{DIC}$ of the more diluted samples to be more enriched. The effect of precipitation on surface water is important from the initial stages of dilution to the equivalence of about 10 hour of reaction time based on the results of this experiment. We suggest that experimentation designed to study carbon evolution in surface waters while minimizing carbon evolution based on the effect of dilution should wait for at least 10 hours after a precipitation event before sampling.

1. Introduction

Precipitation (rainfall or snow-melt) decreases concentrations of dissolved inorganic carbon (DIC) by dilution (e.g., Atekwana and Krishnamurthy, 1998; Howland et al., 2000, Liu and Yuan, 2000; Liu et al., 2010) and the dilution could change the carbon isotopic ratio of the DIC ($\delta^{13}C_{DIC}$) in surface waters (e.g., Cane and Clark, 1999; Doctor et al., 2008). During the wet season, subsurface flow with high content of dissolved soil CO_2 will decrease the $\delta^{13}C_{DIC}$ in surface waters (e.g., Cane and Clark, 1999; Doctor et al., 2008; Liu et al., 2010). High respiration rates will cause isotopic fractionation of soil CO_2 and this could result to increase $\delta^{13}C_{DIC}$ in surface water during the dry season (e.g., Amiotte-Suchet et al., 1999; Telmer and Veizer, 1999; Wachniew, 2006; Doctor et al., 2008; Liu et al., 2010). Studies that investigated the effect of dilution on DIC changes and $\delta^{13}C_{DIC}$ composition in surface water made monthly or seasonal measurements that did not give clear indications if the proportionality of dilution could have any effect on how fast the various diluted water could reach equilibrium (e.g., Cameron et al., 1995; Myrbo and Shapley, 2006; Wachniew, 2006; Doctor et al., 2008; Guo et al., 2008; Liu et al., 2010). Dilution by precipitation as well as increase input of soil CO_2 after a precipitation event could change the $\delta^{13}C_{DIC}$ signature of surface water. Based on the mixing proportion due to the dilution effect from direct precipitation and increased soil CO_2, it is possible that one could track the effect of dilution by sequential monitoring the composition of $\delta^{13}C_{DIC}$ over time and/or space until the system achieves chemical and isotopic equilibrium. In addition to DIC and $\delta^{13}C_{DIC}$ changes, the overall carbonate evolution of a system that is affected by dilution could be determined by carefully monitoring its pH over time and/or space. The change of pH in surface water is a good indication of the buffering state of that particular system and could therefore be a

diagnostic parameter in understanding carbonate species distribution in surface water affected by dilution.

Organic respiration which makes use of oxygen and releases CO_2 and calcite or dolomite dissolution would add carbon to the DIC pool. Photosynthesis which involves using up CO_2 and calcite and dolomite precipitation that remove carbon from the DIC pool occur at variable magnitude and intensity. These conflicting processes that add or remove carbon from surface water DIC pool could have an effect on the DIC concentrations and $\delta^{13}C_{DIC}$ behavior (e.g., Atekwana and Krishnamurthy, 1998; Telmer and Veizer, 1999; Cartwright, 2010; Zeng and Masiello, 2011; Shin et al., 2011). Investigating the effect of dilution on surface water by tracing the behavior of DIC and $\delta^{13}C_{DIC}$ composition to chemical and isotopic equilibrium conditions is difficult in field settings because of the possibility of the continuous addition or removal of carbon from the surface water DIC pool.

In this study, we conducted laboratory experiments to investigate DIC behavior and $\delta^{13}C_{DIC}$ composition in surface waters that are affected by rain or snow-melt with the aim of determining how long a dilution effect would last in surface water systems and how surface water dilution would affect the evolution of DIC and $\delta^{13}C_{DIC}$. We investigated the temporal chemical behavior of DIC and $\delta^{13}C_{DIC}$ composition in diluted and undiluted solution of an artificial $NaHCO_3$, natural lake and river water exposed to atmospheric $CO_{2(g)}$ in a laboratory setting. We prepared the $NaHCO_3$ such that we have a solution with a $\delta^{13}C_{DIC}$ far from equilibrium and a pCO_2 greater than atmospheric $CO_{2(g)}$ ($>10^{-3.5}$ atm). We used $NaHCO_3$ as a model solution to avoid the chemical complexity of natural water so as to better constrain dilution effect on DIC evolution in surface water. The lake water was chosen because its $\delta^{13}C_{DIC}$ was at equilibrium and its pCO_2 greater than atmospheric ($>10^{-3.5}$ atm) and for the river water, its $\delta^{13}C_{DIC}$ was far from

equilibrium and it pCO_2 below atmospheric $CO_{2(g)}$ ($<10^{-3.5}$ atm). We made physical, chemical and isotopic measurements for up to 1000 hour. The pH and DIC changes and the accompanying $\delta^{13}C_{DIC}$ behavior of the samples would allow us to ascertain the chemical and isotopic changes due to dilution in surface waters affected rain or snow-melt.

2. Method

2.1 Sample collection, treatment and measurements

In this study, we used an artificial $NaHCO_3$ solution which was prepared by dissolving 5.5 g of 99% laboratory grade $NaHCO_3$ salt (LCSX-0320-1, EMD Chemicals, Inc.), in 20 L of deionized water. The lake and river water used in this experiment were pumped into acid pre-washed 25 L plastic containers with a submersible pump. The lake water was collected from Lake McMurtry, near Stillwater, Oklahoma (36° 10′ 49.37″ N, 97° 10′ 52.9″ W) and the river water was collected from Arkansas River near Tulsa, Oklahoma (36° 13′ 44.03″ N, 96° 19′ 30.96″ W). A large amount of snowmelt which was used for sample dilution was collected in Stillwater, Oklahoma (36° 7′ 29.73″ N, 97° 4′ 12.37″ W) and homogenized before being used in the experimental treatment. All samples in the field were collected with no headspace, tightly sealed and transported to the laboratory.

We diluted our model $NaHCO_3$ solution, lake and river water with melted snow and had 4 treatments of 20 L for each sample type. One set was undiluted (100%), and three sets were diluted at 25%, 50% and 75% with snow-melt to make 100%, 75%, 50% and 25% $NaHCO_3$, lake and river water proportions. The samples were exposed to the laboratory air in 25 L plastic

buckets that served as reactors immediately after preparation. The samples were agitated by circulating the water in the reactors at a rate of ~10 L/min using a submersible pump (ViaAqua Powerhead, VA 360-906060; Foster and Smith Aquatics) to simulate mixing and turbulence in field settings. All reactors were left opened and in contact with the laboratory atmosphere for up to 1000 hour during which time the solutions evolved isotopic equilibrium with the $CO_{2(g)}$ n the laboratory air.

Physical, chemical and $\delta^{13}C_{DIC}$ measurements were conducted at 0, 0.5, 1, 2, 3, 4, 8 and 24 hours, followed by every 24 hours for 2 weeks and weekly after that, so as to capture any chemical and isotopic changes that could occur immediately after sample dilution and to monitor the sample evolution to equilibrium. Temperature, pH, specific conductance and total dissolved solids (TDS) were measured using a Yellow Springs Instrument (YSI) multi-parameter probe calibrated to manufacturer's specifications. Water samples collected from each reactor were filtered through 0.45 µm nylon filters and the alkalinity concentration was measured immediately after sampling by acid titration (Hach Company, 1992). Samples for anions and cations were collected in high density polyethylene (HDP) bottles; the cation samples were acidified to a pH <2.0 using high purity HNO_3. The anions and cations were measured by ion chromatography (Dionex ICS 3000). Samples for DIC analysis were collected in pre-acidified (1 mL of 85% H_3PO_4) vaccutainer tubes and $CO_{2(g)}$ was extracted as described by Atekwana and Krishnamurthy (1998). The DIC concentrations were calculated from extracted $CO_{2(g)}$, then the $CO_{2(g)}$ was sealed in Pyrex tubes. We periodically collected laboratory air in pre-evacuated 1.5 L glass ampoules and used a vacuum line to purify the $CO_{2(g)}$ which we sealed in Pyrex tubes. The $CO_{2(g)}$ from DIC and the purified $CO_{2(g)}$ from laboratory air were analyzed for $\delta^{13}C$ using a

Finnigan Delta Plus XL isotope ratio mass spectrometer. The stable isotope ratios are reported in the standard delta (δ) notation in per mil (‰):

$$\delta(‰) = \left(\left(R_{sample}/R_{standard}\right) - 1\right)$$

where R is $^{13}C/^{12}C$. The δ values are reported relative to VPDB international standard. Routine $\delta^{13}C$ measurements of in-house standards and replicate samples have an overall precision (1-sigma) of better than 0.1‰.

The computer program PHREEQC Version 2.8 (Parkhurst and Appelo, 1999) was used to model the carbonate species distribution and to calculate the pCO_2 using pH, temperature and DIC.

3. Results

The physical, chemical and stable carbon isotope results for the undiluted and diluted $NaHCO_3$, lake and river water samples are listed in Tables 1, 2 and 3, respectively.

3.1 TDS, pH and alkalinity

At the start of the experiment, the undiluted 100% samples recorded the highest total dissolved solids (TDS) concentrations followed by the diluted 75%, 50% and 25% samples (Figs. III-1a-c). The TDS concentrations stayed almost constant for all samples for the first ~ 100 hour, followed by a slow increase from 100 to ~400 hour and then, increase markedly to the end of the experiment (Figs. III-1a-c). Generally, all samples showed a 3-step behavior in the TDS concentrations over time, (1) a constant concentration, (2) followed by a slow increase, and (3) a

sharp increase to the end of the experiment. The rate of increase of the TDS samples were the same for the $NaHCO_3$ samples, steepest for the 75 and 50% lake samples and steepest for the 100 and 75% river samples.

At the start of the experiment, the highest pH values were recorded for the undiluted (100%), followed by the diluted 75%, 50% and 25% $NaHCO_3$, lake and river samples (Figs. III-2a-c). The pH of the $NaHCO_3$ and lake samples increased continuously throughout the experiments with sharp increases in the first ~ 10 hour, followed by a slow increase from 10 to ~400 hour and then sharp increase to the end of the experiment (Figs. III-2a and b). The river samples showed continuous decrease in pH in the first ~ 10 hour and then, a slow continuous increase from 10 to ~400 hour before increasing sharply to the end of the experiment (Fig. III-2c). Overall, all samples showed a 3-step behavior in the pH; (1) sharp increase in $NaHCO_3$ and lake samples and sharp decrease in the river samples; (2) followed by slow increase and (3) sharp increases to the end of the experiment. The pH increase and decrease was steepest for the diluted 25%, followed by the 50%, 75% and then the undiluted 100% samples.

At the start of the experiment, the highest alkalinity concentrations were recorded for the undiluted samples followed by the diluted 75%, 50% and 25% samples (Figs. III-2d-f). The alkalinity concentrations stayed almost constant for all samples for the first ~ 100 hour, increase slowly from 100 to ~ 400 hour and then increased sharply to the end of the experiment (Figs. III-2d-f). All samples showed a 3-step behavior of (1) constant concentrations, (2) followed by slow increases, and (3) sharp increases to the end of the experiment. Unlike the pH which showed sharp increases and decreases for the diluted 25%, followed by the 50%, 75% and undiluted 100% samples, the rate of increase of the alkalinity samples were the same for the $NaHCO_3$

samples, steepest for the 75% and 50% lake samples and steepest for the 100% and 75% river samples.

3.2 DIC and $\delta^{13}C_{DIC}$

At the start of the experiment, the highest DIC concentrations were recorded for the undiluted 100% samples followed by the diluted 75%, 50% and 25% samples (Figs. III-3a-c). The DIC of the $NaHCO_3$ samples, 100% lake samples and the river samples showed a constant concentrations for the first ~100 hour, followed by a slow increase from ~100 to ~400 hour and then, a markedly sharp increase to the end of the experiment (Fig. III-3a-c). Whereas, the diluted 75%, 50% and 25% lake samples showed a slight decrease in the DIC concentrations for the first ~4 hour before staying almost constant from ~4 to ~100 hour, after which it increased slowly to ~400 hours followed by sharp increase to the end of the experiment (Fig. III-3b). The DIC concentrations of the $NaHCO_3$, 100% lake and the river samples exhibited a 3-behavior characterized by (1) constant DIC concentrations, (2) followed by a slow increase, and (3) markedly increase, whereas, the diluted lake samples showed a 3-step behavior of (1) initial decrease, (2) followed by slow increase and (3) a sharp increase.

At the start of the experiment immediately after dilution, the most enriched $\delta^{13}C_{DIC}$ values were recorded for the 25% samples followed by the 50%, 75% and undiluted 100% samples for the $NaHCO_3$ and river samples, whereas for the lake samples, at the start of the experiment, the most enriched $\delta^{13}C_{DIC}$ values were recorded for the undiluted 100% samples followed by the diluted 75%, 50% and 25% samples (Figs. III-3d-f). The $\delta^{13}C_{DIC}$ of all samples, except the 100% lake sample, showed a 3-step enrichment process described by a slow continuous increase in the first ~100 hour, followed by a sharp increase from ~100 to ~400 hour and then stayed constant

throughout the experiment (Figs. III-3d-f). The $\delta^{13}C_{DIC}$ of the 100% lake sample stayed constant at -4.0 ± 0.5‰ throughout the experiment (Fig. III-3e). All samples (diluted and undiluted) evolved by continuous enrichment to a constant value of ~-4.0‰ for the $NaHCO_3$ and lake samples and -2.0‰ for the river samples.

4. Discussion

4.1 Dilution and carbonate evolution

Rain or melted snow adds DIC and mass to surface water causing solute dilution (e.g., Atekwana and Krishnamurthy, 1998; Liu and Yuan, 2000; Li et al., 2010) and we observed decrease in TDS concentrations according to the initial mixing proportion after which, it stayed almost constant for about 300 hours until evaporation continuously increases it concentrations (Fig. III-1). Dilution had a different effect on carbonate evolution as depicted by the pH (Fig. III-2a-c), alkalinity (Fig. III- 2d-f) and DIC (Fig. III- 3a-c) concentrations and in the $\delta^{13}C_{DIC}$ (Fig. III-3d-f). The effect of dilution on the alkalinity and DIC evolution were equivalent to that of the solute (TDS) which all depended on the dilution ratio. The pH behavior over time was not the same as the TDS, alkalinity and DIC concentrations but evolved differently for the different samples. The $NaHCO_3$ and lake samples according to the pH behavior is a non-buffered system as we observed that immediately after dilution there was a 0.5-1.5 pH unit shift in the samples (Fig. III-2a and b). We described the river as a buffered system as we observed a 0.05-0.2 pH unit in the samples (Fig. III-2c). The $\delta^{13}C_{DIC}$ measured in precipitation ranged from -7.0‰ to -14.0‰ (e.g., Lee and Krothe, 2001; Das et al., 2005) and this is in agreement with the measured

$\delta^{13}C_{DIC}$ value of the snow-melt used in this experiment. However, there was a ~ 2 year gap between the time the $NaHCO_3$ and lake experiments were conducted (February 2011) to the River experiment (January 2013). By the time the River experiment was conducted, isotope fractionation of the DIC had evolved such that the starting $\delta^{13}C_{DIC}$ was -4‰ and not -14‰ as in the fresh snow. Chemical, physical and DIC measurements of the snow-melt at the start of the River experiment yielded almost the same results as fresh snow. We observed that in the samples were there were no pH buffering i.e., in the $NaHCO_3$ and lake samples, the $\delta^{13}C_{DIC}$ shift towards that of precipitation according to the mixing proportions (Fig. III-3d and e) and since there was almost no change in the alkalinity and DIC concentrations for about 100 hours, we define the non-buffered $NaHCO_3$ and lake samples as 'closed systems' in which there was conservation of carbon mass. Likewise, in a pH buffered system i.e., the river samples, the $\delta^{13}C_{DIC}$ shift towards that of precipitation (-4‰) according to the mixing proportions (Fig. III-3f). The $\delta^{13}C_{DIC}$ and DIC evolution of all 3 sets of experimental samples (NaHCO3, Lake and River) all show the same evolutionary trend suggesting that the starting isotopic value was not significant and dilution was the overall controlling parameter. To explain our observations on the carbon evolution in the samples, we look at the pCO_2 behavior of the non-buffered and buffered systems. Generally, if a system has a pCO_2 higher than atmospheric ($10^{-3.5}$ atm), CO_2 outgassing will occur, whereas, if the pCO_2 of the system is less than atmospheric, CO_2 invasion will occur (e.g., Pawellek and Veizer, 1994; Telmer and Veizer, 1999; Richey et al., 2002; Mayorga et al., 2005; Doctor et al., 2008; Ali and Atekwana, 2009). The pCO_2 of the non-buffered $NaHCO_3$ and lake samples were higher than atmospheric ($>10^{-3.5}$ atm) whereas, that of the buffered river sample were slightly lower than atmospheric ($<10^{-3.5}$ atm) (Fig. III-4). We modeled the carbonate species ($H_2CO_3 + HCO_3^- + CO_3^{2-}$) to show their distribution during DIC evolution in non-

buffered and buffered systems. For the non-buffered samples with pCO_2 higher than atmospheric, the continuous increase in pH (Fig. III-2a and b) was from the transformation of HCO_3^- to CO_3^{2-} as the H_2CO_3 continuously decrease during the first ~10 hours (Fig. III-5a and b). As the samples get exposed over long periods of time, the effect of evaporation becomes more pronounced causing solute concentration resulting to increasing concentration of alkalinity, DIC and TDS as observed after about 100 hours of samples exposure (section labeled 3 on figures). Studies have shown that the effect of evaporation on solute concentration are more pronounced over space (e.g., Stiller et al., 1985; Akoko et al., 2013) and over time in samples left exposed to laboratory atmosphere in open containers (e.g., Abongwa and Atekwana, 2013). Since there was transformation of the carbonate species over time but no change in DIC, we therefore considered the $NaHCO_3$ and lake samples as belonging to systems that could be conceptually described as "closed." For the 'open river system' which is buffered with pCO_2 less than atmospheric, the continuous decrease in pH for the first ~10 hours (Fig. III-2c) was due to continuous $CO_{2(g)}$ invasion into river samples forming H_2CO_3 (Fig. III-5c) with no change in the measured DIC and alkalinity concentrations. The relatively lower pCO_2 of the River samples to the $NaHCO_3$ and Lake samples could be attributed to the lower initial DIC of the River samples compared to the $NaHCO_3$ and Lake samples. Continuous invasion of CO_2 into River samples increases the carbon content resulting to increase in the pCO_2 over time (Fig. III-4c). However, the increasing pCO_2 due to CO_2 invasion is not marked by concomitant increase in the carbon concentration as the DIC stays almost constant for the first 100 hours (Fig. III-3c). The observed DIC concentrations did not change over time but calculated carbonate speciation showed that H_2CO_3 follows same trend as the pCO_2 (Fig. III-5c). This could mean that the calculated pCO_2 are related directly more to the pH than DIC concentrations. Because of the differences in the

diffusivities of $^{12}CO_2$ and $^{13}CO_2$ and the preferential incorporation of the heavier ^{13}C into the heavier (liquid) phase (e.g., Vogel et al., 1970; Usdowski and Hoefs, 1990;), the $\delta^{13}C_{DIC}$ of the more diluted samples were more enriched (Fig. III-3f).

4.2 Carbonate evolution and $\delta^{13}C_{DIC}$ composition

The $\delta^{13}C_{DIC}$ of all samples except for the 100% lake sample which was already in isotopic equilibrium by start of experiment were continuously enriched to an equilibrium value of the laboratory air to which they were exposed (~-4.0‰ for $NaHCO_3$ and lake samples and ~-2.0‰ for river samples). We observed a shift in the $\delta^{13}C_{DIC}$ of 1.3 to 1.4‰ for the non-buffered system and a 0.4‰ shift for the buffered system within the first ~ 10 hours (section labeled 1 in Fig. III-3d-f) indicating minimal carbon isotopic fractionation during early times in both pH buffered and non-buffered systems. Since there were no changes in the DIC concentrations for about 400 hour but continuous enrichment in $\delta^{13}C_{DIC}$, we ascribed this observation to the fractionation associated with carbon isotopic exchange between the surface water DIC and atmospheric $CO_{2(g)}$ (e.g., Fonyuy and Atekwana, 2008b). We plotted the concentration of the DIC at any time (C_t) divided by the concentration of the DIC at the start (C_0) (i.e., C_t/C_0 vs. $\delta^{13}C_{DIC}$; Fig. III-6a-c) to describe the behavior of DIC and $\delta^{13}C_{DIC}$ in waters that undergo chemical and isotopic alteration during the interaction with atmospheric $CO_{2(g)}$ (Fig. III-6) (e.g., Gat and Gonfiantini, 1981; Kendall and Caldwell, 1998; Abongwa and Atekwana, 2013). Equilibration of the system was by transformation of bicarbonate to carbonate ion in the non-buffered system and hydration of carbon dioxide to carbonic acid in the buffered system as well as carbon isotopic exchange between the surface water and atmospheric $CO_{2(g)}$ such that the C_t/C_0 stays almost constant but the $\delta^{13}C_{DIC}$ continuously enriched (Fig. III-6). The equilibration process continuous until the

samples achieve isotopic equilibrium with laboratory $CO_{2(g)}$ at ~400 hour and we ascribed the continuous increase in DIC concentration after ~400 hour to evaporation (Fig. III-6).

4.3 Implication of water dilution to DIC evolution

1) Differential dilution of surface water by precipitation would result to differences in pH based on the dilution proportion.
2) Differential dilution would result to differences in the initial evolution of the $\delta^{13}C_{DIC}$ but the overall evolution would be controlled by the isotopic composition of the atmosphere.
3) After initial $\delta^{13}C_{DIC}$ evolution based on dilution proportions, there will be an ultimate convergence of the $\delta^{13}C_{DIC}$ due to surface water DIC-atmospheric $CO_{2(g)}$ interaction.

The effect of precipitation on surface water is important from the initial stages of dilution to the equivalence of about 10 hour of reaction time based on the results of this experiment. The transit time of water may vary between 3 to 19 days in temperate rivers (Basu and Pick, 1996), implying that the effect of dilution which could last for only half a day would not be significant throughout the entire water residence time. However, why half a day could be spatially variable in rivers and streams in terms of sampling after a rain or snow-melt event, the effect of dilution could easily be monitored by sequential sampling over time in lakes. We suggest that experimentation designed to study carbon evolution in surface waters while minimizing the effect of dilution should wait for at least 10 hours after a precipitation event before sampling.

5. Conclusion

Rain or melted snow adds mass into surface water causing solutes dilution according to the mixing proportion. There is initial differential pH immediately after dilution based on the mixing proportion and the buffering capacity of the system such that there is a major pH shift between the various diluted water for a non-buffered system and minimal pH shift between the various diluted water for the buffered system. In non-buffered systems with pCO_2 higher than atmospheric, the $\delta^{13}C_{DIC}$ will be closer to that of precipitation but in buffered system with pCO_2 less than atmospheric, the preferential incorporation of $^{13}CO_2$ into the liquid phase will result to sequentially more enriched water for more diluted systems. According to the results of this experiment, significant changes in pH will last for about 10 hours after a rain event. In this experiment, we considered the NaHCO3 and lake samples as conceptually 'closed system' even at with pCO_2 greater than atmospheric. There was conservation of mass with no carbon change over space and/or time, such that increases in pH could be due to the transformation of bicarbonate to carbonate ion. Whereas, in an open system, in which the pCO_2 is less than atmospheric, the invasion of $CO_{2(g)}$ will result to carbonic acid formation increasing pH. The buffering of pH in surface water results to minimal fractionation of carbon isotopes such that the overall dominant process controlling $\delta^{13}C_{DIC}$ will be carbon isotopic exchange between the surface water DIC and atmospheric $CO_{2(g)}$. Based on the results of this experiment, the effect of dilution appears to be significant for about 10 hours in turbulent surface waters after a rain event and would suggest that hydrological studies in field settings designed to minimize the effect of dilution on carbon evolution should wait for at least half-a-day before sampling.

Acknowledgements

We thank Rawlings Akondi, Emily Guderian, Nicole Paizis, Eric Akoko and Christopher Geyer for field and laboratory assistance.

References

Abongwa, P.T., Atekwana, E.A., 2013. Assessing the temporal evolution of dissolved inorganic carbon in waters exposed to atmospheric $CO_{2(g)}$: A Laboratory Approach. Journal of Hydrology 505, 250-265.

Akoko, E., Atekwana, E.A., Cruse, A.M., Molwalefhe, L. Masamba, W.R.L., 2013. River-wetland interaction and carbon cycling in a semi-arid riverine system: The Okavango Delta, Botswana. Biogeochemistry, 1-22.

Ali, H. N., & Atekwana, E. A., 2009. Effect of progressive acidification on stable carbon isotopes of dissolved inorganic carbon in surface waters. Chemical Geology, 260, 102-111.

Amiotte-Suchet, P., Aubert, D., Probst, J. L., Gauthier-Lafaye, F., Probst, A., Andreux, F., Viville, D., 1999. $\delta^{13}C$ pattern of dissolved inorganic carbon in a small granitic catchment: the Strengbach case study (Vosges mountains, France). Chemical Geology, 159, 129-145.

Atekwana, E.A., Krishnamurthy, R.V., 1998. Seasonal variations of dissolved inorganic carbon and δ13C of surface waters: application of a modified gas evolution technique. Journal of Hydrology 205, 265-278.

Basu, B.K., Pick, F.R., 1996. A large-scale comparison of factors influencing phytoplankton abundance in temperate rivers. Limnology and Oceanography 41, 1572-1577.

Cameron, E.M., Hall, G.E.M., Veizer, J., Krouse, H.R., 1995. Isotopic and elemental hydrochemistry of a major river system: Fraser River, British Columbia, Canada. Chemical Geology 122, 149-169.

Cane, G., Clark, I. D., 1999. Tracing ground water recharge in an agricultural watershed with isotopes. Groundwater, 37, 133-139.

Cartwright, I., 2010. The origins and behaviour of carbon in a major semi-arid river, the Murray River, Australia, as constrained by carbon isotopes and hydrochemistry. Applied Geochemistry 25, 1734-1745.

Das, A., Krishnaswami, S., Bhattacharya, S.K., 2005. Carbon isotope ratio of dissolved inorganic carbon (DIC) in rivers draining the Deccan Traps, India: sources of DIC and their magnitudes. Earth and Planetary Science Letters 236, 419-429.

Doctor, H.D., Kendall, C., Sebestyen, S.D., Shanley, T.B., Ohte, N., Boyer, E.N., 2008. Carbon isotope fractionation of dissolved inorganic carbon (DIC) due to outgassing of carbon dioxide from a headwater stream. Hydrological Processes 22, 2410-2423.

Fonyuy, E. W., Atekwana, E. A., 2008. Dissolved inorganic carbon evolution and stable carbon isotope fractionation in acid mine drainage contaminated streams: Insights from a laboratory study. Applied Geochemistry, 23, 2634-2648.

Gat, J.R., Gonfiantini, R., 1981. Stable isotope hydrology: deuterium and oxygen-18 in the water cycle. IAEA Technical Report Series NO. 210, IAEA Vienna, p. 337.

Guo, X., Cai, W. J., Zhai, W., Dai, M., Wang, Y., Chen, B., 2008. Seasonal variations in the inorganic carbon system in the Pearl River (Zhujiang) estuary. Continental Shelf Research, 28, 1424-1434.

Hach Company, 1992. Water Analysis Handbook. Hach Company, Loveland, Co.

Howland, R. J. M., Tappin, A. D., Uncles, R. J., Plummer, D. H., Bloomer, N. J., 2000. Distributions and seasonal variability of pH and alkalinity in the Tweed Estuary, UK. Science of the total environment 251, 125-138.

Kendall, C., Caldwell, E.A., 1998. Fundamentals of isotope geochemistry.C. Kendall, J.J. McDonnell (Eds.), Isotope Tracers in Catchment Hydrology, Elsevier Science B.V., Amsterdam.

Lee, E.S., Krothe, N.C., 2001. A four-component mixing model for water in karst terrain in south central Indiana, USA. Using solute concentration and stable isotopes as tracers. Chemical Geology 179, 129-143.

Li, S.L., Liu, C.Q., Li, J., Lang, Y.C., Ding, H., Li, L., 2010. Geochemistry of dissolved inorganic carbon and carbonate weathering in a small typical karstic catchment of southwest China: Isotopic and chemical constraints. Chemical Geology 277, 301-309.

Liu, Z., Yuan, D., 2000. Features of geochemical variations in typical epikarst systems of China and their environmental significance. Geology Review 46, 324-327.

Mayorga, E., Aufdenkampe, A.K., Masiello, C.A., Krusche, A.V., Hedges, J.I., Quay, P.D., Richey, J.E., Brown, T.A., 2005. Young organic matter as a source of carbon dioxide outgassing from Amazonian rivers. Nature 436, 538-541.

Myrbo, A., Shapley, M. D., 2006. Seasonal water-column dynamics of dissolved inorganic carbon stable isotopic compositions (δ^{13}_{DIC}) in small hardwater lakes in Minnesota and Montana. Geochimica et Cosmochimica Acta 70, 2699-2714.

Parkhurst, D.L., Appelo, C.A.J., 1999. User's Guide to PHREEQC (Version 2.1)-A Computer Program for Speciation, Batch-Reactions, One-Dimensional Transport and Inverse

Geochemical Calculations. U.S. Geological Survey, Water Resource Investigation Report, 99-4256.

Pawellek, F., Veizer, J., 1994. Carbon cycle in the upper Danube and its tributaries: $\delta^{13}C_{DIC}$ constraints. Isreal Journal of Earth Science 43, 187-194.

Richey, J.E., Melack, J.M., Aufdenkampe, A.K., Ballester, V.M., Hess, L.L., 2002. Outgassing from Amazonian rivers and wetlands as a large tropical source of atmospheric carbon dioxide. Nature 416, 617-620.

Shin, W.J., Chung, G.S., Lee, D., Lee, K.S., 2011. Dissolved inorganic carbon export from carbonate and silicate catchments estimated from carbonate chemistry and δ13CDIC. Hydrology and Earth System Sciences 15, 2551-2560.

Stiller, M., Rounick, J.S., Shasha, S., 1985. Extreme carbon-isotope enrichment in evaporating brines. Nature 316, 434-435.

Telmer, K.H., Veizer, J., 1999. Carbon fluxes, pCO_2, and substrate weathering in a large northern river basin, Canada: Carbon isotope perspectives. Chemical Geology 159, 61-86.

Usdowski, E., Hoefs, J., 1990. Kinetic $^{13}C/^{12}C$ and $^{18}O/^{16}O$ effects upon dissolution and outgassing of CO_2 in the system CO_2-H_2O. Chemical Geology: Isotope Geoscience Section, 80, 109-118.

Vogel, J.C., Grootes, P.M., Mook, W.G., 1970. Isotopic fractionation between gaseous and dissolved carbon dioxide. Zeitschrift fur Physik A (Atoms and Nuclei) 230, 225-238.

Wachniew, P., 2006. Isotopic composition of dissolved inorganic carbon in a large polluted river: the Vistula, Poland. Chemical Geology 233, 293-308.

Zeng, F-W., Masiello, C.A., 2011. Controls on the origin and cycling of riverine dissolved inorganic carbon in the Brazos River, Texas. Biogeochemistry 104, 275-291.

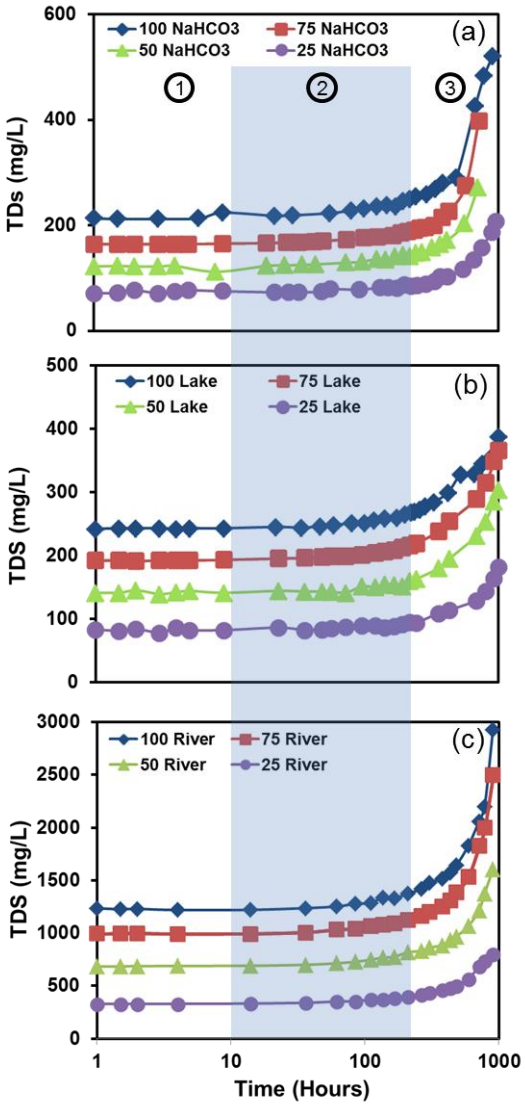

Figure III- 1. Temporal plots of total dissolved solids (TDS) for $NaHCO_3$ (a), lake (b) and river (c) samples exposed to the atmosphere in a laboratory setting. Lowest TDS concentrations were recorded for the 25%, followed by the 50%, 75% and 100% samples. The circled 1, 2 and 3 corresponds to the 3 stages of pH change observed in the samples. [The first sampling points are at time 0 hour but we arbitrary started the x-axis at 1 on the log scale.]

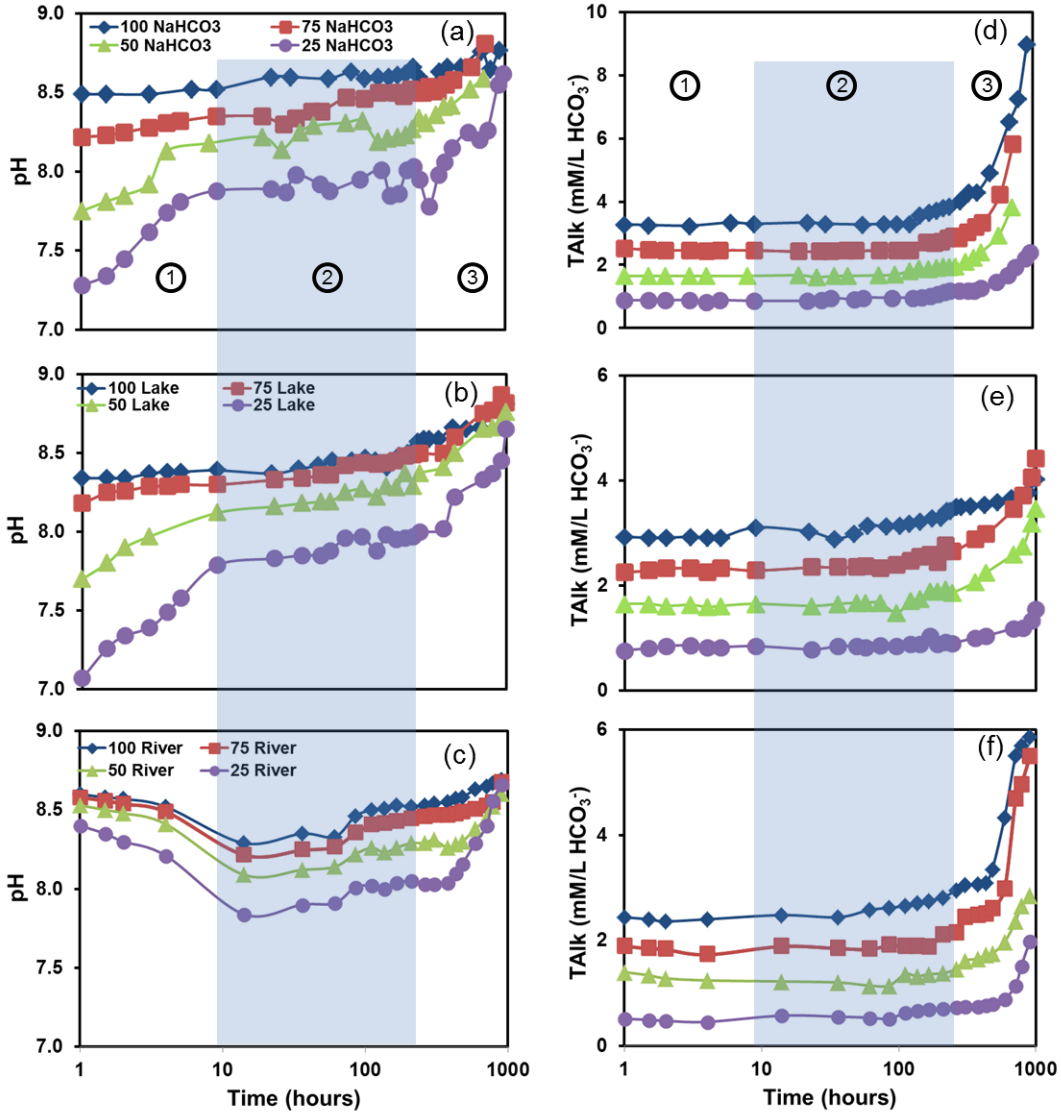

Figure III- 2. Temporal plots of pH and total alkalinity (TAlk) concentrations for 100%, 75%, 50% and 25% $NaHCO_3$ (a and d), lake (b and e) and river (c and f) samples exposed to the atmosphere in a laboratory setting. Lowest pH and alkalinity concentrations were recorded for the 25%, followed by the 50%, 75% and 100% samples. The circled 1, 2 and 3 corresponds to the 3 stages of pH change (sharp increase or decrease (1), slow increase (2) and sharp increase (3)) observed in Figs. 1a-c. [The first sampling points are at time 0 hour but we arbitrary started the x-axis at 1 on the log scale.]

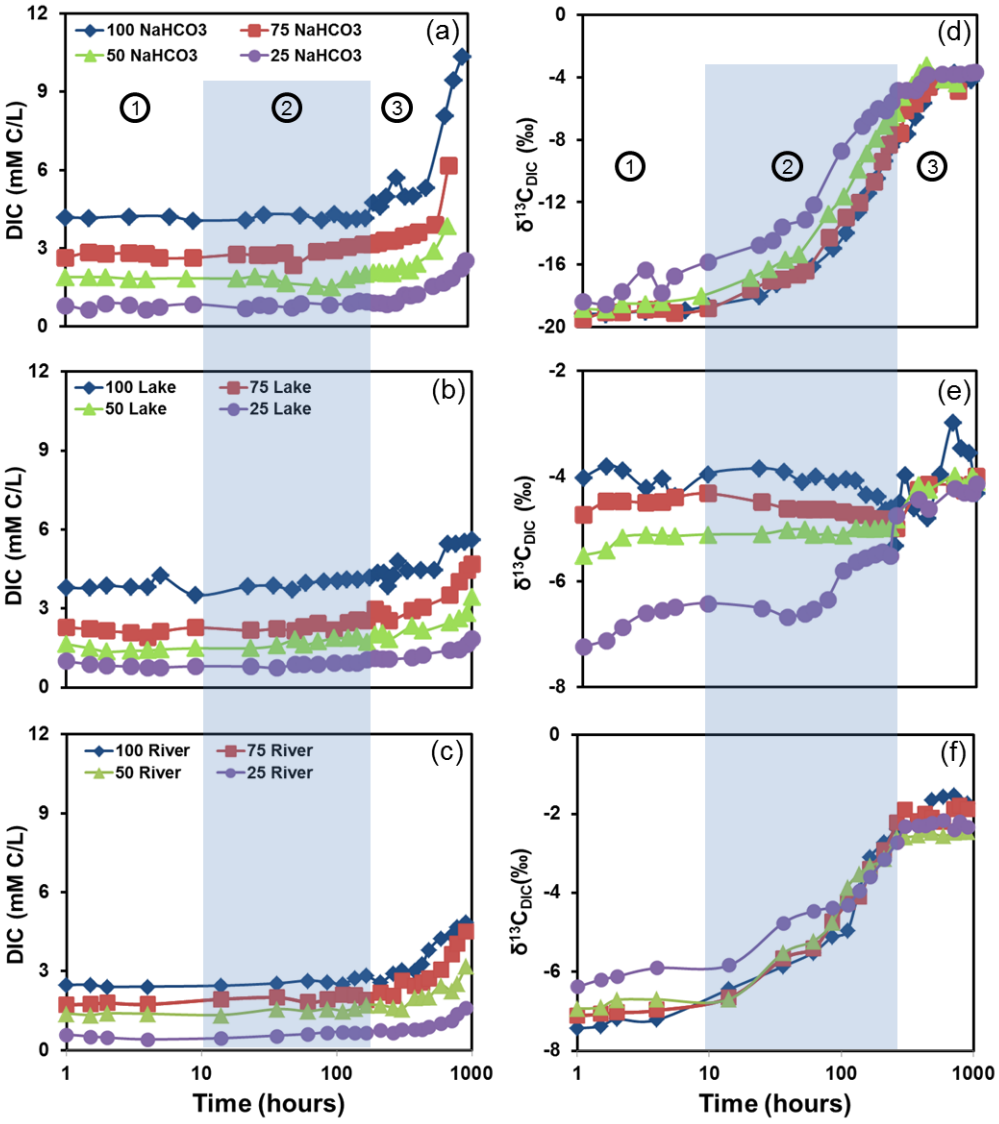

Figure III- 3. Temporal plots of dissolved inorganic carbon (DIC) concentrations and the stable carbon isotope composition of dissolved inorganic carbon ($d^{13}C_{DIC}$) for $NaHCO_3$ (a and d), lake (b and e) and river (c and f) samples exposed to the atmosphere in a laboratory setting. Lowest DIC concentrations were recorded for the 25%, followed by the 50%, 75% and 100% samples. Heaviest $\delta^{13}C_{DIC}$ were recorded for the 25%, followed by the 50%, 75% and 100% $NaHCO_3$ and river samples and for the 100%, followed by the 75%, 50% and 25% lake samples. The circled 1, 2 and 3 corresponds to the 3 stages of pH change observed in Figs. 2a-c. [The first sampling points are at time 0 hour but we arbitrary started the x-axis at 1 on the log scale.]

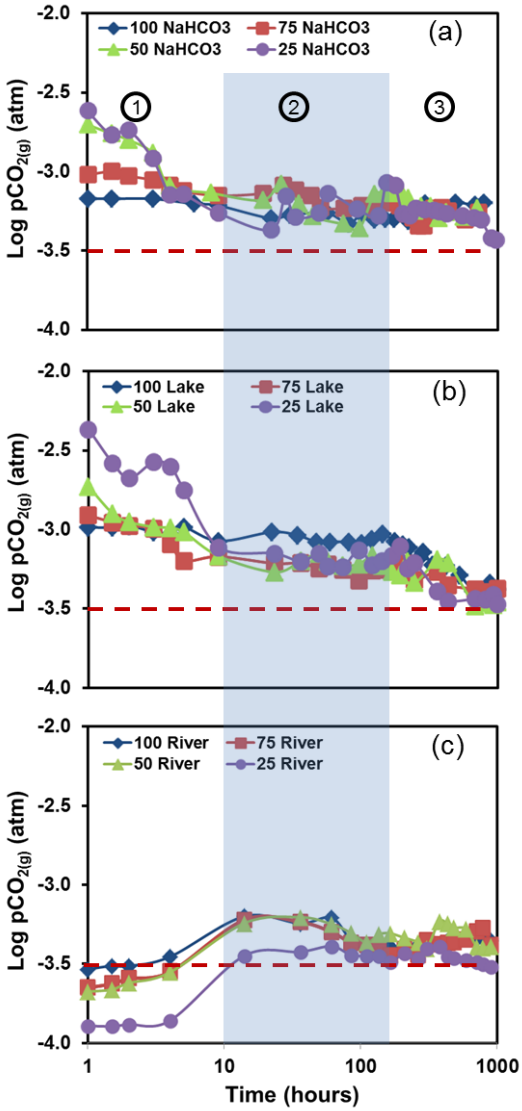

Figure III- 4. Temporal plots of the partial pressure of $CO_{2(g)}$ (pCO_2) for $NaHCO_3$ (a), lake (b) and river (c) samples exposed to the atmosphere in a laboratory setting. The highest $pCO_{2(g)}$ were recorded for the 25%, followed by the 50%, 75% and 100% $NaHCO_3$ and lake samples and for the 100%, followed by the 75%, 50% and 25% river samples. The dashed lines represent an atmospheric $pCO_{2(g)}$ value of $10^{-3.5}$ atmosphere (the accepted average atmospheric $pCO_{2(g)}$). The circled 1, 2 and 3 corresponds to the 3 stages of pH change observed in Figs. 2a-c. [The first sampling points are at time 0 hour but we arbitrary started the x-axis at 1 on the log scale.]

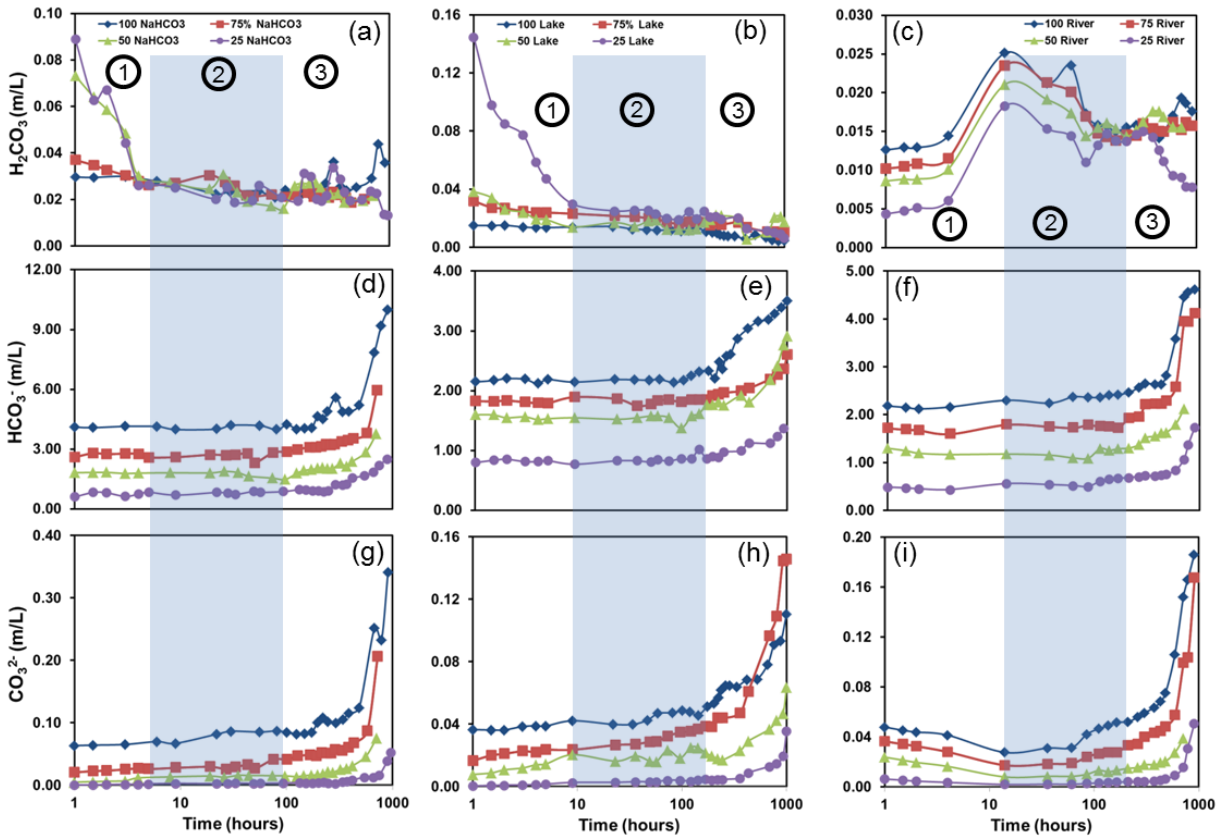

Figure III- 5. Modeled carbonate species (H_2CO_3 + HCO_3^-+ CO_3^{2-}) distribution for the $NaHCO_3$, lake and river samples. H_2CO_3 distribution for $NaHCO_3$ (a), lake (b) and river (c) samples. HCO_3^- distribution for $NaHCO_3$ (d), lake (e) and river (f) samples. CO_3^{2-} distribution for $NaHCO_3$ (g), lake (h) and river (i) samples. The circled 1, 2 and 3 corresponds to the 3 stages of pH change observed in Figs. 2a-c.

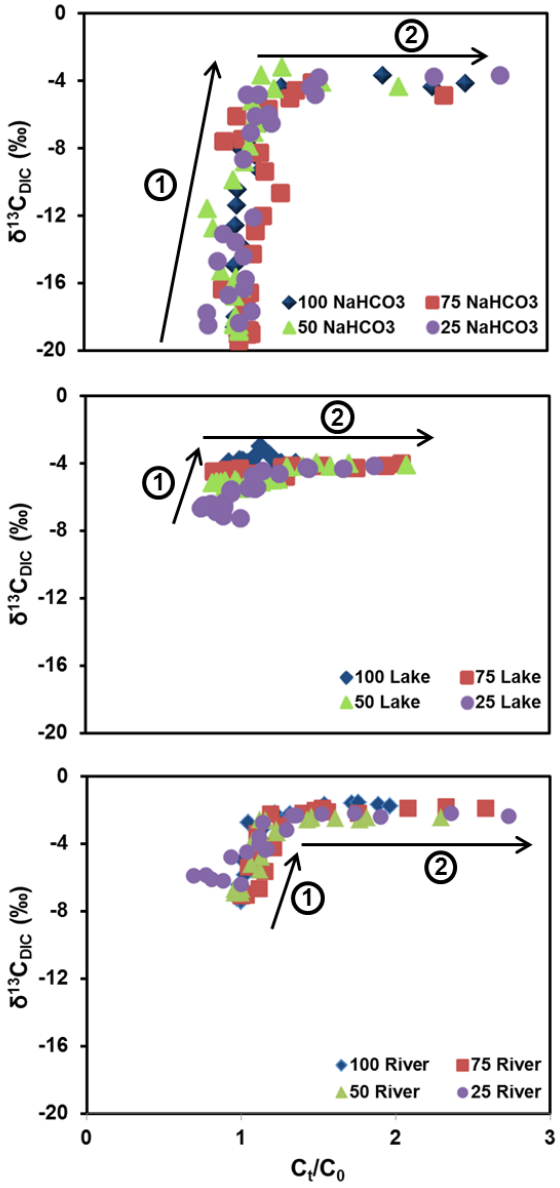

Figure III- 6. Change in the ratio of the concentration at any time (C_t) to the initial concentration (C_0) vs. the stable carbon isotope composition of dissolved inorganic carbon ($\delta^{13}C_{DIC}$) for $NaHCO_3$ (a), lake (b) and river (c) samples exposed to the atmosphere in a laboratory setting. The arrows indicate the direction of evolution of the samples with the upward pointing arrows (1) indicating evolution by carbon isotopic exchange (equilibration) and (2) the forward arrows indicate equilibrium conditions during evaporation.

1

Table III- 1. Physical, chemical and carbon isotope results for the undiluted and diluted $NaHCO_3$ samples.

Sample ID	Time (Hours)	pH	Temp (^{o}C)	Spc (µs/cm)	TDS (mg/L)	Cl^- (mM/L)	SO_4^{2-} (mM/L)	NO_3^- (mM/L)	K^+ (mM/L)	Na+ (mM/L)	Ca^{2+} (mM/L)	Mg^{2+} (mM/L)	Total Alkalinity (mM/L HCO_3^-)	DIC (mM C/L)	$\delta^{13}C_{DIC}$ (‰)	log $pCO_{2(g)}$ (atm.)
100% NaHCO3	1	8.49	22	328	213	-	-	-	-	3.64	-	-	3.29	4.20	-19.1	-3.17
	1.5	8.49	22	327	212	-	-	-	-	3.34	-	-	3.27	4.17	-19.2	-3.17
	3	8.49	22	327	212	-	-	-	-	3.39	-	-	3.25	4.24	-19.0	-3.17
	6	8.52	22	328	213	-	-	-	-	3.39	-	-	3.34	4.23	-18.9	-3.20
	9	8.52	22	330	224	-	-	-	-	3.45	-	-	3.30	4.08	-18.6	-3.21
	22	8.60	22	336	218	-	-	-	-	3.47	-	-	3.34	4.11	-18.0	-3.30
	30	8.60	22	336	219	-	-	-	-	3.48	-	-	3.30	4.30	-17.2	-3.28
	56	8.59	23	343	223	-	-	-	-	3.58	-	-	3.29	4.29	-16.1	-3.26
	81	8.63	22	351	228	-	-	-	-	3.62	-	-	3.30	4.09	-15.0	-3.33
	101	8.59	22	355	231	-	-	-	-	3.65	-	-	3.30	4.34	-14.0	-3.27
	125	8.60	22	361	235	-	-	-	-	3.82	-	-	3.30	4.10	-12.6	-3.30
	149	8.60	22	366	238	-	-	-	-	3.80	-	-	3.58	4.14	-11.4	-3.30
	173	8.61	22	370	235	-	-	-	-	3.83	-	-	3.66	4.16	-10.4	-3.30
	197	8.62	22	379	245	-	-	-	-	3.92	-	-	3.72	4.76	-9.4	-3.25
	221	8.66	23	384	250	-	-	-	-	3.96	-	-	3.82	4.62	-8.4	-3.31
	245	8.60	22	390	254	-	-	-	-	4.11	-	-	3.86	4.18	-7.9	-3.29
	293	8.53	22	396	258	-	-	-	-	4.17	-	-	4.03	4.43	-7.6	-3.20
	341	8.63	21	412	268	-	-	-	-	4.25	-	-	4.31	4.91	-6.5	-3.27
	389	8.66	22	431	280	-	-	-	-	4.79	-	-	4.31	4.94	-5.6	-3.27
	485	8.66	22	504	290	-	-	-	-	5.15	-	-	4.92	5.35	-4.4	-3.20
	675	8.76	24	656	426	-	-	-	-	6.56	-	-	6.53	8.10	-3.7	-3.21
	785	8.65	24	743	483	-	-	-	-	6.82	-	-	7.26	9.46	-4.3	-3.20
	905	8.77	24	800	520	-	-	-	-	6.98	-	-	8.99	10.36	-4.2	-3.20

75% NaHCO3	1	8.22	22	252	164	0.03	0.01	-	0.00	2.65	0.00	0.02	2.54	2.66	-19.5	-3.02
	1.5	8.23	22	252	164	0.03	0.02	-	0.00	2.64	0.00	0.03	2.50	2.86	-19.0	-3.00
	2	8.25	22	252	164	0.03	0.02	-	0.00	2.76	0.00	0.03	2.48	2.81	-19.0	-3.03
	3	8.28	22	253	164	0.03	0.02	-	0.00	2.79	0.00	0.03	2.48	2.84	-18.9	-3.05
	4	8.31	22	253	164	0.03	0.02	-	0.00	2.85	0.00	0.03	2.44	2.82	-18.8	-3.09
	5	8.32	22	253	164	0.03	0.01	-	0.00	2.89	0.00	0.03	2.48	2.64	-19.1	-3.12
	9	8.35	22	254	165	0.03	0.01	-	0.00	2.90	0.00	0.03	2.48	2.65	-18.8	-3.15
	19	8.35	22	256	166	0.04	0.01	-	0.00	2.85	0.00	0.03	2.44	2.78	-17.6	-3.14
	27	8.30	22	257	167	0.04	0.01	-	0.00	2.79	0.00	0.03	2.44	2.76	-17.0	-3.09
	33	8.34	23	258	168	0.04	0.01	-	0.00	2.46	0.00	0.03	2.44	2.77	-16.9	-3.12
	43	8.38	22	260	169	0.04	0.02	-	0.00	2.90	0.00	0.03	2.46	2.84	-16.6	-3.15
	50	8.38	22	262	170	0.04	0.01	-	0.00	2.90	0.00	0.03	2.46	2.37	-16.4	-3.23
	75	8.47	23	266	173	0.04	0.02	-	0.00	2.91	0.00	0.03	2.48	2.89	-14.3	-3.23
	101	8.46	23	270	176	0.04	0.02	-	0.00	2.93	0.00	0.03	2.48	2.94	-12.9	-3.21
	127	8.50	22	273	178	0.04	0.02	-	0.00	3.01	0.00	0.03	2.48	3.06	-12.0	-3.24
	166	8.50	22	279	181	0.04	0.02	-	0.00	3.06	0.01	0.03	2.71	3.37	-10.7	-3.20
	190	8.48	22	284	185	0.04	0.02	-	0.00	3.07	0.01	0.03	2.70	3.10	-9.4	-3.21
	214	8.52	22	289	188	0.05	0.02	-	0.00	3.08	0.01	0.03	2.75	3.02	-8.3	-3.27
	238	8.50	22	293	191	0.05	0.02	-	0.00	3.09	0.01	0.03	2.85	2.71	-7.5	-3.29
	262	8.50	22	299	194	0.05	0.02	-	0.01	3.16	0.01	0.03	2.91	2.40	-7.6	-3.34
	286	8.54	23	302	196	0.05	0.02	-	0.01	3.30	0.01	0.03	2.85	2.62	-6.1	-3.34
	334	8.51	23	308	200	0.05	0.02	-	0.01	3.32	0.01	0.03	3.05	3.17	-5.7	-3.23
	382	8.55	21	330	215	0.05	0.02	-	0.01	3.35	0.01	0.03	3.21	3.54	-5.0	-3.23
	430	8.58	22	347	226	0.06	0.02	-	0.01	3.81	0.01	0.03	3.34	3.64	-4.6	-3.25
	574	8.66	21	423	275	0.06	0.02	-	0.01	4.88	0.01	0.04	4.23	3.92	-4.1	-3.30
	718	8.81	23	612	398	0.07	0.02	-	0.01	6.83	0.02	0.05	5.84	6.18	-4.9	-3.26
50% NaHCO3	1	7.75	22	188	122	0.03	0.02	-	0.01	1.73	0.00	0.04	1.65	1.90	-18.8	-2.70
	1.5	7.81	22	189	123	0.03	0.02	-	0.01	1.84	0.00	0.04	1.65	1.90	-18.9	-2.76

	2	7.85	22	188	122	0.03	0.02	-	0.01	1.88	0.00	0.04	1.65	1.90	-18.5	-2.80
	3	7.92	22	187	122	0.03	0.02	-	0.01	1.89	0.00	0.04	1.65	1.84	-18.5	-2.88
	4	8.13	22	189	123	0.03	0.02	-	0.01	1.90	0.00	0.04	1.65	1.84	-18.4	-3.09
	8	8.18	22	188	112	0.03	0.02	-	0.01	1.91	0.00	0.05	1.65	1.86	-18.0	-3.14
	19	8.22	22	190	123	0.04	0.02	-	0.01	1.91	0.00	0.05	1.67	1.85	-16.8	-3.18
	26	8.14	22	191	124	0.04	0.02	-	0.02	1.92	0.00	0.06	1.61	1.93	-16.3	-3.08
	35	8.25	22	192	125	0.04	0.02	-	0.02	1.93	0.00	0.06	1.65	1.86	-15.7	-3.20
	44	8.29	22	194	126	0.05	0.02	-	0.02	1.99	0.00	0.07	1.65	1.68	-15.3	-3.28
	74	8.31	22	198	129	0.06	0.02	-	0.03	2.04	0.00	0.08	1.67	1.58	-12.7	-3.33
	97	8.32	22	202	131	0.07	0.02	-	0.04	2.06	0.00	0.10	1.69	1.51	-11.6	-3.36
	125	8.19	23	210	136	0.07	0.02	-	0.04	2.09	0.00	0.10	1.81	1.83	-9.9	-3.14
	146	8.21	22	210	135	0.07	0.02	-	0.04	2.13	0.00	0.10	1.89	1.97	-8.8	-3.14
	172	8.22	22	216	141	0.08	0.03	-	0.05	2.15	0.00	0.11	1.87	2.02	-7.9	-3.14
	197	8.23	22	220	143	0.09	0.03	-	0.05	2.20	0.00	0.13	1.91	2.08	-7.1	-3.14
	220	8.27	22	217	141	0.09	0.03	-	0.05	2.42	0.01	0.13	1.97	2.11	-6.5	-3.17
	245	8.34	22	226	147	0.09	0.03	-	0.05	2.49	0.01	0.13	1.93	2.07	-6.3	-3.25
	272	8.31	22	228	148	0.09	0.03	-	0.06	2.63	0.01	0.13	1.97	2.06	-5.2	-3.22
	322	8.36	22	242	158	0.09	0.03	-	0.06	2.67	0.01	0.13	2.10	2.33	-4.5	-3.22
	369	8.41	22	253	164	0.10	0.03	-	0.06	2.71	0.01	0.14	2.24	2.18	-3.7	-3.29
	417	8.42	22	263	171	0.11	0.03	-	0.07	2.79	0.01	0.16	2.40	2.43	-3.2	-3.26
	561	8.52	21	313	204	0.13	0.04	-	0.08	3.41	0.01	0.19	2.93	2.91	-4.1	-3.29
	705	8.59	22	417	271	0.17	0.05	-	0.13	4.66	0.01	0.25	3.84	3.86	-4.4	-3.23
25% NaHCO3	1	7.28	22	109	71	0.09	0.04	-	0.01	0.92	0.01	0.06	0.89	0.83	-18.4	-2.62
	1.5	7.34	22	111	72	0.09	0.04	-	0.01	0.97	0.02	0.06	0.89	0.66	-18.5	-2.77
	2	7.45	22	118	77	0.09	0.04	-	0.01	1.01	0.02	0.06	0.89	0.90	-17.7	-2.74
	3	7.62	22	110	71	0.09	0.04	-	0.01	1.03	0.02	0.06	0.89	0.86	-16.3	-2.92
	4	7.74	22	112	74	0.09	0.04	-	0.01	1.04	0.02	0.06	0.83	0.66	-17.8	-3.15
	5	7.81	22	118	77	0.09	0.04	-	0.01	1.04	0.02	0.06	0.89	0.78	-16.7	-3.14
	9	7.88	22	114	75	0.10	0.04	-	0.01	1.02	0.02	0.06	0.87	0.87	-15.8	-3.26

22	7.89	23	115	73	0.10	0.04	-	0.01	1.03	0.02	0.06	0.87	0.72	-14.7	-3.37
28	7.87	23	111	73	0.10	0.04	-	0.02	1.03	0.02	0.06	0.89	0.86	-14.4	-3.16
33	7.98	23	114	73	0.10	0.04	-	0.02	1.08	0.02	0.06	0.96	0.81	-13.5	-3.29
49	7.92	23	114	74	0.11	0.05	-	0.02	1.09	0.02	0.06	0.90	0.75	-13.1	-3.26
57	7.88	23	120	79	0.12	0.05	-	0.02	1.09	0.02	0.06	0.96	0.91	-12.1	-3.14
93	7.95	23	119	78	0.12	0.05	-	0.03	1.09	0.02	0.06	0.96	0.85	-8.7	-3.24
133	8.01	22	127	82	0.13	0.05	-	0.03	1.11	0.02	0.06	0.96	0.90	-7.1	-3.28
153	7.85	22	127	82	0.13	0.05	-	0.03	1.12	0.02	0.07	0.98	1.01	-6.5	-3.07
177	7.86	22	126	81	0.13	0.05	-	0.03	1.12	0.02	0.07	1.02	0.99	-6.0	-3.09
201	8.01	22	135	87	0.13	0.05	-	0.03	1.16	0.02	0.07	1.08	0.92	-6.1	-3.27
225	8.03	22	128	84	0.13	0.02	-	0.03	1.16	0.02	0.07	1.14	0.93	-5.6	-3.28
249	7.95	22	132	86	0.13	0.02	-	0.04	1.20	0.02	0.10	1.18	0.87	-4.8	-3.23
290	7.78	23	138	89	0.05	0.02	-	0.05	1.29	0.02	0.07	1.18	0.94	-4.8	-3.24
338	7.98	22	146	94	0.06	0.02	-	0.05	1.36	0.02	0.08	1.18	1.24	-4.8	-3.25
372	8.06	23	156	102	0.09	0.02	-	0.05	1.39	0.03	0.08	1.20	1.22	-4.4	-3.25
420	8.15	23	156	102	0.05	0.02	-	0.06	1.49	0.03	0.09	1.28	1.26	-3.8	-3.27
545	8.25	21	181	117	0.05	0.02	-	0.08	1.66	0.03	0.10	1.48	1.58	-3.8	-3.28
661	8.20	22	207	135	0.06	0.02	-	0.10	1.96	0.03	0.11	1.67	1.70	-3.8	-3.29
751	8.26	227	243	158	0.06	0.02	-	0.13	2.46	0.04	0.14	1.93	1.88	-3.8	-3.30
892	8.55	23	288	187	0.06	0.02	-	0.13	2.58	0.05	0.16	2.20	2.24	-3.7	-3.42
964	8.62	23	319	207	0.07	0.03	-	0.13	2.64	0.05	0.16	2.40	2.56	-3.7	-3.43

Spc = Specific conductance
TDS = Total dissolved solids
- = Not applicable

8

Table III- 2. Physical, chemical and carbon isotope results for the undiluted and diluted lake samples.

Sample ID	Time (Hours)	pH	Temp (ºC)	Spc (µs/cm)	TDS (mg/L)	Cl^- (mM/L)	SO_4^{2-} (mM/L)	NO_3^- (mM/L)	K^+ (mM/L)	Na^+ (mM/L)	Ca^{2+} (mM/L)	Mg^{2+} (mM/L)	Total Alkalinity (mM/L HCO_3^-)	DIC (mM C/L)	$\delta^{13}C_{DIC}$ (‰)	log $pCO_{2(g)}$ (atm.)
100% Lake	1	8.34	22.33	372.00	242.00	0.15	0.05	0.00	0.09	0.72	0.77	0.19	2.93	3.78	-4.0	-3.09
	1.5	8.34	22.33	373.00	243.00	0.14	0.05	0.00	0.09	0.71	0.76	0.19	2.91	3.78	-3.8	-3.09
	2	8.34	22.33	373.00	243.00	0.14	0.04	0.00	0.09	0.69	0.73	0.19	2.91	3.87	-3.9	-3.09
	3	8.37	22.33	374.00	243.00	0.14	0.05	0.00	0.09	0.71	0.74	0.19	2.93	3.80	-4.2	-3.12
	4	8.38	22.28	374.00	242.00	0.15	0.05	0.00	0.09	0.70	0.74	0.20	2.91	3.82	-4.0	-3.14
	5	8.38	22.23	374.00	243.00	0.14	0.05	0.00	0.09	0.69	0.74	0.18	2.91	4.24	-4.4	-3.14
	9	8.39	22.14	374.00	243.00	0.15	0.05	0.00	0.09	0.72	0.76	0.19	3.11	3.50	-4.0	-3.12
	22	8.37	22.43	376.00	245.00	0.15	0.05	0.00	0.09	0.72	0.75	0.19	3.03	3.84	-3.9	-3.11
	34	8.40	22.22	377.00	244.00	0.15	0.05	0.00	0.09	0.71	0.76	0.21	2.89	3.86	-3.9	-3.14
	47	8.42	22.23	379.00	246.00	0.15	0.05	0.00	0.09	0.73	0.77	0.19	2.99	3.72	-4.1	-3.18
	59	8.45	21.98	381.00	248.00	0.15	0.05	0.00	0.09	0.72	0.78	0.20	3.15	3.96	-4.0	-3.20
	81	8.45	21.98	385.00	251.00	0.15	0.05	0.00	0.12	0.96	0.75	0.20	3.13	4.02	-4.1	-3.18
	101	8.47	22.26	388.00	252.00	0.16	0.05	0.00	0.10	0.72	0.77	0.22	3.15	4.04	-4.1	-3.20
	119	8.45	22.56	393.00	256.00	0.15	0.05	0.00	0.10	0.73	0.77	0.20	3.19	4.09	-4.1	-3.17
	143	8.41	22.83	398.00	259.00	0.16	0.05	0.00	0.10	0.70	0.74	0.20	3.23	4.10	-4.3	-3.13
	175	8.48	22.00	397.00	260.00	0.16	0.05	0.00	0.11	0.82	0.86	0.22	3.29	4.18	-4.4	-3.20
	202	8.50	22.18	408.00	265.00	0.16	0.05	0.00	0.10	0.74	0.82	0.21	3.30	4.35	-4.6	-3.21
	223	8.52	22.50	414.00	269.00	0.17	0.05	0.00	0.12	0.88	0.87	0.22	3.42	4.34	-4.6	-3.22
	238	8.57	22.42	416.00	270.00	0.17	0.05	0.00	0.10	0.76	0.79	0.22	3.42	3.83	-5.3	-3.26
	261	8.59	22.47	421.00	273.00	0.17	0.05	0.00	0.11	0.80	0.85	0.22	3.50	4.26	-4.5	-3.28
	285	8.59	22.68	427.00	278.00	0.18	0.06	0.00	0.12	0.86	0.89	0.23	3.50	4.79	-4.0	-3.28
	333	8.59	22.01	438.00	285.00	0.19	0.06	0.00	0.13	0.96	1.01	0.25	3.52	4.67	-4.6	-3.35
	420	8.66	21.58	460.00	299.00	0.21	0.07	0.02	0.14	1.04	1.06	0.29	3.44	4.46	-4.8	-3.31
	525	8.65	21.50	490.00	328.00	0.22	0.07	0.00	0.16	1.16	0.66	0.33	4.23	5.14	-4.0	-3.41

	661	8.66	22.19	510.00	329.00	0.24	0.08	0.00	0.16	1.18	0.70	0.34	3.68	4.29	-3.0	-3.40
	761	8.76	22.15	515.00	345.00	0.28	0.09	0.00	0.20	1.42	0.65	0.41	3.70	4.21	-3.5	-3.48
	881	8.79	22.97	546.00	355.00	0.30	0.09	0.01	0.19	1.41	0.62	0.36	3.58	4.53	-3.5	-3.42
	1000	8.81	23.22	597.00	388.00	0.35	0.11	0.01	0.27	1.85	0.61	0.41	4.03	4.61	-4.3	-3.44
75% Lake	1	8.18	18.73	296.00	193.00	0.26	0.09	0.01	0.07	0.40	0.11	2.35	2.26	2.29	-4.7	-2.91
	1.5	8.25	18.96	297.00	193.00	0.32	0.12	0.01	0.07	0.38	0.12	2.39	2.30	2.22	-4.5	-2.95
	2	8.26	19.27	296.00	192.00	0.32	0.12	0.01	0.07	0.40	0.13	2.45	2.34	2.15	-4.5	-2.98
	3	8.29	19.68	296.00	193.00	0.32	0.12	0.01	0.08	0.40	0.13	2.49	2.34	2.08	-4.5	-2.99
	4	8.29	20.06	298.00	193.00	0.32	0.12	0.01	0.08	0.39	0.13	2.51	2.26	1.90	-4.5	-3.09
	5	8.30	20.41	298.00	193.00	0.32	0.12	0.01	0.08	0.40	0.14	2.55	2.34	2.12	-4.4	-3.20
	9	8.30	21.19	299.00	194.00	0.33	0.12	0.01	0.08	0.45	0.13	2.63	2.30	2.28	-4.3	-3.17
	23	8.33	22.41	302.00	196.00	0.33	0.12	0.01	0.08	0.45	0.13	2.69	2.36	2.17	-4.5	-3.21
	36	8.34	22.43	303.00	197.00	0.33	0.12	0.01	0.07	0.45	0.13	2.69	2.36	2.24	-4.6	-3.21
	49	8.36	22.85	305.00	198.00	0.34	0.12	0.01	0.08	0.45	0.13	2.66	2.36	2.16	-4.6	-3.24
	57	8.36	22.61	306.00	199.00	0.33	0.12	0.01	0.09	0.46	0.14	2.80	2.38	2.29	-4.6	-3.22
	73	8.42	22.63	306.00	199.00	0.33	0.12	0.01	0.08	0.45	0.13	2.76	2.34	2.43	-4.6	-3.26
	96	8.44	22.83	310.00	201.00	0.34	0.12	0.01	0.09	0.46	0.14	3.00	2.40	2.18	-4.7	-3.32
	121	8.43	22.99	316.00	205.00	0.35	0.12	0.01	0.09	0.48	0.14	3.01	2.48	2.45	-4.7	-3.26
	142	8.44	22.44	318.00	207.00	0.35	0.12	0.01	0.10	0.51	0.15	3.07	2.56	2.57	-4.7	-3.25
	168	8.45	22.76	322.00	209.00	0.35	0.12	0.01	0.10	0.52	0.16	3.35	2.60	2.55	-4.8	-3.25
	192	8.48	21.73	327.00	213.00	0.37	0.12	0.01	0.10	0.54	0.16	3.39	2.46	2.97	-4.8	-3.24
	219	8.49	21.64	333.00	216.00	0.37	0.12	0.01	0.10	0.55	0.16	3.43	2.77	2.78	-5.0	-3.21
	245	8.50	22.54	338.00	220.00	0.38	0.12	0.01	0.11	0.57	0.16	3.44	2.66	2.53	-5.0	-3.32
	360	8.50	21.63	367.00	239.00	0.38	0.12	0.01	0.11	0.61	0.17	3.49	2.89	2.91	-4.3	-3.27
	432	8.60	22.12	392.00	255.00	0.40	0.14	0.02	0.11	0.81	0.18	3.49	2.99	3.05	-4.2	-3.35
	686	8.75	22.52	447.00	290.00	0.44	0.15	0.02	0.12	1.09	0.19	3.76	3.46	3.51	-4.2	-3.38
	806	8.77	23.12	484.00	315.00	0.45	0.15	0.02	0.13	1.28	0.20	3.97	3.72	4.01	-4.3	-3.40
	926	8.87	23.21	536.00	349.00	0.46	0.16	0.02	0.13	1.32	0.39	4.07	4.07	4.45	-4.2	-3.45
	1000	8.82	24.21	564.00	367.00	0.46	0.17	0.03	0.15	1.36	0.40	4.17	4.43	4.68	-4.0	-3.38

50% Lake	1	7.97	20.00	218.00	141.00	0.27	0.10	0.00	0.05	0.40	0.09	1.69	1.65	1.65	-5.5	-2.73
	1.5	8.02	20.11	219.00	141.00	0.26	0.10	0.00	0.05	0.38	0.09	1.64	1.65	1.49	-5.4	-2.90
	2	8.12	20.27	220.00	145.00	0.27	0.10	0.00	0.05	0.40	0.09	1.69	1.61	1.35	-5.2	-2.95
	3	8.16	20.49	217.00	139.00	0.27	0.10	0.00	0.05	0.40	0.09	1.70	1.63	1.39	-5.1	-2.98
	4	8.24	20.69	217.00	142.00	0.27	0.10	0.01	0.05	0.39	0.09	1.70	1.59	1.40	-5.1	-2.99
	5	8.25	20.88	221.00	144.00	0.27	0.10	0.01	0.05	0.40	0.09	1.72	1.61	1.44	-5.1	-3.02
	9	8.38	22.36	216.00	141.00	0.27	0.10	0.02	0.06	0.45	0.10	1.70	1.65	1.49	-5.1	-3.17
	23	8.29	22.16	222.00	144.00	0.27	0.10	0.02	0.06	0.45	0.10	1.77	1.61	1.49	-5.1	-3.27
	36	8.36	22.34	219.00	143.00	0.27	0.10	0.03	0.06	0.45	0.11	1.80	1.65	1.59	-5.0	-3.20
	49	8.27	22.57	220.00	143.00	0.26	0.10	0.03	0.06	0.45	0.11	1.84	1.67	1.81	-5.0	-3.15
	57	8.26	22.44	221.00	143.00	0.26	0.10	0.03	0.06	0.46	0.11	1.87	1.67	1.62	-5.1	-3.20
	73	8.43	22.60	218.00	141.00	0.27	0.10	0.03	0.06	0.45	0.11	1.87	1.67	1.74	-5.1	-3.23
	96	8.38	22.54	232.00	151.00	0.28	0.10	0.03	0.06	0.46	0.11	1.89	1.48	1.87	-5.1	-3.22
	121	8.45	22.93	231.00	150.00	0.28	0.10	0.03	0.06	0.48	0.11	2.07	1.71	1.87	-5.0	-3.17
	142	8.44	22.37	238.00	155.00	0.30	0.11	0.03	0.06	0.51	0.11	2.20	1.75	1.92	-5.0	-3.23
	168	8.34	22.17	236.00	154.00	0.29	0.11	0.03	0.07	0.52	0.12	2.24	1.89	1.72	-5.0	-3.26
	192	8.30	21.55	242.00	151.00	0.32	0.12	0.03	0.07	0.54	0.12	2.34	1.89	2.00	-5.0	-3.29
	219	8.25	21.47	248.00	160.00	0.32	0.11	0.04	0.07	0.55	0.12	2.37	1.93	2.06	-5.0	-3.20
	245	8.24	21.74	251.00	163.00	0.33	0.12	0.04	0.07	0.57	0.12	2.42	1.87	1.82	-4.8	-3.33
	360	8.33	21.50	276.00	180.00	0.33	0.12	0.03	0.08	0.61	0.13	2.63	2.07	2.32	-4.2	-3.19
	432	8.84	22.09	300.00	195.00	0.33	0.12	0.04	0.11	0.81	0.17	3.46	2.24	2.15	-4.3	-3.21
	686	8.63	22.47	355.00	231.00	0.41	0.15	0.05	0.16	1.09	0.22	4.72	2.60	2.46	-4.0	-3.48
	806	8.38	23.26	390.00	254.00	0.44	0.16	0.04	0.19	1.28	0.26	5.57	2.75	2.61	-4.2	-3.46
	926	8.42	23.45	439.00	286.00	0.65	0.21	0.04	0.20	1.32	0.27	5.77	3.19	2.81	-4.0	-3.47
	1000	8.52	24.47	467.00	304.00	0.75	0.24	0.04	0.21	1.36	0.28	5.97	3.46	3.42	-4.1	-3.46
25% Lake	1	7.07	21.30	127.00	83.00	0.17	0.07	0.07	0.03	0.21	0.05	0.83	0.77	0.99	-7.2	-2.37
	1.5	7.26	21.36	125.00	81.00	0.17	0.07	0.07	0.03	0.22	0.05	0.83	0.81	0.88	-7.1	-2.58

2	7.34	21.40	129.00	84.00	0.17	0.07	0.07	0.03	0.22	0.05	0.87	0.85	0.83	-6.9	-2.68
3	7.39	21.49	125.00	78.00	0.17	0.07	0.07	0.04	0.23	0.06	0.96	0.87	0.79	-6.6	-2.57
4	7.49	21.59	132.00	86.00	0.18	0.07	0.07	0.03	0.23	0.06	0.95	0.83	0.75	-6.5	-2.60
5	7.58	21.86	125.00	82.10	0.17	0.07	0.07	0.03	0.23	0.06	0.94	0.83	0.76	-6.5	-2.75
9	7.79	21.93	125.00	82.00	0.18	0.07	0.07	0.03	0.24	0.06	0.94	0.85	0.80	-6.4	-3.11
23	7.83	22.51	133.00	86.00	0.19	0.07	0.07	0.03	0.24	0.06	0.94	0.79	0.79	-6.5	-3.15
36	7.85	22.53	127.00	82.00	0.17	0.07	0.07	0.03	0.24	0.06	0.96	0.85	0.74	-6.7	-3.20
49	7.85	22.81	127.00	83.00	0.18	0.07	0.07	0.03	0.24	0.06	0.98	0.85	0.88	-6.6	-3.15
57	7.88	22.72	131.00	85.00	0.18	0.08	0.07	0.04	0.24	0.06	1.02	0.83	0.88	-6.5	-3.23
73	7.96	22.93	132.00	87.00	0.18	0.07	0.07	0.03	0.25	0.06	1.02	0.87	0.88	-6.3	-3.24
96	7.97	23.00	139.00	90.00	0.18	0.07	0.07	0.04	0.24	0.07	1.04	0.85	0.93	-5.8	-3.13
121	7.88	23.26	138.00	90.00	0.19	0.08	0.07	0.03	0.24	0.07	1.05	0.89	0.93	-5.6	-3.23
142	7.98	22.78	132.00	86.00	0.19	0.08	0.08	0.04	0.25	0.07	1.06	0.89	0.93	-5.5	-3.20
168	7.95	22.49	137.00	89.00	0.19	0.08	0.08	0.04	0.25	0.07	1.07	1.04	1.04	-5.5	-3.16
192	7.96	21.99	141.00	92.00	0.19	0.08	0.08	0.04	0.27	0.07	1.07	0.89	1.10	-5.4	-3.10
219	7.97	21.86	147.00	95.00	0.19	0.08	0.08	0.04	0.27	0.07	1.07	0.92	1.09	-5.5	-3.25
245	8.00	22.13	143.00	94.00	0.21	0.09	0.08	0.05	0.27	0.07	1.08	0.90	1.07	-4.7	-3.21
360	8.02	21.87	168.00	109.00	0.26	0.09	0.09	0.09	0.31	0.08	1.27	1.00	1.14	-4.4	-3.39
432	8.22	22.51	174.00	114.00	0.27	0.09	0.10	0.09	0.31	0.08	1.26	1.04	1.24	-4.6	-3.45
686	8.33	22.38	199.00	129.00	0.30	0.10	0.10	0.10	0.33	0.08	1.32	1.18	1.41	-4.2	-3.44
806	8.37	23.05	223.00	144.00	0.36	0.13	0.13	0.12	0.41	0.10	1.66	1.20	1.43	-4.3	-3.44
926	8.45	23.23	252.00	164.00	0.42	0.13	0.14	0.17	0.46	0.12	1.86	1.34	1.65	-4.3	-3.41
1000	8.65	24.04	280.00	182.00	0.50	0.14	0.15	0.29	0.52	0.13	2.11	1.55	1.85	-4.1	-3.47

Spc = Specific conductance
TDS = Total dissolved solids

Table III- 3. Physical, chemical and carbon isotope results for the undiluted and diluted river samples

14

Sample ID	Time (Hours)	pH	Temp (ºC)	Spc (µs/cm)	TDS (mg/L)	Cl^- (mM/L)	SO_4^{2-} (mM/L)	NO_3^- (mM/L)	K^+ (mM/L)	Na^+ (mM/L)	Ca^{2+} (mM/L)	Mg^{2+} (mM/L)	Total Alkalinity (mM/L HCO_3^-)	DIC (mM C/L)	$\delta^{13}C_{DIC}$ (‰)	log $pCO_{2(g)}$ (atm.)
100% River	1	8.6	15	1854	1235	12.09	1.04	0.02	0.21	11.74	1.86	0.97	2.44	2.40	-7.4	-7.43
	1.5	8.58	15.2	1843	1227	11.96	1.03	0.02	0.22	11.58	1.98	1.00	2.40	2.48	-7.4	-7.38
	2	8.57	15.5	1847	1230	12.02	1.03	0.02	0.21	11.76	1.96	0.96	2.36	2.41	-7.2	-7.20
	4	8.52	16.8	1831	1219	12.32	1.06	0.01	0.23	11.50	2.04	1.05	2.40	2.41	-7.2	-7.22
	14	8.29	19.2	1833	1221	12.87	1.10	0.02	0.24	11.81	1.92	0.96	2.48	2.45	-6.4	-6.45
	36	8.35	19.5	1854	1237	12.87	1.11	0.02	0.25	11.57	1.95	1.01	2.44	2.54	-5.9	-5.87
	61	8.33	19.4	1881	1253	12.50	1.07	0.01	0.28	11.91	2.07	1.08	2.58	2.64	-5.5	-5.52
	85	8.46	19.2	1919	1277	12.73	1.09	0.01	0.27	12.09	2.10	1.09	2.62	2.58	-5.1	-5.12
	111	8.5	19.3	1933	1286	12.90	1.10	0.02	0.32	12.48	2.23	1.18	2.66	2.50	-5.0	-4.97
	136	8.51	19.5	2000	1338	13.29	1.14	0.01	0.31	12.61	2.21	1.21	2.71	2.74	-4.0	-3.95
	165	8.53	19.4	2010	1330	13.69	1.17	0.01	0.33	12.70	2.47	1.25	2.75	2.83	-3.1	-3.11
	210	8.52	19.7	2060	1375	14.21	1.21	0.01	0.28	12.75	2.74	1.32	2.81	2.59	-2.7	-2.74
	262	8.53	19.6	2130	1418	14.96	1.28	0.01	0.27	12.95	2.81	1.45	2.95	2.91	-2.4	-2.40
	303	8.54	19.3	2220	1475	16.83	1.43	0.05	0.32	13.32	2.81	1.53	3.05	3.05	-2.4	-2.35
	377	8.55	21.3	2280	1516	16.83	1.44	0.02	0.44	15.23	2.90	1.65	3.07	3.02	-2.2	-2.19
	432	8.57	21.7	2360	1570	19.57	1.65	0.01	0.56	17.41	2.99	1.68	3.09	3.26	-2.2	-2.22
	481	8.58	21.6	2460	1641	19.05	1.61	0.02	0.59	17.85	3.08	1.81	3.34	3.81	-1.7	-1.67
	590	8.63	20	2740	1826	22.30	1.88	0.02	0.77	21.75	3.62	2.13	4.33	4.25	-1.6	-1.58
	711	8.65	22	3100	2060	31.89	2.64	0.04	1.07	23.93	3.56	2.95	5.51	4.36	-1.5	-1.55
	783	8.67	22.3	3200	2200	36.29	2.98	0.04	1.24	25.91	3.45	3.53	5.70	4.68	-1.7	-1.69
	903	8.69	22.5	3400	2930	51.82	4.15	0.07	1.72	30.44	3.18	4.78	5.86	4.87	-1.7	-1.74
75% River	1	8.58	16.9	296	995	9.24	0.80	0.03	0.16	9.00	1.43	0.74	1.91	1.94	-7.1	-3.65
	1.5	8.56	17	297	997	9.21	0.80	0.06	0.16	9.13	1.40	0.70	1.87	1.77	-7.1	-3.62
	2	8.54	17.2	296	998	9.32	0.81	0.03	0.18	9.30	1.43	0.65	1.85	1.81	-7.0	-3.59

	4	8.49	17.7	296	992	9.17	0.80	0.03	0.16	9.35	1.39	0.65	1.75	1.76	-7.0	-3.55
	14	8.22	19	298	994	9.25	0.80	0.03	0.17	9.61	1.46	0.67	1.91	1.96	-6.7	-3.22
	36	8.25	19.3	298	1007	9.44	0.82	0.02	0.17	9.78	1.46	0.66	1.87	2.02	-5.7	-3.23
	61	8.27	19.1	299	1033	9.66	0.84	0.03	0.18	9.87	1.53	0.70	1.85	1.84	-5.4	-3.30
	85	8.36	18.9	302	1040	10.22	0.89	0.03	0.17	10.04	1.49	0.71	1.93	1.94	-4.7	-3.37
	111	8.41	19	303	1070	10.05	0.88	0.03	0.18	10.35	1.52	0.72	1.91	2.12	-4.2	-3.38
	136	8.42	19.2	305	1082	10.62	0.93	0.03	0.18	10.43	1.60	0.77	1.91	2.11	-4.1	-3.39
	165	8.43	19	306	1095	10.91	0.95	0.03	0.18	10.61	1.65	0.78	1.89	1.93	-3.4	-3.44
	210	8.45	19.6	306	1128	11.37	0.99	0.02	0.19	11.00	1.79	0.75	2.12	2.21	-2.9	-3.40
	262	8.46	19.3	310	1167	11.94	1.04	0.03	0.21	11.78	1.87	0.90	2.16	2.08	-2.2	-3.44
	303	8.47	19	316	1204	12.98	1.13	0.03	0.21	12.48	2.08	0.89	2.46	2.67	-1.9	-3.35
	377	8.47	21.6	318	1255	13.75	1.20	0.03	0.24	13.04	2.17	1.04	2.50	2.45	-2.2	-3.38
	432	8.48	21.4	322	1308	14.72	1.28	0.06	0.25	15.22	2.33	1.09	2.52	2.59	-2.0	-3.37
	481	8.49	21.4	327	1385	17.19	1.48	0.05	0.28	18.35	2.63	1.31	2.62	2.73	-2.1	-3.36
	590	8.51	20.2	333	1536	23.99	2.07	0.07	0.32	18.83	3.55	1.41	2.99	3.08	-2.2	-3.34
	711	8.53	21.9	338	1826	27.60	2.36	0.08	0.44	21.74	3.94	2.33	4.70	3.65	-1.9	-3.29
	783	8.55	23	367	2000	3.40	2.92	0.10	0.79	25.09	5.08	3.79	4.98	4.08	-1.8	-3.27
	903	8.68	24.21	392	2500	42.23	3.56	0.14	0.86	34.78	5.50	4.08	5.51	4.53	-1.9	-3.38
50% River	1	8.53	17.9	1027	684	6.20	0.55	0.06	0.09	7.09	0.82	0.42	1.40	1.39	-6.9	-3.68
	1.5	8.5	18	1029	685	6.24	0.56	0.07	0.10	7.06	0.82	0.47	1.34	1.34	-6.9	-3.66
	2	8.48	18.1	1032	687	6.09	0.54	0.06	0.10	7.21	0.85	0.45	1.28	1.40	-6.7	-3.62
	4	8.41	18.4	1037	689	6.15	0.55	0.06	0.09	7.09	0.83	0.45	1.24	1.38	-6.7	-3.55
	14	8.09	19.1	1038	691	6.17	0.55	0.06	0.10	7.40	0.85	0.46	1.22	1.34	-6.7	-3.24
	36	8.12	19.4	1050	700	6.27	0.56	0.08	0.10	7.56	0.90	0.45	1.20	1.56	-5.5	-3.21
	61	8.14	19.3	1071	714	6.39	0.57	0.06	0.11	7.68	0.92	0.50	1.14	1.48	-5.2	-3.25
	85	8.22	19	1093	729	6.50	0.58	0.06	0.11	7.94	0.96	0.50	1.14	1.57	-4.8	-3.30
	111	8.26	19.2	1125	749	6.66	0.59	0.06	0.10	7.93	0.96	0.48	1.36	1.50	-3.9	-3.37
	136	8.23	19.4	1152	767	6.84	0.61	0.06	0.12	7.93	1.03	0.53	1.32	1.58	-3.5	-3.31
	165	8.26	19.3	1165	776	6.94	0.62	0.06	0.12	8.43	1.06	0.54	1.36	1.71	-3.3	-3.31

	210	8.29	20.1	1227	819	7.11	0.63	0.06	0.12	8.60	1.06	0.55	1.38	1.71	-3.1	-3.34
	262	8.29	19.9	1249	831	7.39	0.66	0.06	0.13	8.55	1.14	0.58	1.46	1.61	-2.6	-3.36
	303	8.31	18.9	1296	863	7.79	0.69	0.06	0.15	9.51	1.17	0.63	1.61	1.56	-2.6	-3.40
	377	8.26	22.5	1328	885	8.28	0.74	0.07	0.16	10.15	1.28	0.62	1.65	1.99	-2.6	-3.23
	432	8.28	22	1403	936	8.69	0.77	0.07	0.16	10.59	1.34	0.70	1.73	2.03	-2.4	-3.25
	481	8.3	21.9	1453	968	9.04	0.80	0.07	0.18	11.05	1.40	0.81	1.75	2.02	-2.5	-3.27
	590	8.38	20.9	1607	1066	10.23	0.91	0.08	0.23	12.73	1.89	0.94	1.97	2.46	-2.6	-3.28
	711	8.45	21	1822	1214	12.40	1.10	0.10	0.27	14.06	2.00	1.12	2.36	2.24	-2.5	-3.40
	783	8.52	22.6	1914	1376	14.93	1.32	0.10	0.32	15.69	2.11	1.24	2.66	2.52	-2.5	-3.40
	903	8.6	23.07	2000	1604	15.69	1.38	0.12	0.43	17.47	2.57	1.30	2.85	3.20	-2.5	-3.39
25% River	1	8.4	19.4	494	329	2.81	0.28	0.06	0.04	3.38	0.42	0.39	0.51	0.65	-6.4	-3.89
	1.5	8.35	19.4	495	330	2.78	0.27	0.06	0.04	3.39	0.42	0.38	0.49	0.52	-6.2	-3.89
	2	8.3	19.4	496	330	2.79	0.27	0.05	0.04	3.32	0.39	0.36	0.47	0.48	-6.1	-3.88
	4	8.21	19.3	495	330	2.82	0.28	0.06	0.05	3.27	0.40	0.37	0.45	0.41	-5.9	-3.86
	14	7.84	19.3	500	333	2.81	0.27	0.05	0.05	3.27	0.42	0.37	0.57	0.46	-5.8	-3.45
	36	7.9	19.2	510	340	2.90	0.28	0.05	0.07	3.34	0.42	0.36	0.55	0.55	-4.8	-3.42
	61	7.91	19.3	528	352	2.94	0.29	0.06	0.07	3.34	0.45	0.36	0.53	0.61	-4.5	-3.39
	85	8.01	19.01	534	355	3.01	0.29	0.05	0.09	3.45	0.50	0.36	0.51	0.68	-4.4	-3.44
	111	8.02	19.1	555	371	3.11	0.30	0.06	0.08	3.67	0.47	0.37	0.63	0.69	-4.3	-3.45
	136	8	19	560	373	3.15	0.30	0.05	0.09	3.68	0.51	0.38	0.67	0.66	-4.0	-3.45
	165	8.04	19.1	577	385	3.20	0.32	0.06	0.09	3.52	0.53	0.34	0.69	0.66	-3.6	-3.49
	210	8.05	19.5	595	396	3.25	0.35	0.07	0.12	3.75	0.54	0.37	0.71	0.76	-3.2	-3.43
	262	8.03	20	628	418	3.58	0.37	0.07	0.12	3.78	0.59	0.38	0.73	0.67	-2.7	-3.47
	303	8.031	19.8	652	434	3.65	0.38	0.07	0.15	4.02	0.63	0.36	0.75	0.79	-2.3	-3.40
	377	8.04	21.7	693	462	3.71	0.39	0.08	0.15	4.24	0.62	0.37	0.75	0.80	-2.3	-3.39
	432	8.1	22	721	480	4.11	0.40	0.08	0.15	4.48	0.66	0.38	0.77	0.79	-2.3	-3.45
	481	8.16	22	747	498	4.31	0.41	0.08	0.20	4.63	0.84	0.37	0.79	0.90	-2.2	-3.46
	590	8.29	20.9	842	561	4.78	0.46	0.08	0.20	5.20	0.93	0.46	0.89	1.03	-2.2	-3.47
	711	8.4	21	1029	686	5.86	0.56	0.09	0.31	6.68	0.98	0.46	1.14	1.12	-2.4	-3.49

	783	8.56	22.9	1105	736	6.42	0.61	0.11	0.33	7.12	1.05	0.49	1.51	1.39	-2.2	-3.50
	903	8.66	23	1278	800	7.53	0.72	0.12	0.43	9.02	1.36	0.58	1.99	1.61	-2.3	-3.52

Spc = Specific conductance
TDS = Total dissolved solids

CHAPTER IV

GENERAL CONCLUSION

This work addressed three related and outstanding problems on DIC evolution and $\delta^{13}C_{DIC}$ composition in surface waters:

(1) The chemical and isotopic equilibrium state of surface water and its temporal evolution to chemical and isotopic equilibrium,

(2) The temporal and spatial chemical and isotopic evolution of surface water with potential to precipitate carbonates and

(3) The effect of precipitation which adds water into surface water causing solute and DIC dilution on the chemical and isotopic evolution of DIC to equilibrium.

The problems were approached by conducting laboratory and/or field experiments on three separate projects that involved tracing DIC behavior and $\delta^{13}C_{DIC}$ composition over space and/or time in surface waters that interacts with atmospheric $CO_{2(g)}$. The objectives of the research were:

(1) to develop models that characterize the evolutionary pathways of DIC in surface water exposed to atmospheric $CO_{2(g)}$ over time,

(2) to generate information on DIC-$\delta^{13}C_{DIC}$ models from field and laboratory data that characterize water evolution through calcite saturation and,

(3) to conduct a comparative assessment of the effect of DIC dilution by precipitation on DIC chemical and isotopic evolution.

The following outcome resulted from the experiments:

1) Generated models based on DIC concentrations and $\delta^{13}C_{DIC}$ that can be used to assess the temporary trajectory during carbon cycling in surface waters,

2) Information on DIC evolutionary phases and fractionation of $\delta^{13}C_{DIC}$ as water evolve from undersaturation to saturation with respect to calcite, and

3) Information on changes on DIC concentration and $\delta^{13}C_{DIC}$ composition due to surface water dilution by precipitation

I. Generated models based on DIC concentrations and $\delta^{13}C_{DIC}$ that can be used to assess the temporary trajectory during carbon cycling in surface waters

The first project involved conducting laboratory experiments in which artificial $NaHCO_3$ solution, natural groundwater and lake water were exposed to laboratory air for up to 1000 hours to monitor the behavior of DIC and $\delta^{13}C_{DIC}$ composition over time. The results from this experiment showed that there was $CO_{2(g)}$ loss, $CO_{2(g)}$ gain and carbon exchange between DIC in surface waters and atmospheric $CO_{2(g)}$ that resulted to varied DIC concentration and $\delta^{13}C_{DIC}$ behavior over time. Conceptualizing the possible pathways of DIC in a system in which carbon cycling is dominated by surface water DIC - atmospheric $CO_{2(g)}$ interaction, we came out with five possible models based on the results of the chemical and stable carbon isotopic analyses: (1) loss of $CO_{2(g)}$ to the atmosphere with enrichment in $\delta^{13}C_{DIC}$; (2) DIC gain from evaporative enrichment and exchange of carbon in DIC with the atmospheric $CO_{2(g)}$ to cause the $\delta^{13}C_{DIC}$ to

increase; (3) no net gain or loss of DIC as carbon is exchanged between DIC and atmospheric $CO_{2(g)}$ which causes the $\delta^{13}C_{DIC}$ to increase; (4) increases in the DIC concentrations from evaporative enrichment accompanied by no change in the $\delta^{13}C_{DIC}$; (5) increases in the DIC concentrations accompanied by depletion in $\delta^{13}C_{DIC}$.

Models based on the DIC concentrations and $\delta^{13}C_{DIC}$ can be used to assess the temporary trajectory during carbon cycling in surface waters and are applicable in systems where the dominant carbon-cycling process is controlled by atmospheric $CO_{2(g)}$-surface water DIC interaction. We tested the models with field data and showed how changes in the DIC and the $\delta^{13}C_{DIC}$ can be explained in surface waters where the cycling of carbon is dominated by DIC-atmospheric $CO_{2(g)}$ interaction. However, the models developed in this study should not be applied to field scenarios in which the dominant carbon-cycling process is not controlled by surface water DIC-atmospheric $CO_{2(g)}$ interaction.

II. Information on DIC evolutionary phases and fractionation of $\delta^{13}C_{DIC}$ as water evolve from undersaturation to saturation with respect to calcite

The second project involved performing field and laboratory experiments on carbonate springs that evolved to saturation with respect to calcite and to equilibrium with atmospheric $CO_{2(g)}$. We made measurements of DIC and $\delta^{13}C_{DIC}$ and calculated the calcite equilibrium state of the springs over time in agitated and non-agitated laboratory samples and over distance in field settings to assess the DIC behavior and $\delta^{13}C_{DIC}$ composition as the water evolved to calcite supersaturation conditions. We observed here that outgassing of CO_2 drives the DIC evolution towards calcite supersaturation and to equilibrium with atmospheric $CO_{2(g)}$ resulting to

decreasing carbon concentration over time. Based on the calculated saturated index of calcite we defined four evolutionary phases: increasing saturation, increasing supersaturation, decreasing supersaturation and increasing supersaturation. We identified the DIC evolutionary phase to increasing saturation and increasing supersaturation and the fractionation of the $\delta^{13}C_{DIC}$ during these phases which were by kinetic isotopic fractionation were accompanied by a 1 to 2‰ shift $\delta^{13}C_{DIC}$. We also found that significant enrichment of about 5‰ in the $\delta^{13}C_{DIC}$ occurred during the phase of decreasing supersaturation when DIC decrease was controlled by DIC equilibration with atmospheric $CO_{2(g)}$ and the isotopic fractionation driven by equilibrium isotopic fractionation. Based on our results, field samples only evolved to the stage of increasing supersaturation and thus its $\delta^{13}C_{DIC}$ was controlled mainly by kinetic isotopic fractionation from $CO_{2(g)}$ loss from the samples whereas, laboratory samples evolved beyond calcite supersaturation and its $\delta^{13}C_{DIC}$ enrichment was by equilibrium isotopic exchange due to carbon equilibrium exchange with atmospheric $CO_{2(g)}$. Significant enrichment of the $\delta^{13}C_{DIC}$ of carbonate springs only occur in the decreasing calcite supersaturation state which is not commonly achieved in field settings because of the limited flow distance which hampers investigation of carbonate evolution beyond calcite saturation.

The results of this study could be applied to any highly charged $CO_{2(g)}$ system that evolve to calcite supersaturation conditions such as flowing rivers or lakes that are fed by $CO_{2(g)}$ dominated groundwater. Our results show that considering a non-turbulent or non-mixed $CO_{2(g)}$ charged system, it could take up to 2 days from the time the CO_2 is supplied to the time it precipitate $CO_{2(g)}$ and would take as little as 5 hours to precipitate calcite in a well-mixed or turbulent system.

III. Information of changes on DIC concentration and $\delta^{13}C_{DIC}$ composition due to surface water dilution by precipitation

The third project involved conducting laboratory experiments in which an artificial $NaHCO_3$ solution, lake water and river water were undiluted (100%) and diluted by 25, 50 and 75% with snow-melt and exposed to laboratory air for up to 1000 hours. Measurements of DIC concentrations and $\delta^{13}C_{DIC}$ composition were made over time to determine the effect of dilution on carbonate speciation, DIC and $\delta^{13}C_{DIC}$ behavior on precipitation impacted surface waters. The most diluted water resulted in the lowest pH and solutes concentrations and the $\delta^{13}C_{DIC}$ value was closer to that of the precipitation. Based on dilution proportion, there was an initial evolution of the $\delta^{13}C_{DIC}$ which was different for the different mixtures, but over time there was a convergence of the $\delta^{13}C_{DIC}$ due to surface water DIC-atmospheric $CO_{2(g)}$ interaction. In non-buffered waters with pCO_2 higher than atmospheric, the $\delta^{13}C_{DIC}$ will be closer to that of precipitation but in buffered system with pCO_2 less than atmospheric, the preferential incorporation of $^{13}CO_2$ into the liquid phase will result to sequentially more enriched water for more diluted water. According to the results of this experiment, pH buffering will last for about 10 hours after a rain event. In a 'closed system' in which the pCO_2 is greater than atmospheric, there is conservation of mass with no carbon change over space and/or time, such that increases in pH could be due to the transformation of bicarbonate to carbonate ion. Whereas, in an 'open system, in which the pCO_2 is less than atmospheric, the invasion of $CO_{2(g)}$ will result to carbonic acid formation increasing pH. The buffering of pH in surface water results to minimal fractionation of carbon isotopes such that the overall dominant process controlling $\delta^{13}C_{DIC}$ will be carbon isotopic exchange between the surface water DIC and atmospheric $CO_{2(g)}$.

Based on the results of this experiment, the effect of dilution appears to be significant for about 10 hours in turbulent surface waters after a rain event and would suggest that hydrological studies in field settings designed to minimize the effect of dilution on carbon evolution should wait for at least half-a-day before sampling.

APPENDIX I

Table AI-1. The DIC concentrations and $\delta^{13}C_{DIC}$ of the laboratory and outside air measured during the experiments

	Sample ID	Date	DIC (mmol/L)	$\delta^{13}C_{DIC}$ (‰)
Experiments for Chapter I	Lab Air	6/7/2011	0.04	-10.2
	Lab Air	6/11/2011	0.04	-11.0
	Lab Air	8/1/2011	0.02	-12.9
	Outside Air	6/7/2011	0.04	-11.9
	Outside Air	6/11/2011	0.04	-11.6
	Outside Air	8/1/2011	0.02	-10.5
Experiments for Chapter II	Lab Air	6/7/2011	0.04	-10.2
	Lab Air	6/11/2011	0.04	-11.0
	Lab Air	8/1/2011	0.02	-12.9
	Lab Air	12/17/2012	0.09	-12.3
	Lab Air	1/3/2013	0.01	-11.9
Experiments for Chapter III	Lab Air	5/21/2012	0.04	-9.5
	Lab Air	5/24/2012	0.01	-10.7
	Lab Air	5/30/2012	0.01	-11.0
	Lab Air	9/10/2012	0.04	-12.0
	Lab Air	9/15/2012	0.00	-11.8

VITA

Pride Tamasang Abongwa

Candidate for the Degree of

Doctor of Philosophy

Dissertation: ASSESSING THE EVOLUTION OF DISSOLVED INORGANIC CARBON AND STABLE CARBON ISOTOPES IN SURFACE WATERS

Major Field: Geology

Biographical:

Education:

Completed the requirements for the Doctor of Philosophy in geology at Oklahoma State University, Stillwater, Oklahoma in July, 2004.

Completed the requirements for the Master of Science in hydrology and water resources at UNESCO-IHE Institute of Water Education, Delft, The Netherlands in 2004.

Completed the requirements for the Bachelor of Science in geology at University of Buea, Buea, Cameroon in 1999.

Experience:

Teaching and Research Assistant, Oklahoma State University, Jan 2011-July 2014.
Summer Intern, Energy and Environmental Research Center, May-Aug 2012 & 2013.

Professional Memberships:

- American Association of Petroleum Geologists (AAPG)
- National Association of Black Geoscientists (NABG)
- Geological Society of America (GSA)
- Oklahoma City Geological Society (OCGS)